Studies on the role of Oxygen-regulated protein ORP150 in Alzheimer's disease

Thesis submitted to the Jawaharlal Nehru University in partial fulfilment for the award of the degree of

**DOCTOR OF PHILOSOPHY
IN
BIOTECHNOLOGY**

By

Neha Chanana

**SCHOOL OF BIOTECHNOLOGY
JAWAHARLAL NEHRU UNIVERSITY
NEW DELHI-110067
INDIA**

2017

CERTIFICATE

This is to certify that the work entitled **"Studies on the role of Oxygen-regulated protein ORP150 in Alzheimer's disease"** submitted to the School of Biotechnology, Jawaharlal Nehru University, New Delhi in partial fulfillment of the requirements for the award of the degree of Doctor of Philosophy, embodies faithful record of original research work carried out by **Neha Chanana**. This work is original and has not been submitted so far in part or full for any other degree or diploma of any other university.

Neha Chanana

(Ph.D. Candidate)
School of Biotechnology
Jawaharlal Nehru University
New Delhi-110067, India

Prof. Uttam Pati
(Supervisor)
School of Biotechnology
Jawaharlal Nehru University
New Delhi-110067, India

Prof. Uttam Pati
(Dean)
School of Biotechnology
Jawaharlal Nehru University
New Delhi-110067, India

Dedicated to my family.....

Acknowledgement

I thank god for blessing me with the best in life.

Special thanks to:

My seniors – Anuj Sir, Amir Sir and Kamia Ma'am for their immense support and suggestions in helping me find ways through hard times of my research work.

My lab friends - Deepak and Meenu, for being there whenever I needed them both personally as well as professionally.

My cheerful juniors in lab - Deepa, Sapna, Ambarish, Shashank, Priyanka, Akanksha, Sagarika, Rekha and Simran for their cordial attitude and invaluable support all through my PhD tenure.

Shashank for helping me in FRET calculations and Deepa for sharing her room with me when I needed it the most.

Our ex-MSc students – Rahul, Madan, Mitali, Nilesh, Suraj, Anando, Nikita, Paresh and Vikas for maintaining a friendly atmosphere in the lab.

All the short trips, coffee/tea/lunch sessions, get-togethers, birthday cakes/treats and the fun we all had together will stay captured in my memory forever.

My journey became a lot easier with:

My besties Divya, Priya, Raman, Deepak, Vineet and Aditi who were always by my side, encouraging and cheering me up for all that came my way.

My heartfelt gratitude to:

My 2010 PhD batch friend's–Deepak and Mahima (with whom I started my journey of PhD), Vinay, Vidya Sagar, Fatima, Deepshikha, Ravi, Soumya, Vikas, Damini, Vinod, Neetu and Deepti for their love and support.

My badminton group - Nilesh, Deepak, Shirish, Shailender and Dileep and my lawn-tennis partner- komal, for instilling in me sportsman spirit, which also brought a welcome change and relaxation to the daily routine.

My friends Shailaja, Akruti, Mahima Bansal, Himanshu, Tripti di, Merenli, Indu and Kavita for elevating my spirits in times of need.

I also extend my gratitude to

Two of my favourite seniors from the department – Reema Ma'am and Gaurav Sir for their affection and professional help.

My colleagues– Ajeena, Manish, Shikha, Shailesh Sir, Vijeta Ma'am, Neha Ma'am, Sunita Ma'am, Manjul Ma'am, Atul Sir, Manish Sir, Amit Rahi Sir.

My special juniors in the department - Vatika, Sonal, Monisha, Sonam, Priyanka chowdhary, Pratibha, Sree, Shweta, Rashmi, Richa, Abhishek, Titas, Mriganko, Himanshu, Bala, Roshan, Jeetesh, Pallavi, Aditi, Ritu, Sneha, Priyanka Singh, Supriya, Vasudha, Alka, Jasweer and Radha for their high-spirited, cordial attitude and their invaluable help all through my stay in the department.

Some of my colleagues in other departments/institutes – Shalini, Ravi, Sandhya, Mukesh, Pawan, Monika, Usha, Himanshi, Pallavi and Vijay for sharing information and basic lab necessities.

I would also like to thank:

All Technical and Non-Technical staff of CIF and Lab Attendants for assisting me to get going with the research work and to use departmental facility. Particular thanks to two of my Lab Assistants, Mukesh and Deepak, for providing me with the basic lab necessities. I extend my thanks to our Office Staff Mr. M. K Manuj, Mr. Vinod, Tiwariji, Shobha Ma'am, Vedpalji, Ajay bhaiya and others for their full support with respect to my official formalities during my stay.

Naipalji, Sindhu Ma'am and Yadavji for their co-operation.

Rajesh Bhaiya for preparing all the coffees and snacks fresh which kept me going through the strenuous working hours.

Finally, ***I deeply acknowledge***

The financial support from CSIR and DST-PURSE which helped me carry out my research work.

I dedicate my thesis to my family.

Best
NC ☺

Abbreviations

%	Percentage
β ME	Beta mercaptoethanol
α	Alpha
β	Beta
μg	Microgram
μl	Microliter
μM	Micromolar
~	Approximately
^{o}C	Degree celsius
A_{260}	Absorbance at 260 nm
A_{280}	Absorbance at 280 nm
A_{600}	Absorbance at 600 nm.
Ab	Antibody
Aβ42	Amyloid beta 42
Amp	Ampicillin
AP	Alkaline phosphatase
APS	Ammonium persulphate
ATP	Adenosine Triphosphate
BCIP	5-bromo-4-chloro-3-indolyl phosphate
bp	Base pair
BSA	Bovine Serum Albumin
CO_2	Carbon dioxide
CHIP	Carboxyl terminus of HSC70-interacting protein
CHX	Cycloheximide
C-terminal	Carboxy terminal
ddH_2O	Double distilled water
ddNTP	Di-deoxyribose nucleotide triphosphate
DMSO	Dimethyl sulfoxide
DNA/RNA	Deoxyribose/Ribose nucleic acid
dNTP	Deoxyribose nucleotide triphosphate
DTT	Dithiothreitol
EDTA	Ethylene diamine tetracetic acid
ELISA	Enzyme Linked Immuno Sorbent Assay
ER	Endoplasmic Reticulum
EtBr	Ethidium Bromide
FCS/FBS	Fetal calf/bovine serum
g	Gravitational force
Gms	Grams
h/hrs	Hour/hours
Ig	Immunoglobulin

IP	immunoprecipitation
IPTG	Isopropyl-β-D-thio-galactopyranoside
Kan	Kanamycin
kb	Kilo base
kD/kDa	Kilo Dalton
LB	Luria Bertani medium
M	Molar
mg	Milligram
min/mins	Minute/Minutes
ml	Millilitres
mM	Millimolar
MG-132	Z-Leu-Leu-Leu-CHO
N	Normailty
NBT	Nitro blue tetrazolium chloride
NCCS	National centre for cell science
ng	Nanogram
NIMHANS	National Institute of Mental Health and Neuro Sciences
Ni^{2+}-NTA	Nickel-nitrilotriacetic acid
N-terminal	Amino terminal
O/N	Overnight
OD	Optical Density
OS	Oxidative Stress
PAGE	Poly Acrylamide Gel Electrophoresis
PBS	Phosphate Buffer Saline
PCR	Polymerase Chain Reaction
Pen	Penicillin
PMSF	Phenyl Methyl sulfonyl fluoride
RNase	Ribonuclease
rpm	Revolution per minute
RT	Room Temperature
SDS	Sodium Dodecyl Sulphate
SDS-PAGE	SodiumDodecyl Sulphate-Poly acrylamide Gel Electrophoresis
sec	Seconds
Strep	Streptomycin
SWDBB	South-west dementia brain bank
TAE	Tris acetate EDTA
TBE	Tris-borate EDTA
TE	Tris-EDTA
TEMED	N,N,N′,N′ tetramethyl ethylene diamine
Tris	Tris (hydroxymethyl) amino acid
U	Unit(s)
UPR	Unfolded protein response
UV	Ultra Violet
Ub	Ubiquitin
v/v	volume/volume

w/v   weight/volume
WT   Wild type

Table of Contents

Results

Summary

Altered expression of molecular chaperones in AD affected brain regions indicates their role in development and progression of Alzheimer's disease. Oxygen regulated protein ORP150, an endoplasmic reticulum-resident chaperone, elevated in cellular and transgenic mouse models of Alzheimer's disease (AD) is responsible for folding and maturation of secretory and membrane proteins. BACE1, a key membrane protein involved in amyloidogensis in AD, is shown to be negatively regulated by cellular chaperone CHIP. In this study, the role of ORP150 is established in stabilizing stress-induced BACE1 levels. ORP150 increases cellular Aβ42 production by enhancing BACE1-mediated APP-processing. An increase in ORP150 level results in rise of cellular BACE1 protein level resulting in cleavage of APP into CTF99 and Aβ42 whereas silencing of ORP150 alleviates BACE1 levels under oxidative and ER stress. Moreover, ORP150 and CHIP inversely control cellular Aβ42 generation. The glycosylated ORP150 is shown to stabilize BACE1 although both glycosylated and unglycosylated ORP150 physically interact with BACE1. Furthermore, a direct relation between ORP150 and BACE1 and an inverse relation between CHIP and BACE1 is observed *in vivo* in both male and female AD patients. Thus, a simultaneous synergy and antagonism is observed between ORP150 and CHIP in AD patients in gender-specific manner in regard to BACE1 and Aβ42 production. The expression and activity of molecular chaperones is known to be regulated at both transcriptional and post-transcriptional level under pathological stress conditions. The effect of ER-resident chaperone ORP150 on the cellular chaperone CHIP and vice versa was further established under pathological stress conditions. Interestingly, ORP150 regulates cellular BACE1 levels by inversely regulating CHIP under ER, oxidative and hypoxic stress conditions. By contrast, CHIP reduces ORP150 and BACE1 levels specifically under oxidative stress. In conclusion, opposing actions of ORP150 and CHIP in controlling BACE1 levels and Aβ42 production is thus confirmed in this study in both cellular models of AD as well as *in vivo* in human AD brain. Thus, this finding might help future implications in designing chaperone-mediated new therapeutics for AD.

INTRODUCTION

Introduction

Alzheimer's disease

Alzheimer's di sease (AD) i s one of t he m ost common pr ogressive ne urodegenerative disorders involving a gradual decline in many cognitive processes ultimately leading to dementia and death. It alone accounts for 60-70% of the cases of dementia (Reitz et al. 2012). Worldwide, nearly 44 million people have Alzheimer's or related dementia. There are t wo types of Alzheimer's disease, on e which a ccounts f or 95% of the c ases i .e. sporadic l ate ons et A lzheimer's di sease (LOAD) and the ot her w hich is less pr evalent (5% of cases) is early onset familial AD (FAD). LOAD occurs late in life, usually after 65 years, due to combination of both genetic and environmental factors. Also, presence of specific pol ymorphisms in A po l ipoprotein E g ene (APOE4) i s g enetically associated with an increased risk of AD (Bertram et al. 2010; Verghese et al. 2011). Other factors include a ge, br ain i njury, de pression or hypertension (Thornton et al. 2006; Bruijn and Ikram 2014). The epigenetic f actors l ike hi stone m odification a nd a bnormal D NA methylation also inc rease the risk for LOAD (Chouliaras et al. 2010). O n the c ontrary, FAD occurs early in age due to the presence of autosomal dominant mutations in the gene involved i n A D l ike amyloid pr ecursor pr otein-1 (APP), pr esenillin-1 (PS1) or presenillin-2 (PS2). Duplication of chromosome 2 1 in the case of Down syndrome (also where APP gene is located) is also a cause for early-onset FAD. Alzheimer's disease has been s een t o e ffect m en a nd w omen di fferently with i ts i ncreased i ncidence i n w omen attributed to factors like lowered levels of estrogen with age, influence of Apolipoprotein E-ε4 and their increased life span (Hebert et al. 2001; Viña and Lloret 2010; Laws et al. 2016).

So f ar, t here i s no c ure f or A lzheimer's di sease. S ome m edications l ike acetylcholinestarase inhibitors and NMDA Receptor antagonists are used to treat AD, but they only delay the pr ogression of s ymptoms associated w ith AD (Parson et al. 2013). Thus, insights into the pathogenesis of AD are essential for discovery of targeted therapy which can block the progression of the disease (i.e. clinical symptoms) and for designing of drugs targeting various molecular pathways.

Amyloid Precursor Protein, APP and its processing in Alzheimer's disease

APP, a transmembrane protein, is the precursor molecule for the amyloid beta-peptides, the fibrillar form of which forms the neurotoxic amyloid beta plaques (Hardy and Selkoe 2002). APP gene spans 290kb on chromosome 21 and has 18 exons. It is known to be expressed by many tissues specially concentrated at the neuronal junctions. Structurally, APP is an integral membrane protein with a large extracellular N-terminus containing cystein domain, followed by an acidic domain, a Kunitz domain (also known as KPI, Kunitz protease inhibitor domain), a glycosylated domain containing OX2 domain, followed by a single-membrane spanning (transmembrane) domain and a shorter, C-terminal cytoplasmic domain. The Aβ peptide encoding region is part of the luminal glycosylated domain (Coburger et al. 2013) **(Figure 1)**.
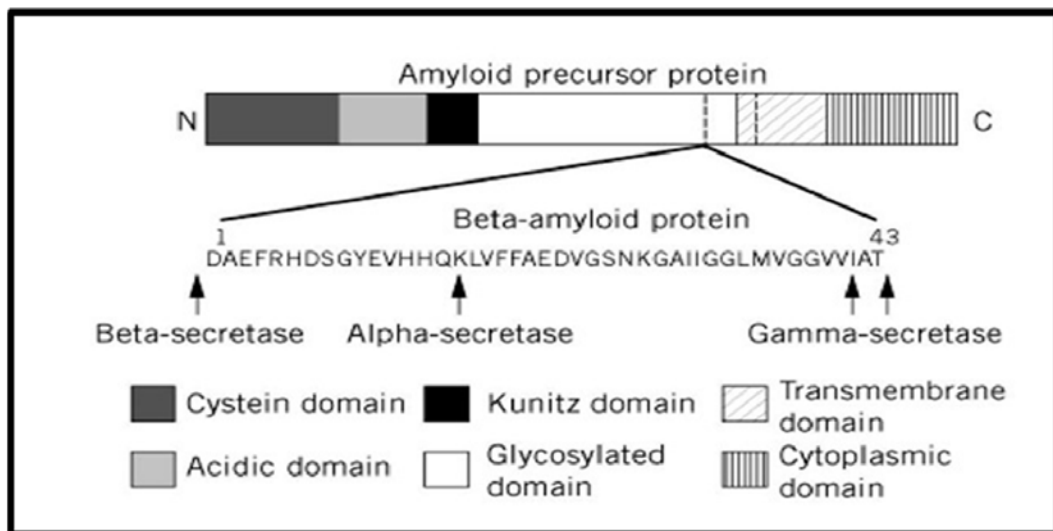
Figure1: Structural organization of Amyloid Precursor Protein, APP domains (Molecular Biology).

APP is composed of 770 amino acid residues and alternate splicing of exon 7 and 8 (encoding KPI domain and OX2 domain respectively) generates three major isoforms namely APP770, APP751 and APP695. The APP770 isoform contains both the KPI and OX2 domains, however APP751 isoform lacks KPI domain and APP695 lacks both the KPI and an OX2 domain. The shortest APP695 form is expressed at higher levels in AD brain as compared to the APP751 and APP770 forms. In particular, a Swedish mutation of two base pair transversion (G to T and A to C) resulting in two amino acid substitutions (lysine to asparagine and methionine to leucine) at N-terminal of Aβ was observed in some Swedish families (De Strooper et al. 1994). Swedish mutant APP is

more pa thogenic a s BACE1 enzyme shows an enhanced β-processing act ivity ov er swAPP695 and an increased Aβ production (Mullan et al. 1992).

APP i s pr ocessed b y one of t he t wo pa thways i .e. a myloidogenic a nd t he non - amyloidogenic pa thway (Cole a nd V assar 2007). N ormally i n c ells, non -amyloidogenic pathway i s f ollowed w here i n A PP i s c leaved by α-secretase w ithin the be ta-amyloid peptide generating an extracellular sAPPα fragment and a membrane anchored CTFα fragment (C83). sAPPα fragment is known to have neuro-protective effects (Thornton et al. 2006) . The C83 fragment further is cleaved by γ-secretase enzyme r eleasing an extracellular P 3 fragment and a m embrane an chored AICD fragment. P3 fragment i s degraded and the AICD plays role in nuclear gene regulation through its interactions with a multimeric complex that includes Histone Acetyl Transferase, Tip60 (Cao and Su 1999; Muller e t a l. 2007) . H owever, i n A lzheimer's disease, t he a myloidogenic pa thway i s followed wherein APP is cleaved by the β-secretase, BACE1 enzyme at the β-secretase site that ge nerates an extracellular sAPPβ fragment and a membrane anchored CTFβ fragment (C99). The CTFβ fragment is further cleaved by γ-secretase releasing toxic Aβ peptides extracellularly ranging in length from 37-43 amino acid residues and generating membrane anchored A ICD fragment (Selkoe 20 01; Laferla et al. 2007; Thinakaran and Koo 2008). Aggregation of toxic β-amyloid peptide as ex tracellular pl aques an d hyperphophorylated t au pr oteins as int racellular ne urofibrillary ta ngles a re the w ell- known hi stopathological ha llmarks of AD (Selkoe 2001; T anzi a nd B ertram 2005). Aβ has recently been shown to be a natural antibiotic that forms aggregate trap to imprison bacterial pathogens thus protecting the brain from infection (Kumar et al. 2016). Images below show t he br ain changes t hat ar e obs erved in AD w here accumulation of extracellular β-amyloid plaques a t ne uron-neuron j unctions hi nders t he synaptic s ignal transmission **(Figure 2)**.
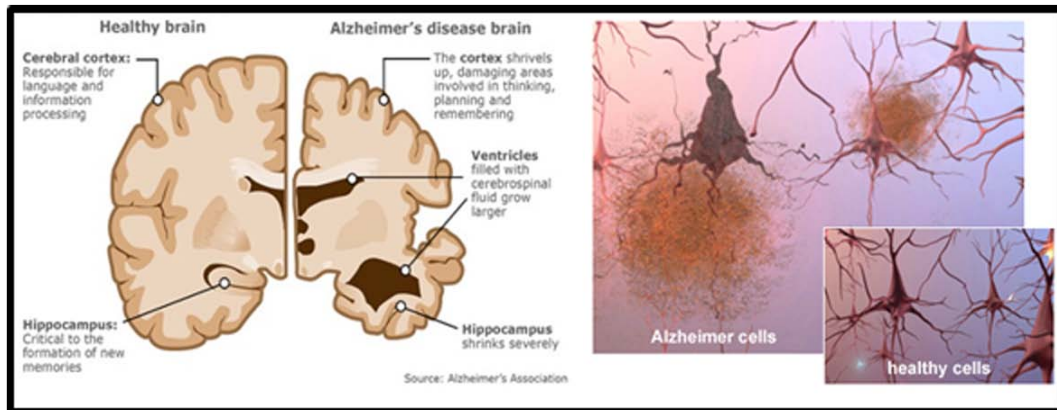
Figure 2: Brain changes that are observed in Alzheimer's disease and microscopic view of the Amyloid beta plaques (Alzheimer's Association. Alz.org research centre).

The m ajor r egions a ffected a re c ortex a nd t he hi ppocampus, s o a re t he obs erved symptoms of le arning and memory d eficits which i nclude short te rm memory los s, language pr oblems, di sorientation, m ood s wings, l oss of m otivation. G radually, bodi ly functions are lost, thus ultimately leading to death. (Cole and Vassar 2007).

BACE1 and Alzheimer's disease

BACE1, a transmembrane aspartyl protease, is the rate limiting and principal enzyme in the ge neration of t oxic a myloid β peptides. BACE1 gene spans 30kb o n c hromosome 11q23.2 and has 9 exons (Sinha et al. 1999; Dislich et al 2012). Deletion of BACE1 via homologous recombination in mouse models of AD completely abolishes Aβ generation in the brain without any developmental abnormalities (Cai et al. 2001; Luo et al. 2001; Roberds et al. 2001) thus making it s uitable drug target for AD. Structurally, BACE1 is composed of 505 amino acids and has an N-terminal signal peptide domain (residues, 1-21), followed by a propeptide domain (residues, 22-45), a protease domain (residues, 46-460) which contains two luminal catalytic motifs (DTGS, at residues 93-96, and DSGT, at residues 289-292) characteristic of an aspartyl protease active site, followed by a single transmembrane dom ain (residues, 461 -477) a nd a s hort C -terminal c ytosolic dom ain (residues, 478 -501) **[Figure 3]** (Hussain e t a l. 1999; V assar et a l. 1999; Capell et al. 2000; Benjannet et al. 2001) . Signal peptide helps in its localization into the endoplasmic reticulum. In t he E R, B ACE1 unde rgoes s ome pos t-translational modi fications like phosphorylations, glycosylations at four asparagines residues $(N^{153,172,223,354})$, transient acetylation a t s even arginine r esidues and di sulfide bond formation (Huse a nd D oms 2001; Maxwell et al. 2 008). The pr o-peptide o f B ACE1 is t hen cleaved before i t i s

transported to Golgi network where in further extensive glycosylation takes place which includes S-palmitoylation at Cys 474, Cys 478, Cys 482, and Cys 485. All these post-translation modifications of BACE1 increase the molecular weight of BACE1 from 50kD to 75kD. The membrane targeted BACE1 is then internalized to endosomes. Owing to its acidic pH -optimum (Vassar et al . 1999; Shimizu et al. 2008), BACE1 cleaves its substrates mostly in the acidic early endosomal and trans-Golgi compartments, also sites of Aβ generation (Haass et al. 1994). However, studies also show Aβ generation in the endoplasmic reticulum (Chyung et al. 1997; Cook et al. 1997).
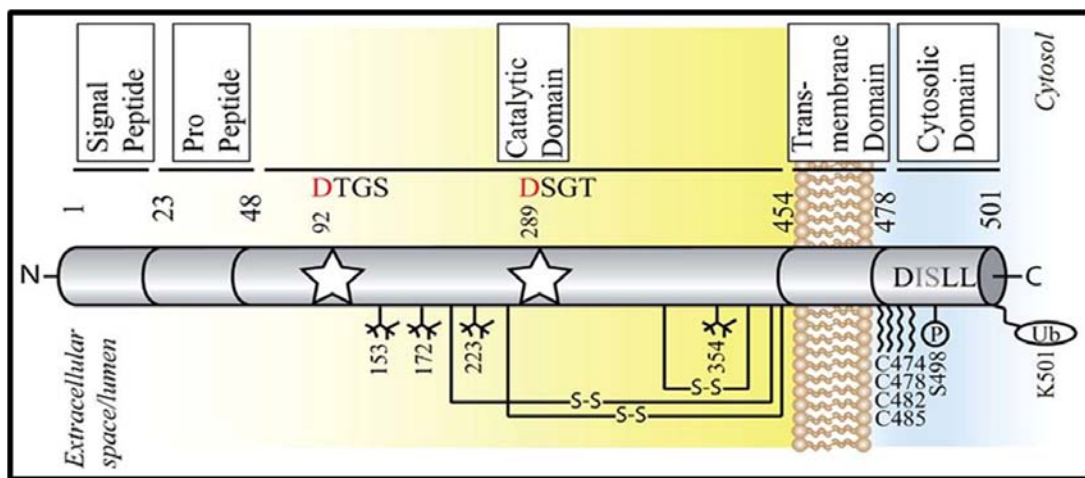
Figure 3: Structural organization of BACE1 (Dislich and Lichtenthaler 2012).

Apart from proteolytic processing of APP, BACE1 is involved in multiple physiological roles including synaptic transmission. Recently it has been shown that BACE1 via its transmembrane domain interacts with adenylate cyclase resulting in reduction of CREB phosphorylation, PKA activity and cAMP levels. And, this reduced cAMP/PKA/CREB pathway contributes to the observed impaired memory and cognitive deficits in BACE1 transgenic mice independently of Aβ (Chen et al. 2012). Another publication shows a copper binding site as a 24 -residue peptide in the cytoplasmic domain of BACE1 identifying a possible link to metal homeostasis and oxidative stress in AD. It shows that BACE1 competes for and interacts with CCS (the copper chaperones for SOD1) through domain 1 and thus reduces the activity of SOD1 (Angeletti et al. 2005; Dingwall 2007).

Regulation of BACE1

I. Transcriptional control of BACE1

Previous studies show BACE1 to be regulated by a number of transcription factors like Sp1, NF-κB, HIF1 and PPARγ amongst others. Sp1, belonging to the Sp/KLF (Specificity protein/Krüppellike factor) family, was the first transcriptions factor to be studied in BACE1 regulation and was found to be an activator of BACE1 expression (Christensen et al. 2004). NF-κB (nuclear factor kappa-light-chain-enhancer of activated B cells) is known to regulate BACE1 in a cell-type dependent manner by binding to distinct subunits while acting as an activator or a repressor. In differentiated neuronal cultures and nonactivated glial cultures it acts as a repressor for BACE1 transcription whereas in activated astrocytic and Aβ-exposed neuronal cultures it acts as an activator (Bourne et al. 2007; Chami et al. 2012). Hypoxia inducible factor-1 (HIF1), a heterodimeric transcription factor composed of oxygen sensitive alpha subunit (HIF1α) and constitutively expressed beta subunit (HIF1β), is another major transcription factor known to upregulate BACE1 gene transcription under hypoxic conditions (Sun et al. 2006; Zhang et al. 2007). Lastly, PPARγ, a ligand induced transcription factor is known to act as a repressor for BACE1 transcription (Sastre et al. 2006).

II. Translational and Post-translational control

Previous studies show a large number of molecules including proteins and lipids regulating BACE1 levels and amyloid β-peptide biogenesis. Ceramide, a membrane lipid acting as a second messenger in many biological events, is found to be elevated in brain of AD patients. It has been shown to stabilize BACE1 post-translationally and promote Aβ peptide biogenesis (Puglielli et al. 2003). Reticulon family of proteins consisting of four members, RTN1, RTN2, RTN3 and RTN4 have been shown to be binding partners of BACE1 where colocalization with RTN3 was observed in neurons while colocalization with RTN4 was found to be more enriched in oligodendrocytes. RTN proteins have been shown to be negative modulators of BACE1, thus blocking its activity over APP and inhibiting Aβ peptide generation (He et al. 2004; Murayama et al. 2006). Golgi-localized, γ-ear-containing, ADP ribosylation factor-binding (GGA) proteins have been shown to regulate retrograde transport of BACE1 from endosomes to the trans-Golgi network in a phosphorylation dependent manner (Wahle et al. 2005). The C-terminus ACDL (acid

cluster dileucine motif) domain of BACE1 containing DISLL motif interacts with the VHS (Vps-27, Hours, and STAM) domain of GGA proteins. Thus, GGA proteins interact with the phosphorylated foms of BACE1 and direct their transport from the endosomes to the TGN, while the unphosphorylated BACE1 is transported to the cell surface (He et al. 2005). Another study shows Seladin1 (selective Alzheimer disease indicator-1), a neuroprotective protein, to be selectively downregulated in the brain of AD patients. The study further shows downregulation of Seladin1 in oxidative stress-induced apoptosis in turn reduces GGA3, thus stabilizing BACE1 and promoting amyloidogenesis (Sarajärvi et al. 2009). Another negative modulator of BACE1 studied is sorting nexin 6 (SNX6, a PX domain protein), a putative component of retromer, a multiprotein cargo complex that mediates the retrograde trafficking of BACE1 in the endocytic pathway (Okada et al. 2010). Another member of this family, SNX12 interacts with BACE1 and also negatively regulates BACE1-mediated APP processing (Zhao et al. 2012). Thus, changes in the expression of these proteins in the human brain are likely to affect cellular amyloid β-production and the formation of amyloid plaques.

III. BACE1 degradation

It is known that ubiquitination of BACE1 occurs at lysine 501 in its C-terminus domain. However, there are conflicting reports on whether BACE1 is degraded via the proteosomal pathway or the lysosomal pathway, where both pathways degrade ubiquitinated proteins. Proteosomal mediated degradation of BACE1 has been shown using proteosome inhibitors (lactacystin) (Qing et al. 2004). However, a few studies have shown lysosome as the major route of BACE1 degradation where inhibition of lysosomal proteases by chloroquine and NH_4Cl has shown increase in BACE1 levels and its localization in LAMP2 positive compartments, a specific marker for lysosomes. The dileucine motif (DDISLLK-leu499/leu500) in its C-terminal domain is observed to be responsible for its lysosmal mediated degradation (Koh et al. 2005).

IV. Physiological stress and BACE1

Unfolded protein response (UPR) plays an important role in AD pathogenesis (Hoozemans et al. 2005; Hoozemans et al. 2012). Endoplasmic reticulum is the site of synthesis and processing of nearly all the proteins passing through the secretory pathway. In response to the accumulation of unfolded proteins in the ER, UPR is activated involving activation of PERK, IRE1 and ATF6 which further controls translation attenuation of proteins and expression of ER-resident chaperones. Altered induction of ER-resident UPR responsive proteins including GRP78/BiP, PDI, PERK, eIF2α-P and IRE1α have been observed in AD patients brain (Yoo et al. 2001, Plácido et al. 2014). Stroke and cerebral infarction have been known to be significant risk factors for Alzheimer's disease. Hypoxia is known to alter APP processing via increasing the activity of both β and γ-secretase thus increasing amyloid biogenesis. A biphasic mechanism is shown to be involved in BACE1 upregulation under hypoxia with ROS (generated by sudden interruption of mitochondrial ETC) mediating the early response while transcriptional activation by HIF1 mediating the late post-hypoxic response (Zhang 2007; Gugleilmotto, Aragno et al. 2009; Guglielmotto, Tamagno et al. 2009). Oxidative stress is observed to be a major contributor to ageing and is known to play potential causative role in the pathogenesis of Alzheimer's disease. The brain is particularly vulnerable to oxidative stress (OS) because of its high utilization of oxygen, low levels of anti-oxidants and an increased level of polyunsaturated fatty acids. A large number of studies have shown upregulation of BACE1 transcription, expression and activity under oxidative stress condition with JNK/AP1 acting as the transcriptional controller (Chami and Checler 2012) and PKR/eIF2α acting as the translational controller (Mouton-liger et al. 2012). It is also observed that mild oxidative stress do not increase BACE1 levels but induce its subcellular rearrangement from lighter to denser fractions promoting APP processing (Tan et al. 2013). Also, pharmacological inhibitors of energy (insulin, 2-deoxyglucose, 3-nitropropionic acid, kainic acid) have been shown to increase both BACE1 levels and activity (Velliquette et al. 2005). Recently, bisecting N-acetylglucosamine modification was found to stabilize BACE1 under oxidative stress conditions (Kizuka et al. 2016)

Chaperones in Alzheimer's disease

I. Oxygen-regulated protein (ORP150) in Alzheimer's disease

ORP150, also known as hypoxia upregulated protein (HYOU1), is a known endoplasmic reticulum (ER) - resident chaperone belonging to the heat shock protein 110 family (a HSP70 subfamily) (Easton et al. 2000; Du et al. 2016). ORP150 was first discovered expressing under low oxygen conditions in cultured astrocytes (Heacock and Sutherland 1990), which was then followed by its purification and characterization (Kuwabara et al. 1996). It is encoded by HYOU1 gene present on chromosome 11 and has 26 exons. Three mRNA transcripts are known to be induced from its alternative promoters: Exon1A, Exon1B (ER-resident forms) and Exon2 (truncated cytoplasmic form) with ATF4, ATF6 and Nrf2 as its transcriptional activators (Kaneda et al. 2000; Zong et al. 2016). Polymorphism in the ORP150 gene has been found to be associated with insulin resistance in PIMA Indians (Ozawa et al. 2005). The expression of ORP150 is increased in a range of pathologic situations such as brain ischaemia (Matsushita et al. 1998), atherosclerotic plaques (Tsukamoto et al. 1996) and malignant tumours (Stojadinovic et al. 2007). Structurally, ORP150 is a 999 amino-acid residue protein having an N-terminal signal peptide domain (responsible for ER targeting), followed by an ATPase domain, a peptide binding domain, an α-helical lid domain and a C-terminal KNDEL ER retention sequence **(Figure 4)** (Takeuchi 2006).
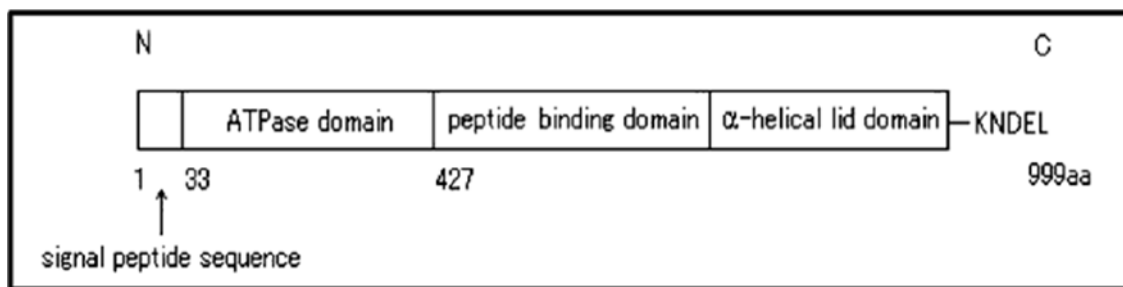
Figure 4: Human Heart ORP150 (Takeuchi 2006).

Functionally, ORP150 has not been fully elucidated, but its cytoprotective effects are observed in renal, neural and cardiac models of ischemia-reperfusion injury (Matsushita et al. 1998; Ozawa et al. 1999; Kitano et al. 2004; Kitao 2004; Aleshin et al. 2005). It is induced in response to environmental stress with its elevated levels observed specifically in the pathology of ER stress related diseases like diabetes, neurodegenerative diseases,

cardiovascular diseases and cancer (Arrington et al. 2008; Wang et al. 2011; Kusaczuk and Cechowska-Pasko 2013; Wu et al. 2013). Together with other chaperones such as 78- and 94-kDa glucose regulated proteins (GRP78 and GRP94), it assists in the folding and assembly of secretory and membrane proteins (Flores-diaz et al. 2004) and of large oligomeric proteins including immunoglobulins (Lin et al. 1993; Kuznetsov et al. 1997). The expression of ORP150 has also been observed in higher stages of bladder cancer and its correlation with metalloproteinases (MMP2) expression signifies its role as a molecular chaperone for MMP's and in tumor invasiveness (Asahi et al. 2002). ORP150 is implicated in angiogenesis where it is seen to co-express with VEGF and increase its secretion in human wound macrophages (Ozawa, Kondo, et al. 2001; Ozawa, Tsukamoto, et al. 2001; Semenza 2001). Also, ORP150 mediates lysophosphatidic acid induced VEGF secretion as observed in mesenchymal stem cells (Wei et al. 2013). Furthermore, ORP150 has been shown to provide anti-apoptotic signals in a variety of cancers such as prostate, breast and bladder (Asahi et al. 2002; Miyagi et al. 2002). Thus, induction of ORP150 in cancers is thought to be a cause for resistance to chemotherapy and is involved in tumor progression (Krętowski et al. 2013). ORP150 in complex with tumor specific antigens is studied as a potential vaccine and has been shown to produce tumor specific immune response *in vivo* (Arnouk et al. 2010; Chen et al. 2013; Yu and Wang 2013). While most of the studies of ORP150 involve the endoplasmic form, one study states the presence of a cytosolic form of ORP150 transcribed from exon 2 that lacks the ER-targeted signal peptide. This cytosolic form of ORP150 was found to have a role in nuclear transport and was found to be co-immunoprecipitated with Ran-GTP, the complex involved in NLS-dependent nuclear import of proteins. Thus, ORP150 also seems to play some role in nuclear transport of proteins (Yu et al. 2002).

Development of neurological disorders has been associated with ER chaperones and co-chaperones in which ORP150 was found to be associated with Alzheimer's disease (Ni and Lee 2007). Same study shows knockout of ORP150 in mouse models is associated with embryonic lethality. Studies in HEK293-APP stable cells showed overexpression of GRP170/ORP150, GRP78, calnexin suppressed the production of β-amyloid peptides (Aβ), a major component of extracellular senile plaques in Alzheimer's disease. On the other hand, overproduction of swAPP or addition of synthetic Aβ42 caused upregulation of the mRNA of various ER chaperones in cells including that of ORP150. Cytoprotective role of ORP150 along with its critical role in neuronal survival to

ischemic stress and excitory stimuli has previously been reported (Tamatani et al. 2001; Kitao et al. 2004). Thus, it is concluded that ORP150 and other ER chaperones are highly induced to ameliorate the accumulation of misfolded proteins and protect neuronal cells against neurotoxicity (Hoshino et al. 2007). Another study shows induction of cytoprotective ORP150 by s APPalpha, the non-amyloidogenic product of APP processing (Hartl et al. 2013).

II. C-terminus of HSC70 interacting protein (CHIP) in Alzheimer's disease

As chaperones have been known to regulate proteins associated with Alzheimer's progression (Koren et al. 2009), another such Tetracopeptide repeat (TPR)-containing cellular chaperone is C-terminus of HSC70 interacting protein (CHIP), also known as STUB1 (STIP1 homology and U-box containing protein 1). CHIP is a 35kD ubiquitously expressed cellular protein possessing dual function both as a molecular chaperone and as an E3 ubiquitin ligase (kumar et al. 2012). Stress-induced chaperone response is a characteristic protective response to environmental stress (Feder and Hofmann 1999). CHIP, activates HSF1−the central transcriptional activator of stress-response signalling, and also confers protection against apoptosis and cellular stress (Dai et al. 2003). CHIP critically plays role in quality control and is known to degrade several AD related misfolded or aggregating proteins like tau (shimura et al. 2004), CFTR (Meacham et al. 2001), p53 (Esser et al. 2005) and Aβ (Kumar et al. 2012). Recently it was shown that CHIP stabilizes APP via proteasomal degradation and p53-mediated trans-repression of BACE1 (Singh et al. 2015). Elevated CHIP levels protect against NFT formation in early stages of AD (Sahara et. al. 2005); conversely decrease in CHIP has been correlated with an increase in neuroprotective NQO1 protein in aged brain (Tsvetkov et al. 2011). Another paper shows proteosome-dependent CHIP-HSP70 complex in stabilization of APP and degradation of cellular Aβ levels (Kumar et al. 2007). CHIP has also been seen as a mechanistic link between Aβ and Tau pathology where Aβ induced progression of tau pathology could be reversed by addition of CHIP (Oddo et al. 2008). Thus, CHIP is found to be a potential target for therapeutics in AD. CHIP along with USP47 enzyme is known to antagonistically regulate katanin-p60 mediated axonal growth (Yang et al. 2013). Antogonistic interactions has also been observed between yeast chaperones, Hsp104 and Hsp70 in Prion curing (Newnam et al. 1999).

Rationale

The mechanism of action of molecular chaperones in Alzheimer's disease is still not completely understood. However, enough evidence in literature encourages development of chaperone-mediated therapy for treatment of AD (Marino Gammazza et al. 2016). Chaperone-mediated therapy would include chaperone replacement via gene or protein administration in case a chaperone is protective to AD and blocking or elimination of chaperone if a chaperone is pathogenic to AD. As BACE1 is at the crossroad of a toxic vicious cycle involving cellular stress and Aβ production (Chami and Checkler 2012), thus studying the regulation of BACE1 by stress-responsive chaperones will help us find new strategies for therapeutic intervention in Alzheimer's progression.

Increased levels of ORP150 has been observed in cellular and transgenic mouse models of AD (Hoshino et al. 2007). As ORP150 is a chaperone involved in folding and assembly of secretory proteins it was hypothesized in this study whether ORP150 plays role in regulating BACE1-mediated APP processing and cellular Aβ42 generation. An inverse relation exists between CHIP and BACE1 in neuronal cells by virtue of CHIP's ability in destabilizing BACE1 (Singh and Pati 2015). CHIP, along with HSP70, have been found to be a critical regulator of neuronal cell fate after stress (Stankowski et al. 2011). In addition, CHIP-HSP70 complex plays neuroprotective role by maintaining steady state levels of APP and attenuating Aβ toxicity (Kumar et al. 2007). As multiple chaperones are shown to be simultaneously functional in Alzheimer pathology it was further hypothesized whether any chaperonic synergy or antagonism between ER chaperone, ORP150 and cellular chaperone, CHIP might constitute Aβ pathology under pathological stress conditions.

Expression levels of a large number of heat shock proteins and chaperones have been found to be elevated in effected regions from AD brain tissue (Hamos et al. 1991). The primary role of these proteins is to protect substrates following synthesis and during stress and only as a last alternative do they promote protein degradation (Koren et al. 2009). To further probe the role of ORP150 and CHIP in the pathogenesis of AD, the levels of these chaperones were compared with that of BACE1 and Aβ42 in human AD brain.

Aims and Objectives

I.   To analyze the effect of ORP150 on BACE1 levels and on BACE1-mediated APP-processing in HEK293 and Neuronal cells.

II. To establish the role of ORP150 on stress-mediated (oxidative stress, ER-stress, hypoxia) BACE1 regulation.

III. To study the subcellular colocalization and interaction between ORP150 and BACE1.

IV. To study inverse relation between ORP150 and CHIP under stress conditions.

V.   To analyze and compare *in vivo* expression profile of ORP150, CHIP, BACE1 and Aβ42 in cortex of AD patients.

MATERIALS

AND

METHODS

Materials

Human brain tissue

Post-mortem frontal cortex and temporal cortex tissue of an Asian origin were obtained from NIMHANS, Bangalore, India and frontal cortex of White British origin were obtained from South West Dementia brain bank, University of Bristol, Bristol. All patient samples were approved by Institutional Ethical Review Board, JNU.

Chemicals

Acrylamide, Ammonium Acetate, Ammonium Persulphate, Bis-Acrylamide, Boric Acid, Bovine Serum Albumin, Bromophenol Blue, *p*-Coumaric acid, Calcium Chloride, Chloroform, Cycloheximide (CHX), Dithiothreitol, Ethidium Bromide, Ethylene Diamine Tetracetic Acid (EDTA), Formaldehyde, Glacial Acetic acid, Glutathione Sepharose, Glycine, Glycerol, Guanidium Hydrochloride, HEPES, Imidazole Hydrochloride, Isoamyl Alcohol, Isopropyl Alcohol, L-glutamine, Lithium chloride, Luminol, Magnesium chloride, Methanol, MG-132, N, N, N', N'-Tetramethyl-Ethylenediamine (TEMED), Ni^{2+}-NTA bead, Nonidet P-40, Phenol, Phenyl Methyl Sulphonyl Fluoride (PMSF), Potassium Dihydrogen Phosphate, Potassium Acetate, Potassium Chloride, Protein A Sepharose, Reduced Glutathione, Sodium Acetate, Sodium Azide, Sodium Bicarbonate, Sodium Chloride, Sodium Deoxycholate, Sodium dodecyl (lauryl) sulphate, Sodium hydroxide, Sodium pyruvate, Tris Base (Trizma Base), Triton X-100, Tween-20, Trypsin Inhibitor, Xylene Cyanol, β-mercaptoethanol and other chemicals were purchased from Sigma-Aldrich, USA, Amersham Pharmacia, UK, Amresco, USA and Calbiochem, USA. Absolute alcohol was purchased from E. Merck, Germany. Luria Bertani (LB) medium, Luria agar for bacterial growth was obtained from BD Difco™, USA. Concentrated HCl, Concentrated Nitric acid, Glucose, Potassium dichromate, Sodium carbonate and Sodium thiosulphate were purchased from Qualigens Chemicals, India. Bradford reagent for protein quantitation was obtained from Bio-Rad, USA. Nitrocellulose membrane purchased from MDI, India and Millipore, USA. Dialysis tubing for removing the extra salts from the purified proteins was bought from Sigma-Aldrich, USA.

Enzymes, Reagents and Antibodies

RNase A, T4 DNA ligase and restriction endonucleases ClaI, EcoRI, NheI, SalI were purchased from New England Biolabs, USA. Taq DNA polymerase was purchased from Bangalore Genei India. Pfu and phusion DNA polymerase were purchased from Fermentas, USA. All the oligonucleotides used were obtained from Sigma-Aldrich, USA. Mini and midi plasmid DNA isolation kits, Genomic DNA isolation kit, and agarose gel extraction kit were purchased from Qiagen, Germany. Bradford protein detection kit was procured from BIO-RAD. Human Aβ42-specific sandwich ELISA kit was obtained from Invitrogen, Carlsbad, CA. TRIzol for total RNA isolation was purchased from Sigma-Aldrich, USA. cDNA synthesis and SYBR green Real-Time PCR Master mix were purchased from Thermofischer scientific, USA. Anti-BACE1 (M-83 and Z-183), anti-CHIP (G-2), anti-myc (9E10), anti-HA (F-7), anti-GST (B-14), anti-GAPDH (0411), and anti-β amyloid (H-43, 6A 6 and 2C 8) antibodies were purchased from Santa-Cruz Biotechnology, USA. Anti-ORP150 antibody (2F07) was purchased from IBL, Japan. Anti-Mouse and Anti-Rabbit secondary antibodies (poly HRP-conjugated) were purchased from Pierce Biotechnology, USA.

Bacterial strains and bacterial expression vectors

Escherichia.coli DH5α strain (*E. coli* DH5α) were routinely used for plasmid DNA preparation and *E. coli* BL21(DE3) strain was used for protein expression. pGEX vector systems was used for expression of GST-tagged proteins.

Cell culture reagents, cell lines and mammalian expression vectors

Dulbecco's Modified Eagle Media (DMEM) was purchased from Hi-media, India. Pen-Strep (Mixture of two antibiotics: Penicillin and Streptomycin), Phosphate buffered saline (PBS) and Trypsin-EDTA were obtained from Sigma-Aldrich, USA. Fetal bovine serum was purchased from Gibco-BRL, USA. DMSO for preservation of cell lines was purchased from Sigma-Aldrich, USA. Transfection reagent lipofectamine 3000 was bought from Invitrogen, USA. Cell culture plastic wares were obtained from BD Falcon, USA. All cell lines were obtained from National Centre for Cell Sciences, Pune, India. Expression vectors used in the studies were ORP150-pMD18-T (procured from Sinobiological), pCHA (from Prof. Uttam Pati), ORP150-pCHA (sub-cloned in lab),

pcDNA3.1 BACE1-FLAG (from Prof. Bart De Strooper), pcDNA3.1 APP-HA (from Dr. María), pcDNA3.1 CHIP-myc (from Dr. Suzanne), ORP150-EGFP (sub-cloned in lab), BACE1-DsRED Ex (sub-cloned in lab), GST-BACE1 (from Dr. Georges Levesque).

siRNA ORP150 construct

Mission e siRNA, poo l of s iRNA, targetted a gainst O RP150 and n egative c ontrol (scramble) siRNA was procured from Sigma Aldrich.

Table 1: Oligonucleotide's used in the study

S.No.	Oligo. Name (RS)	Oligonucleotide sequence (5'-3')	No. of bases	Purpose of use
1	ORP150 fwd (Nhe1)	CTAGCTAGCTATGGCAGACAAAGTTAGGAGGC	32	ORP150-pCHA Clone
2	ORP150 rev (Cla1)	CCCATCGATTAGTTCGTCGTTCTTCAAAGG	30	
3	ORP150 fwd (Nhe1)	CTAGCTAGCTATGGCAGACAAAGTTAGGAGGC	32	ORP150-EGFP clone
4	ORP150 rev (EcoR1)	CGGGAATTCTAGTTCGTCGTTCTTCAAAGG	31	
5	BACE1 fwd (EcoR1)	CGGAATTCATGGCCCAAGCCCTGCCC3	26	BACE1-DsRED Ex clone
6	BACE1 rev (Sal1)	ACGCGTCGACCTTCAGCAGGGAGATGTC	28	
7	BACE1 fwd	AGACGCTCAACATCCTGGTG	20	Real time
8	BACE1 rev	CCTGGGTGTTAGGGCACATAC	21	
9	ORP150 fwd	CCCTCGATAATCTCCTCAA	19	Real time
10	ORP150 rev	CTAACGTTGTCATCTCCAC	19	
11	GAPDH fwd	CCACTTTGTCAAGCTCATTTCC	22	Real time
12	GAPDH rev	CTCTCTTCCTCTTGTGCTCTTG	22	

The following samples were procured from Dr. S.K Shankar, NIMHANS, Bangalore and from SWDBB, UK.

Table 2: Patient Samples Used in the Study

S. No.	ID	PMI	Age / Sex	Diagnosis	Tissue region	Braak stage
1	BBN_9299	5.5	90 / M	CONTROL	Frontal Cortex	2
2	BBN_9408	42	87 / M	CONTROL	Frontal Cortex	2
3	BBN_9413	67	82 / M	CONTROL	Frontal Cortex	2
4	BBN_9429	57.5	74 / M	CONTROL	Frontal Cortex	0
5	BBN_19626	35.75	81 / M	CONTROL	Frontal Cortex	3
1'	BBN_8989	13	90 / M	AD	Frontal Cortex	3
2'	BBN_9275	36	87 / M	AD	Frontal Cortex	6
3'	BBN_26011	68.5	80 / M	AD	Frontal Cortex	4
4'	BBN_9148	55	74 / M	AD	Frontal Cortex	≤3
5'	BBN_9394	32	81 / M	AD	Frontal Cortex	4
6	08B203	20.3	77 / F	CONTROL	Temporal Cortex	-
7	08B203	20.3	77 / F	CONTROL	Frontal Cortex	-
8	BBN_9422	39.5	74 / F	CONTROL	Frontal Cortex	1
9	BBN_9399	50	73 / F	CONTROL	Frontal Cortex	2
10	BBN_8728	62	88 / F	CONTROL	Frontal Cortex	2
11	BBN_9365	32	86 / F	CONTROL	Frontal Cortex	2
12	BBN_8671	24	78 / F	CONTROL	Frontal Cortex	2
6'	15B271	4.36	92 / F	AD	Temporal Cortex	-
7'	15B271	4.36	92 / F	AD	Frontal Cortex	-
8'	BBN_9123	35	74 / F	AD	Frontal Cortex	3-4
9'	BBN_9371	50.5	73 / F	AD	Frontal Cortex	5
10'	BBN_9346	64	88 / F	AD	Frontal Cortex	6
11'	BBN_9173	31	86 / F	AD	Frontal Cortex	5
12'	BBN_9189	21	78 / F	AD	Frontal Cortex	6

Methods

Maintenance of mammalian cell lines and cell culture

HEK-293 and SHSY5Y cell lines were maintained for whole cell lysate preparations, cell biology experiments, and transfection experiments. The cells were grown in a CO_2 incubator at 37°C and 5% CO_2. The medium used for these cell lines was Dulbecco's modified eagle's medium (DMEM) supplemented with 10% Fetal Calf Serum (FCS). Trypsinization was done when confluency reached 90-100% for splitting of cells for further use. For trypsinization of the cell lines, the cells were first washed with 1X PBS. The cells were treated with 1X Trypsin-EDTA solution for 2 minutes in the 37°C incubator. After incubation, the cells were detached from the plate surface and trypsin-EDTA solution was neutralized by adding 1.0 mL of complete DMEM media to the plate. Cells were centrifuged and re-suspended in the complete media. Equal number of cells were added to fresh plates and then allowed to grow for further growth.

Generation of HEK293-BACE1 and HEK293-APP stable cell line

The HEK-293 cells stably expressing BACE1 and swAPP695 were generated as follows. HEK-293 cells were seeded on polylysine-coated 6-well plate. At 70% confluency, cells were independently transfected with 1 µg/well of linearised FLAG-BACE1 and pcDNA3.1 APP695 vector each using Lipofectamine 3000 reagent (Invitrogen). G418 (Calbiochem) was added at a concentration of 1000 µg/mL after 48 hours of transfection and drug resistant cells were collected after 2-3 weeks for single cell cloning, in which cells were diluted, and seeded in 96-well plates at one cell per well. Wells that contained more than one cell were marked and excluded from further investigation. Fifty per cent of the medium in each well was replaced twice a week. After 4-6 weeks, surviving clones reached confluency and were expanded for experiments and cryo-preservation. Resistant clones were analyzed by western blot to confirm the overexpression of BACE1 and FL-APP.

Preservation of cell lines

For the preservation of cell lines, freeze downs were prepared and stored at -80°C for short-term storage and at -196°C (liquid nitrogen) for long-term storage. Healthy growing cells were harvested at ~70-80% confluent stage for preservation. After trypsinization, cells were collected in a 15 mL centrifuge tube by centrifuging at 1,000 rpm for 3 minutes followed by thorough washing with 1X PBS. PBS was then removed and cells were re-suspended in the preservation solution containing 90% FCS and 10% DMSO and added to cryo-vials. The vials were immediately transferred to -80°C deep freezer/liquid nitrogen. For best revival efficiency ~ 1×10^6 cells were added per vial. After a week post storage, one freeze down per cell type was revived and checked for the cell viability.

Revival of mammalian cell lines

Cells were taken out from the liquid nitrogen cylinder, thawed at 37°C and added to falcon tube having 1.0 mL of complete DMEM media. The cells were centrifuged at 1,000 rpm for 3 minutes, the supernatant was discarded and the cells were washed with 1X PBS solution. Again cells were homogeneously re-suspended in 1.0 mL of complete media and plated in 60 mm petri-plates.

Transient transfections

Transient transfections were done using lipofectamine reagent (Invitrogen) according to manufacturer's protocol. A day before transfection, cells were trypsinized and then plated equally into culture plates. 24 hours later, on the day of transfection, cells were around 70-80% confluent. The required amount (1.0 μg) of DNA was suspended in 100 μL of incomplete medium and mixed with 1.0 μL of Plus reagent. After 5 minutes of incubation at room temperature 1.5 μL of lipofectamine was added to the mixture and was mixed again. Mixture was incubated for 15 minutes to form the complexes. When incubation period was over, transfection mixture was added to the petri-plates drop by drop; plates were rocked gently and kept in CO_2 incubator at 37°C. Cells were further allowed to grow and processed according to experiments.

Preparation of whole cell lysate

Cells were harvested and centrifuged at 7,000 rpm for 5 minutes. The pellet was washed with PBS and centrifuged at 7,000 rpm for 5 minutes. After decanting the supernatant, pellet was re-suspended in appropriate volume of RIPA lysis buffer (50 mM Tris, pH 7.4, 150 mM NaCl, 0.1% SDS, 1 mM EDTA, 1% Triton X-100, 1X PIC, 1.0 mM PMSF). It was incubated on ice for 15-20 minutes and then centrifuged at 13,000 rpm for 10 minutes. Supernatant was aliquoted in fresh tubes, and protein concentration of whole cell lysate was estimated using Bradford protein detection kit (BIO-RAD).

Preparation of human brain tissue lysate

25 mg cortex from each of an AD patient and an age-matched non-demented control was weighed, minced and collected in respective labelled eppendorf and 250 µL of RIPA lysis buffer was added to the tissue. Pippetting was performed for re-suspension of tissue. It was incubated on ice for 30-40 minutes and then centrifuged at 13,000 rpm for 20 minutes. Supernatant was aliquoted in fresh tubes, and protein concentration of whole tissue lysate was estimated using Bradford protein detection kit (BIO-RAD).

Quantitation of proteins using bio-rad protein assay kit

The BIO-RAD protein assay kit is based on the Bradford dye binding procedure (Bradford, 1976). The assay makes use of BSA as a protein standard. The micro assay was used here to detect protein in the range of 1.25 µg/mL to 25 µg/mL. Different concentrations of BSA ranging from 1.0 µg to 25 µg diluted in 800 µL miliQ water sample was taken. 200 µL of the BIO-RAD reagent was added to it and incubated for 15 minutes in dark. O.D. was taken immediately at 595 nm. The same procedure was performed for the cell lysates, tissue lyastes and recombinant protein samples. A standard linear curve was plotted for estimation of the cell/tissue lysates and recombinant proteins. The complex formed with the dye reagent is photosensitive and stable for a maximum period of 30 minutes.

Immunoprecipitation assay

Cells were harvested and lysed in NP-40 buffer (50 mM Tris-HCl pH 7.4, 150 mM NaCl, 1.0% NP-40, 1.0 mM PMSF, supplemented with protease inhibitor cocktail) at 4°C for 20 minutes. After centrifugation at 13,000 rpm supernatant was transferred to fresh tubes. 5% of whole cell lysate was used as input. About 1 mg of whole cell lysate was incubated with 1.0 µg of anti-BACE1 or anti-HA antibody and incubated for 3-4 hours at 4°C. 25 µL of protein A agarose (50%) was added to the lysate and further incubated at 4°C for 2 hours. Washing was done 5 times with NP-40 buffer. Immunocomplex was released by addition of SDS loading dye, boiled for 5 minutes and loaded to 10% SDS-PAGE. Transfer of proteins to nitrocellulose membrane was done and immune-blotted with target antibodies.

Western blotting

After protein samples were resolved on SDS-PAGE, gel was equilibrated with transfer buffer for 10 minutes, followed by transfer of proteins on to the nitrocellulose membrane by wet blot system (Bio-Rad). Post-transfer, membrane was transferred to blocking buffer (PBS containing 5% BSA, and 0.1% Tween-20) for 2 hours at room temperature. After incubation, blot was washed three times (5 minutes each) with wash buffer (PBS containing 0.1% Tween-20). Subsequently, the membrane was incubated with primary antibody diluted (1:2,000) in PBS containing 0.1% BSA and 0.05% Tween-20 for 2 hours followed by washing thrice (5 minutes each) with wash buffer. The membrane was then incubated with secondary antibody (1:10,000 dilution) conjugated to poly-horseradish peroxidase (HRP) for another 1 hour. After subsequent washing, blot was developed with ECL™ Western Blotting Detection Reagents.

For further detection of the GAPDH (loading control) in the lysates, the membrane was incubated with stripping buffer (62.5 mM Tris-HCl (pH 6.8), 2% SDS, and 100 mM β-mercaptoethanol) for 30 minutes at 50°C. The membrane was then washed three times with wash buffer and incubated with blocking buffer. After blocking, the membrane was re-incubated with anti-GAPDH antibodies (1:5,000 dilution), subsequently with HRP-conjugated anti-mouse antibodies (1:10,000 dilution) and treated as described previously. The intensity of bands was quantified using ImageJ densiometry software (NIH), USA.

ELISA for amyloid-beta (Aβ42) analysis

Cells (for intracellular Aβ42) and 10 mg of brain tissue were extracted overnight in 5 M guanidine-HCl at room temperature (RT). The lysate were further diluted 50-fold in BSAT-DPBS with 1X protease inhibitor cocktail (pierce), centrifuged at 16,000g for 20 minutes at 4°C. For extracellular Aβ42, conditioned media was TCA precipitated and re-suspended in BSAT-DPBS with 1X protease inhibitor cocktail (pierce). Total Aβ42 levels in diluted samples were determined using a human Aβ42-specific sandwich ELISA (Invitrogen, Carlsbad, CA) according to manufacturer's recommendations. In brief, cell lysates were loaded onto (N-terminal) antibody pre-coated ELISA plate which was further loaded with C-terminal specific amyloid antibody (rabbit) and incubated for 3 hours on shaking at room temperature. After incubation, solution was decanted and plate was washed thrice with wash buffer. After patting dry the plate on tissue, plate was loaded with HRP-conjugated detection antibody (anti-rabbit) and incubated for 30 minutes. After decanting the solution, plate was washed thrice with wash buffer. Chromogen TMB substrate was then added on to the wells and incubated for 20-30 minutes. Blue colour was developed where substrate i.e. amyloid β-42 was present. After 20-30 minutes, the reaction was stopped using stop solution and yellow colour developed. Absorbance was measured at 480 nm.

Cycloheximide (CHX) chase assay

HEK-293 cells were transfected with ORP150-HA along with an empty vector. After 16 hours of transfection, cells were treated with cycloheximide (CHX) (100 µg/mL) for the indicated time points (0, 3, 6, 9 and 12 hours) and samples were collected at these time points and were processed for western blotting. BACE1 and ORP150-HA protein level was detected by anti-BACE1 (M83) and anti-HA antibody.

RNA isolation and first strand cDNA synthesis

Expression of endogenous BACE1 transcripts in HEK293 cells were examined by real time PCR. HEK293 cells were transfected with BACE1 expression plasmids along with empty plasmid or increasing amount of ORP150. Total RNA was isolated by using Trizol reagent (Invitrogen) according to the manufacturer's instructions. Cells were harvested and the cell pellet was dissolved in 1 mL of Trizol reagent. After 5 minutes incubation at

room temperature, 200 µL of chloroform per ml of Trizol reagent was added to the samples and the tubes were vigorously shaken for 15 seconds and further incubated for 5 minutes at room temperature. Samples were centrifuged at 10,000 rpm for 10 minutes. After centrifugation, of the three visible layers, upper aqueous layer consisted RNA, middle layer consisted white precipitated DNA and bottom layer consisted organic phase and proteins. The upper aqueous layer containing RNA (which is about 60% of the trizol reagent used) was transferred to another fresh eppendorf tube. 500 µL of isopropanol per ml of Trizol reagent was added to the aqueous phase and mixed gently. After 15 minutes incubation, samples were centrifuged at 14,000 rpm for 25 minutes. Supernatant was discarded and pellet was washed with 1 mL of 70% ethanol and centrifuged for 5 minutes at 14,000 rpm at 4°C. Pellet was dried and dissolved in 50 µL RNase free water. The first strand cDNA was synthesized from 1 µg of total RNA using a cDNA synthesis kit (Verso, Thermo scientific) with an oligo dT primer according to the manufacturer's instructions. An appropriate volume of cDNA for each gene was determined during qPCR optimization.

cDNA thermal cycle conditions

	Temperature	Time	No. of cycles
Step 1 (cDNA synthesis)	42°C	30 minutes	1
Step 2 (Inactivation)	95°C	2 minutes	1

Real-Time PCR

Quantitative PCR reactions were performed on an Agilent Mx3000P, using SYBR-Green Master Mix (Dynamo Colorflash), Agilent 96 well optical reaction plates and Agilent optical adhesive plate sealers. All reactions were completed in triplicate. Each 20 µL PCR reaction contained 0.02 to 0.1 µg cDNA, 2X SYBR-Green Master Mix, and primers diluted to a final concentration of 0.5 µM. The following cycling parameters were used: 95°C for 7 minutes, followed by 40 cycles of 95°C for 10 seconds, an annealing of 58°C for 15 seconds and an extension temperature of 60°C for 15 seconds. During each cycle of the PCR the fluorescence emitted by the binding of SYBR-Green dye to the double stranded DNA produced in the reaction was measured. To confirm the specificity of the reactions, dissociation curves were constructed for each amplicon with a single cycle of

95°C f or 1 minute, 55°C f or 30 s econds a nd 95°C f or 30 s econds a fter P CR amplification.

Analysis of quantitative PCR

The S YBR-Green fluorescent spectra col lected during the PCR were analysed us ing the Sequence Detection System Software (Agilent). Firstly, background threshold levels were set at t he num ber of c ycles be fore an y S YBR-Green fluorescence w as de tected. The detection threshold was set at the point where the increase in SYBR-Green fluorescence became e xponential. Assuming s pecific amplification, the cycle num ber a t which t he sample's fluorescence intersected with the detection threshold, was directly proportional to the amount of DNA in the sample, and was expressed as C_T values. Method of relative quantification was employed to quantify PCR products.

Determination of t he r elative a bundance w as a chieved us ing a ubi quitously expressed gene (GAPDH) as a calibrator. Calibrator used in this thesis, and their primer sequences are listed in **Table 1**. This approach requires the calibrator/sample reactions to have the same am plification efficiency w hich was de termined by titr ating the c alibrator a nd sample 1,000 fold, where the gradient of the titration series equates to the amplification efficiency of the r eaction. Calibrator/sample pr imer pa irs w ith similar a mplification efficiencies (< 0.01) were used for further analysis.

The calculation for quantitation first determined the difference (ΔC_T) between the C_T values of the target and the calibrator:

$$C_T = C_T \text{ (target) - } C_T \text{ (calibrator)}$$

This va lue w as cal culated for each sample after which one s ample (either t ime = 0 for time c ourse experiments) w as de signated as t he r eference s ample. T he com parative ($\Delta\Delta C_T$) calculation was then used to determine the difference between each sample's ΔC_T and the reference's ΔC_T.

Comparative expression level = C_T (target) - C_T (reference)

Finally, t hese va lues w ere t ransformed t o absolute va lues us ing t he f ormula: A bsolute comparative expression level = $2^{-\Delta\Delta C_T}$

Confocal imaging and FRET

For confocal imaging of ORP150-EGFP and BACE1-DsRED Ex constructs, cells were grown in 35 mm plate on coverslip. The two plasmids were transfected individually and in 1:1 ratio of both. In another set, EGFP and DsRED plasmids were transfected for negative control experiment. 24 hours post-transfection, cells were fixed in 4% paraformaldehyde for 20 minutes, and after washing twice with PBS, nuclear staining was performed with DAPI. Coverslips were mounted on glass slide and cells were monitored by laser confocal microscope, Zeiss LSM510 for colocalization and FRET.

Images were captured for FRET calculations by sensitized emission. Three sets of images were captured: pure GFP channel image (Donor channel - Exc. 488nm/Emi. BP 505nm-530nm), Pure DsRED Ex channel image (Acceptor channel - Exc. 543nm /Emi. LP 560nm), and FRET channel image (FRET channel - Exc. 488nm and LP 560nm). Bleed-through of donor in acceptor channel and cross-excitation of acceptor by donor excitation wavelength was calculated using FRET analyzer plugin (Hachet-Haas et al. 2006) for Fiji software (https://imagej.nih.gov/ij/plugins). Only EGFP and DsRED Ex fluorophore constructs were used as negative control. FRET efficiency calculations were performed as mentioned below:

Donor Image In donor channel Exc. 488nm/Emi. BP 505nm-530nm $I^{D\,Pure}$	Acceptor Image In acceptor channel Exc. 543nm/Emi. LP 560nm $I^{A\,Pure}$	Raw FRET Image In FRET channel Exc. 488nm and LP 560nm $I^{Raw\,FRET}$

1) nFRET = $I^{Pure\,FRET}$ = $I^{Raw\,FRET}$ - [BT_D + CE_A]

Where, $I^{Pure\,FRET}$ is Intensity of Pure FRET image in FRET channel

$I^{Raw\,FRET}$ is Intensity of Raw FRET image in FRET channel

BT_D is Bleed through of Donor in acceptor channel

CE_A is Cross Excitation of Acceptor by donor excitation wavelength

The BT_D and CE_A were calculated separately using only Donor (GFP) and only Acceptor Ds-RED) constructs.

$$BT_D = \alpha \times [I^{D\ Pure}] \quad ; \quad \alpha = \frac{I^{D\ FRET}}{I^{D\ Pure}} \quad \text{of donor only sample}$$

Where, α is Bleed through coefficient

$I^{D\ FRET}$ is Intensity of donor in FRET channel

$I^{D\ pure}$ is Intensity of donor in donor channel

$$CE_A = \beta \times [I^{A\ Pure}] \quad ; \quad \beta = \frac{I^{A\ FRET}}{I^{A\ Pure}} \quad \text{of acceptor only sample}$$

Where, β is Cross excitiation coefficient

$I^{A\ FRET}$ is Intensity of acceptor in FRET channel

$I^{A\ pure}$ is Intensity of acceptor in acceptor channel

2)

$$\text{FRET efficiency} = \frac{nFRET}{I^{D\ Pure} + nFRET}$$

For calculations of FRET efficiency by acceptor photobleaching, BACE1 signal was approximately 95% bleached by 543 nm laser with 100% transmittance, a corresponding increase in ORP150 signal was measured. FRET eff. was calculated as below:

$$\text{FRET Efficiency} = \frac{I^D\ Prebleach - I^D\ Postbleach}{I^D\ Prebleach}$$

Where, $I^D\ Prebleach$ is Intensity of donor before bleaching Acceptor

$I^D\ Postbleach$ is Intensity of donor after bleaching Acceptor

Bacterial culture

All the bacterial cultures were grown in LB medium at 37°C with shaking in the presence of appropriate antibiotics. The medium was sterilized by autoclaving at pressure of 15

lbs/square inch for 15 minutes. For preserving the bacterial cultures, cells were allowed to grow in LB medium with appropriate antibiotic concentration. When the cells reached log phase, 500 µL of culture was added into the microcentrifuge tube containing 500 µL of 100% glycerol solution. The cells were vortexed thoroughly till the solution became homogeneous and stored at -80°C.

Preparation of competent cells

The *E. coli* (DH5α and BL21) competent cells were prepared with slight modifications in the standard protocol (Sambrook, 1989). The glycerol stock of *E. coli* was streaked on the LB agar plate using streak-plate method. A single colony was picked and inoculated in 10 mL of LB broth and incubated overnight at 37°C with shaking. After 16 hours, 500 µL of the culture was used as inoculum (1% final volume) for a 50 mL LB broth. The cells were grown to an OD_{600} of 0.3-0.5. The cells were chilled on ice and then transferred to a pre-chilled sterile oakridge tube under aseptic conditions. The cells were centrifuged at 4,000 rpm for 5 minutes at 4°C. The supernatant was discarded and the pellet was re-suspended in 25 mL of chilled 100 mM $CaCl_2$ and incubated on ice for 30 minutes. The cells were centrifuged again at 4,000 rpm for 5 minutes at 4°C. The pellet was re-suspended in 5 mL of 100 mM $CaCl_2$ and 50% glycerol was added to it to a final concentration of 15%. The cells were kept on ice for 2-3 hours and were finally stored at -80°C as 200 µL aliquots. For checking the efficiency of the cell, an aliquot was taken out the next day and transformed with 10 ng of a standard plasmid DNA. The efficiency of the competent cells was calculated as the number of transformants per microgram of the supercoiled plasmid DNA.

Transformation

A 200 µL aliquot of competent cells was thawed on ice. 10 ng of plasmid DNA was added to the thawed cells and incubated on ice for 30 minutes. The cells were given heat shock by keeping the tube containing cells in a water bath at 42°C for 45 seconds. The cells were immediately transferred onto ice for 2 minutes and 800 µL of autoclaved LB broth was added to it. The cells were kept on incubator shaker at 37°C for 1 hour. Out of one ml culture, 25 µL of cells were plated on a LB agar plate containing appropriate antibiotics for selection of transformants. The LB plate was incubated at 37°C for 12-16 hours.

Plasmid DNA isolation

Small-scale plasmid isolation (mini-prep)

Plasmids were isolated by Qiagen Miniprep plasmid isolation kits which are based on a modified alkaline lysis procedure, followed by binding of plasmid DNA to QIAGEN Anion-Exchange Resin under appropriate low-salt and pH conditions. RNA, proteins, dyes, and low-molecular-weight impurities are removed by a medium-salt wash. 5 mL of overnight grown (15-16 hours) bacterial culture was transferred to a microcentrifuge tube and centrifuged at 6,000 g for 15 minutes at 4°C. Supernatant was discarded and bacterial pellet was re-suspended in 300 µL of buffer P1 (containing RNaseA) and mixed by vortexing/pipetting up/down until no cell clumps remained. 300 µl of Buffer P2 was added, mixed thoroughly by vigorously inverting the sealed tube 4–6 times, and incubated at room temperature (15–25°C) for not more than 5 minutes. After that, 300 µL of buffer P3 was added to it, mixed immediately and thoroughly by vigorously inverting the tube 4-6 times and left on ice for 5 minutes. The tubes were spun at 4°C for 10 minutes at 13,000 rpm. The clear supernatant containing plasmid DNA was transferred and passed through the qiagen column by centrifugation at 10,000 rpm for 1 minute. The flow through was discarded. The plasmid containing column was washed with 750 µl of buffer PE and spun at 10,000 rpm for 1 minute. The flow through was discarded and the column was spun for another 1 minute to remove any residual buffer PE. EB buffer was added to the column for elution and the column was allowed to stand for 2-3 minutes and spun at 13,000 rpm for 2 minutes. The eluted plasmid was collected in a microcentrifuge tube. Plasmid DNA was run on 1% agarose gel at constant voltage of 75 volts and the DNA bands were visualized under UV trans-illuminator following EtBr staining.

Large scale plasmid isolation (midi-prep)

The large scale plasmid isolation was also done using the Qiagen Plasmid Midi Kit according to manufacturer's protocol. 25 mL of the overnight grown (16 hours) bacterial culture was transferred to an autoclaved oakridge tube and centrifuged at 6,000 rpm for 15 minutes at 4°C. The supernatant was discarded and the pellet was resuspended in 4 mL of Buffer P1 by vortexing. 4 mL of Buffer P2 was then added and mixed well by inverting 4-6 times and incubated at room temperature for 5 minutes. 4 mL of pre-chilled

Buffer P 3 was add ed and mixed by inve rting 4-6 t imes a nd i ncubated on i ce f or 15 minutes. The oakridge tube was then centrifuged at 12,000 r pm for 30 minutes at 4 °C. The supernatant was col lected and re-centrifuged a t 12,000 r pm for 30 minutes at 4 °C. Meanwhile, QIAGEN-tip 100 column was e quilibrated with 4 mL Buffer Q BT and allowed t o e mpty b y gravity f low. F inally, t he s upernatant w as c ollected a nd pa ssed through the QIAGEN - tip column and allowed to pass by gravity flow. The column was washed t hrice with 10 mL o f Buffer Q C. Finally the D NA w as e luted w ith 5 mL o f Buffer QF. DNA was precipitated by adding 0.7 volumes of iso-propanol and centrifuged immediately at 12,000 rpm for 30 minutes at 4°C. The supernatant was decanted and the pellet w as w ashed with 2 mL of pr e-chilled 70% ethanol b y c entrifugation a t 13,000 rpm for 10 minutes at 4°C. The pellet was air dried and re-dissolved in TE buffer.

Agarose gel electrophoresis and DNA quantitation

The agarose gel was made in 1X TAE buffer. The percentages of agarose gel varied from 0.8% to 1.2 % a ccording t o t he s ize o f t he D NA f ragments of i nterest t o be analyzed. Ethidium B romide w as added t o i t (from a s tock of 10 m g/mL i n w ater) t o a final concentration of 0.5 μg/mL. The agarose was dissolved by boiling and the solution was poured i n t he gel casting m ould and c ombs were i nserted. T hickness o f t he gel was approximately 3 -5mm. The gel w as a llowed to s olidify f or a pproximately 30 minut es. Meanwhile, 500 mL s olution of 1X TAE w as m ade and pour ed i nto the e lectrophoresis tank. The comb was removed carefully and the gel was kept in the electrophoresis tank. The D NA s ample s m ixed with tracking d ye were loaded i nto t he w ells a nd electrophoresis was carried out at constant voltage 60-75 V till bromophenol blue moved to a bout 2/3rd length of the gel. The b ands were then vi sualized under s hort wavelength UV transilluminator. For quantitation of the DNA by spectrophotometer, DNA was taken in a qua rtz cuve tte and m easured OD at 260 nm a nd 280 nm. 1.0 O D a t 260 nm equivalent to 50 μg/mL DNA concentration. The ratio of OD_{260}/ OD_{280} nm was taken to check the purity of the DNA preparation. The ratio of the protein free pure DNA ranges from 1.8-1.9.

Restriction enzyme digestion of DNA

Desired amount of plasmid DNA or PCR amplicons were taken and re-suspended in ddH$_2$O containing 1X restriction digestion buffer. Appropriate amount of enzyme was then added and the sample was incubated at the prescribed temperature. After completion of incubation, 3M NaOAc (Sodium acetate), pH 5.2 was added to the reaction mixture to a final concentration of 0.2 - 0.3 M. Then 2.5 volumes of ethanol was added and kept at -80°C for 30 -45 minutes to precipitate the DNA. The sample was then centrifuged at 14,000 rpm at 4°C for 30 minutes. It was then washed with 70% ethanol and the DNA pellet was allowed to air dry before proceeding to the next step of loading on the gel.

Phosphatase treatment

Calf Intestinal alkaline Phosphatase (CIAP) catalyzes the hydrolysis of 5'-phosphate groups from DNA, RNA and ribo- and deoxyribo-nucleoside triphosphates. It is used to deposphorylate restriction digested cloning vector to prevent self-ligation thus lowering background. 0.01 units/pmol of CIAP enzymes was used to dephosphorylate DNA ends, in a total reaction volume of 100 μL having 1X CIAP buffer. The sample was then incubated at 37°C for 30 minutes and the reaction was stopped by adding 2 μL of 0.5 M EDTA and heated at 65 °C for 10 minutes. The DNA was extracted with PCI (phenol:chloroform:isoamyl alcohol) and ethanol precipitated. The DNA pellet was dried and used for further experiments.

DNA extraction from agarose gels

Qiagen QIAquick gel extraction kit was used to extract PCR amplified products and restriction enzyme digested DNA fragments to obtain DNA free of all salts, proteins and other interfering agents. The purified DNA was then used for ligation and other purposes. For Gene-clean, desired DNA band was excised from the gel and put in a microcentrifuge tube. The weight of agarose piece was measured. Three volumes of buffer QG was added and the gel slice in the tube was heated at 50°C for 10 minutes (until the agarose slice dissolved). Once the gel was completely dissolved, one gel volume of isopropanol was added to the tube. The sample was then loaded onto the QIAquick column placed on 2 ml collection tube and centrifuged at 12000 rpm for 1 minute. The flow through was discarded. The column bound DNA was washed with 750 μl of buffer PE and centrifuged

for 1 minute. Flow through was discarded and column was centrifuged for an additional minute to remove any residual ethanol (of buffer PE). The QIAquick column was placed on a 1.5 ml microcentrifuge tube and DNA was eluted using EB buffer. The eluted DNA product was analyzed on agarose gel.

Ligation

Vector and insert DNA were digested with complementary restriction sites. The plasmid vector and insert were added in a molar ratio of 1:3 or 1:5 along with 1 μL of ligation buffer (10x) and 1 unit of T4 ligase in a total reaction volume of 10 μL. The reaction mixture was incubated for 16 hours at 16°C. The cohesive end ligation needs the final concentration of 1 mM ATP. After the completion of the incubation period, samples were transformed or stored at -20°C until further use.

Overexpression of the recombinant proteins

The expression plasmids containing the desired gene (10 ng) were transformed in competent *E. coli* BL21(DE3) cells. A single colony was picked from the plate and inoculated into fresh LB medium and incubated overnight at 37°C. From this overnight grown culture, LB flask was inoculated and incubated at 37°C for 3-4 hours till A_{600} reached 0.8 to 0.9. Cultures of GST-BACE1 as well as GST-only were induced with 0.5 mM IPTG for overexpression and incubated at 30°C for 4 hours. Expression was confirmed by lysis of 1.0 mL cell pellet with lysis buffer and loaded on 10-12% SDS-PAGE.

Purification of proteins by glutathione sepharose

For the purification of GST-tagged proteins, glutathione agarose affinity chromatography was used. The Glutathione Agarose beads were procured from Amersham Biosciences. The induced cell culture containing GST-tagged protein was centrifuged at 7,000 rpm at 4°C for 10 minutes to harvest the cells, the cell pellet was resuspended in lysis buffer (PBS pH-7.4, 0.1% Triton X-100 and 0.5 mM PMSF) and sonicated with 20 seconds on and 40 seconds off cycle till the lysate became clear. Cell lysate was centrifuged at 12,000 rpm at 4°C for 30 minutes to separate the soluble protein from the inclusion bodies and membrane fractions. The supernatant fraction was taken and passed through

the pre-packed lysis buffer equilibrated glutathione sepharose column for binding of the GST tagged protein to the glutathione sepharose beads. To remove the non-specifically adhered proteins, the column was washed with 10 bed volumes of lysis buffer 3-4 times. The elution of the proteins was done by passing the elution buffer (20 mM reduced glutathione in 50 mM Tris-HCl, pH 8.0) to the column and flow through was collected. The eluted protein was dialyzed against PBS (pH 7.4) for 4-5 hours to remove the reduced glutathione from the protein. The purification as well as the dialysis was done at 4°C.

Proteins	LB Broth	IPTG Concentration	Induced Temperature	Induced Time	Glutathione Concentration
GST-BACE1	1X	0.5 mM	30°C	4 hours	20 mM
GST-only	1X	0.5 mM	30°C	4 hours	20 mM

Sodium dodecyl sulphate-Polyacrylamide gel electrophoresis

Sodium dodecyl sulphate-Polyacrylamide gel (SDS-PAGE) was used for visualization of proteins showing overexpression, purification, protein-protein interactions and western blot studies. Different percentages of gel were used according to the size of proteins. Percentages of acrylamide in normal gels used for various studies were from 8 and 10%, and in gradient gels from 4% to 20%. Stacking gel used was either 4% or 5%. Samples were prepared in 4X SDS-loading dyes. Running buffer used was 1X Tris-glycine. The stock solutions of buffers used for the preparation of gel were 1.5 M Tris-HCl, pH 8.8 (for resolving) and 1.0 M Tris-HCl pH 6.8 (for stacking gel). The compositions of SDS-PAGE used in the study were as follows:

Composition of SDS-Polyacrylamide gel

Resolving gel (10 mL)

Components	4%	8%	10%	20%
MQ water	4.60 mL	4.00 mL	3.30 mL	0.6 mL
30% Acrylamide	2.70 mL	3.30 mL	4.00 mL	6.6 mL
1.5 M Tris-HCL (pH 8.8)	2.50 ml	2.50 mL	2.50 mL	2.6 mL
10% SDS	100 μL	100 μL	100 μL	100 μl
10% APS	100 μL	100 μL	100 μL	100 μl
10% APS	6 μL	4 μL	4 μL	4 μl

Stacking gel (5 ml)

Components	4 %
MQ water	3.56 mL
30% Acrylamide	0.67 mL
1.0 M Tris-Hcl (pH 6.8)	0.63 mL
10% SDS	50 μL
10% APS	50 μL
TEMED	5 μL

Coomassie blue staining

After running the gel, it was transferred to the Coomassie brilliant blue stain solution and incubated for 30 minutes with constant shaking at room temperature. Gel was then de-stained by placing it in the destain solution and incubating it at room temperature with constant shaking. Used de-stain was replaced with a fresh de-stain solution until the

background was cleared and the bands became evident.

GST pull down assay

1 mg of whole cell lysate prepared from ORP150 transfected HEK293 cells was incubated either with 5 μg of purified GST only or GST-BACE1 recombinant protein. After 1 hour incubation at 4°C, glutathione sepharose beads were added and further incubated for 3 hours at 4°C. After Incubation, beads were washed extensively five to six times with 1 ml of PBS (containing 0.01% Triton X-100) and complexes were eluted from the beads with elution buffer containing 10 mM reduced glutathione in 50 mM Tris HCl (pH 8.0). SDS loading dye was added to the eluted proteins, boiled for 5 minutes and subjected to SDS-PAGE analysis followed by western blotting with anti-ORP150 antibody and anti-GST antibody.

Statistical analysis

Data is presented as means and standard errors of the mean (SEMs, represented by error bars in histograms). Comparisons of the difference in mean of two groups (±SEM) were carried out using the Student's t-test. Comparisons were two-tailed. All statistical tests were carried out using SigmaPlot, version 11 statistics software where $P \leq 0.05$ was accepted as significant mean values (±SEM) for each experiment.

RESULTS

Results

β-secretase BACE1, i s a ke y e nzyme i nvolved i n t he a myloidogenic processing of Amyloid precursor protein (APP) and generation of toxic β-amyloid peptide; hence is a suitable dr ug ta rget f or tr eatment of A lzheimer's di sease (AD) (Ghosh e t al. 2014) . BACE1 expression level is tightly regulated in cells. Pathological s tructures, amyloid plaques and neurofibrillary t angles, t ypical of A D harbour molecular chaperones which are eminent r egulators o f pr oteins de trimental to Alzheimer's pr ogression (Koren et al. 2009). ORP150, a n E R-resident ch aperone, chaperones a num ber of glycosylated a nd secretory proteins (Lin et al. 1993, K uznetsov et al. 1997). mRNA levels of ORP150 are upregulated in cellular and transgenic mouse models of AD (Hoshino et al. 2007). It has already b een shown that cel lular chaperone, C-terminus of H SC70 Interacting P rotein (CHIP), stabilizes APP via CHIP-BACE1-p53 feedback loop (Singh and Pati, 2015).

In this study, the role of ORP150 was investigated in regulating cellular BACE1 levels and its β-processing activity over APP. Further, crosstalk between ORP150 and CHIP in regulating BACE1 l evels w as s tudied unde r s tress c onditions. L astly, t he e xpression profile of O RP150, C HIP, BACE1 a nd Aβ42 *in vivo* in cor tex of A D pa tients w as examined.

Effect of ORP150 on BACE1 levels and on BACE1-mediated APP-processing in HEK293 and Neuronal cells

I. Sub-cloning of ORP150 from pMD18-ORP150 construct into pCHA mammalian expression vector

To e xamine w hether O RP150 pl ays role i n regulating cellular BACE1 levels and BACE1-mediated APP pr ocessing, first HA-tagged ORP150 m ammalian e xpression vector was generated. ORP150 cDNA construct (3kb) was PCR amplified with specific primers by using pMD18-ORP150 as template and subsequently amplified PCR products were di gested with Nhe1 and Cla1 restriction e ndonucleases. Digested PCR pr oducts were then ligated on the same restriction sites (Nhe1 and Cla1) in pCHA plasmid. Ligated products were transformed in *E. coli* DH5α strain. Screening of clone was done by colony

PCR and positive clones were confirmed by restriction digestion, PCR amplification and sequencing **(Figure 1)**.
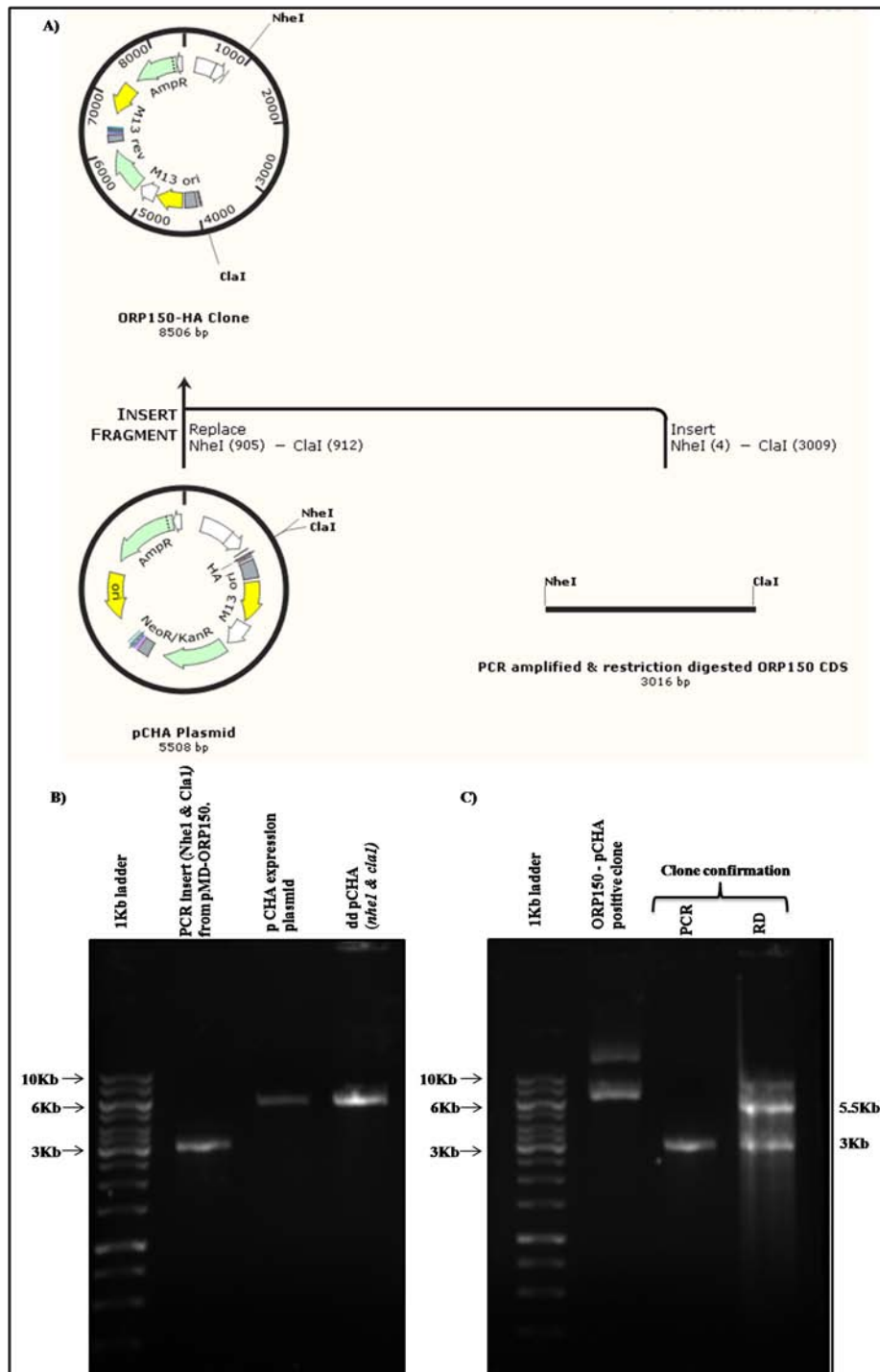
Figure 1: Construction of ORP150-HA mammalian expression vector. A) Schematic representation of cloning strategy of ORP150 cDNA in pCHA mammalian expression vector. **B)** PCR a mplicon e ncoding O RP150 c DNA w as a mplified f rom pM D18-ORP150 pl asmid a nd double digested (Nhe1/Cla1). pCHA ba ckbone vector was also double digested (Nhe1/Cla1). Each was purified for ligation **C)** Clone confirmation of ORP150 in pCHA vector was confirmed by PCR and by restriction digestion (Nhe1/Cla1) on 1% agarose.

II. Generation of HEK293-BACE1 and HEK293-APP stable cells

To analyze the effect of ORP150 on BACE1 levels and its functional activity upon APP, HEK293-BACE1 and HEK293-APP stable cells were generated by transfecting BACE1 and s wAPP695 pl asmid c onstructs i nto H EK293 c ells. E ach of H EK293-BACE1 and HEK293-APP stable cell lines were collected from respective single cell colony by using G418 a s s election a ntibiotic, r esistance t o which was conf erred by t he ne omycin resistance gene pr esent i n B ACE1 a nd A PP pl asmid c onstructs. C onfirmation of s table cells was performed by western blot using BACE1 and APP specific antibodies **(Figure 2– lane 2)**. HEK293 only cells were used as negative control **(Figure 2- lane 1)**.
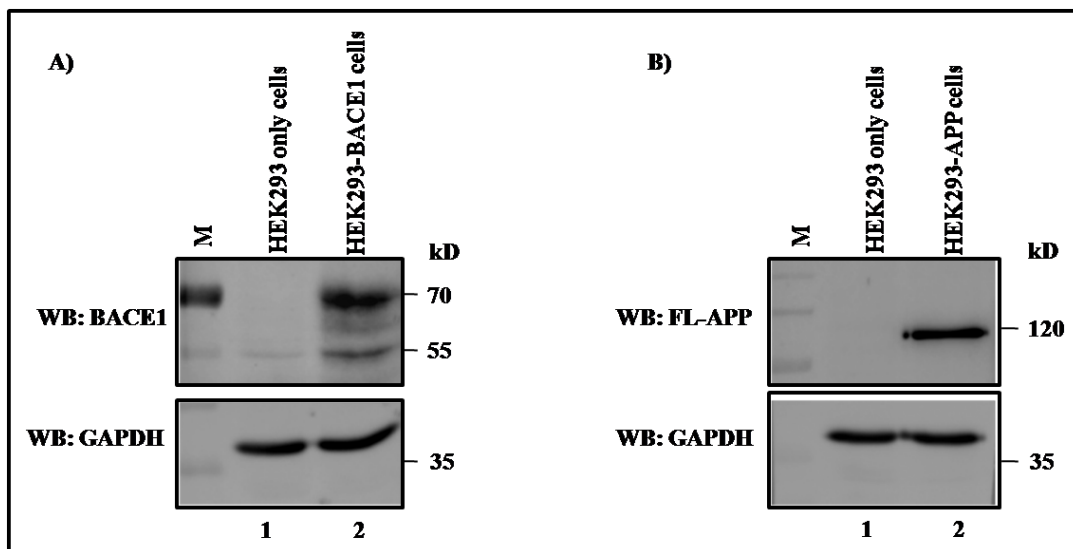
Figure 2: Generation of A) HEK293-BACE1 and B) HEK293-APP stable cells. HEK293-BACE1 stable and APP st able ce ll l ines w ere g enerated by t ransfecting H EK293 cells w ith BACE1-FLAG pl asmid and APP-HA plasmids r espectively. S election w as pe rformed us ing (1 mg/ml) G418 selection antibiotic. Western blot showing expression of BACE1 (A) and APP (B) in comparison to only HEK293 cells. M is protein molecular weight marker.

III. Effect of ORP150 on BACE1 level and BACE1-mediated APP processing in a dose-dependent manner

To determine the role of ORP150 in regulating BACE1 levels and BACE1-mediated APP processing, H EK293 c ells w ere t ransiently t ransfected w ith a c onstant a mount of expression vector encoding BACE1 along with an empty vector or HA-tagged ORP150. 24 hours post-transfection, cells were lysed in RIPA lysis buffer and western blotting was performed to analyze the expression of ORP150, BACE1 and GAPDH. Overexpression of ORP150 was found to increase ectopic expression of BACE1 by 1.5 fold in HEK293

cells **(Figure 3A – lane 2 and 1)**. APP is t he ke y s ubstrate of B ACE1 i nvolved i n amyloidogenesis. N ext t o de termine t he e ffect of O RP150 upon BACE1 a nd A PP, HEK293-BACE1 stable cells w ere co-transfected w ith a constant a mount of expression vector encoding swAPP695 along with an empty vector or HA-tagged ORP150. Western blotting w ith specific antibodies r evealed stabilization of B ACE1 by 1.5 f old a nd a corresponding decrease in the levels of FL-APP by 1.2 fold in the presence of ORP150 in HEK293-BACE1 stable cells **(Figure 3B – lane 2 and 1)**.
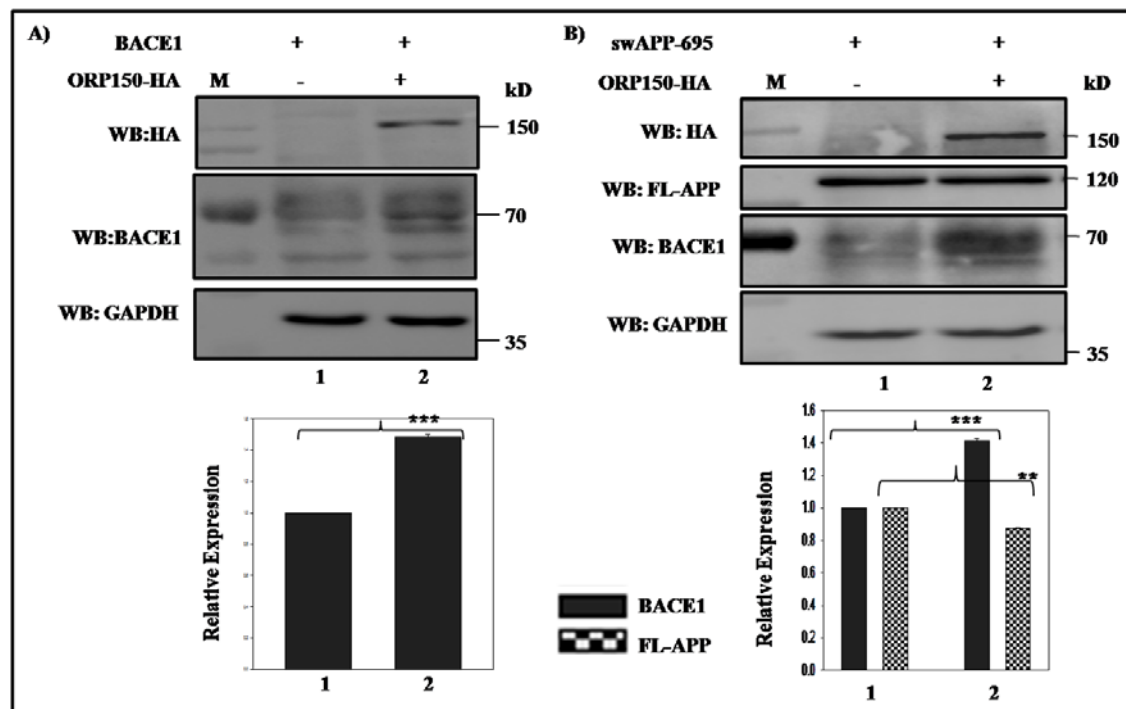
Figure 3: ORP150 stabilizes BACE1 levels both transiently in HEK293 cells and in HEK293-BACE1 stable cells. A) BACE1 was transiently co -expressed w ith o r w ithout ORP150-HA expression p lasmid in HEK293 c ells. Total a mount o f D NA f or transfection w as kept c onstant in e ach r eaction w ith e mpty vector. 24 hour s p ost-transfection, O RP150 a nd BACE1 expression were analyzed by western blotting. GAPDH was used as a loading control. **B)** Western blot analysis of BACE1 and FL-APP upon overexpression of ORP150-HA in HEK293-BACE1 stable cells. M is protein molecular weight marker. Data was expressed as mean ± SE from three independent experiments. Statistical analysis was performed by two-tailed t-test for the significance at the * $P \leq 0.05$, ** $P \leq 0.01$ and *** $P \leq 0.001$.

Next, to determine if O RP150 has a ny direct ef fect ov er F L-APP, HEK293-APP s table cells were transfected with empty vector or HA-tagged ORP150 both in the presence and absence of t ransiently t ransfected BACE1. Western blotting results de monstrated that ORP150 di d not directly affect t he l evels of F L-APP in the abs ence of B ACE1 i n HEK293-APP stable cells **(Figure 4 – lane 4 and 3)** but decreased FL-APP levels by 1.3

fold via stabilization of ectopic expression of BACE1 by 1.7 fold (**Figure 4 - lane 2 and 1**). This result suggests that ORP150 stabilizes BACE1 protein level in cells and hence enhances BACE1-mediated APP processing.
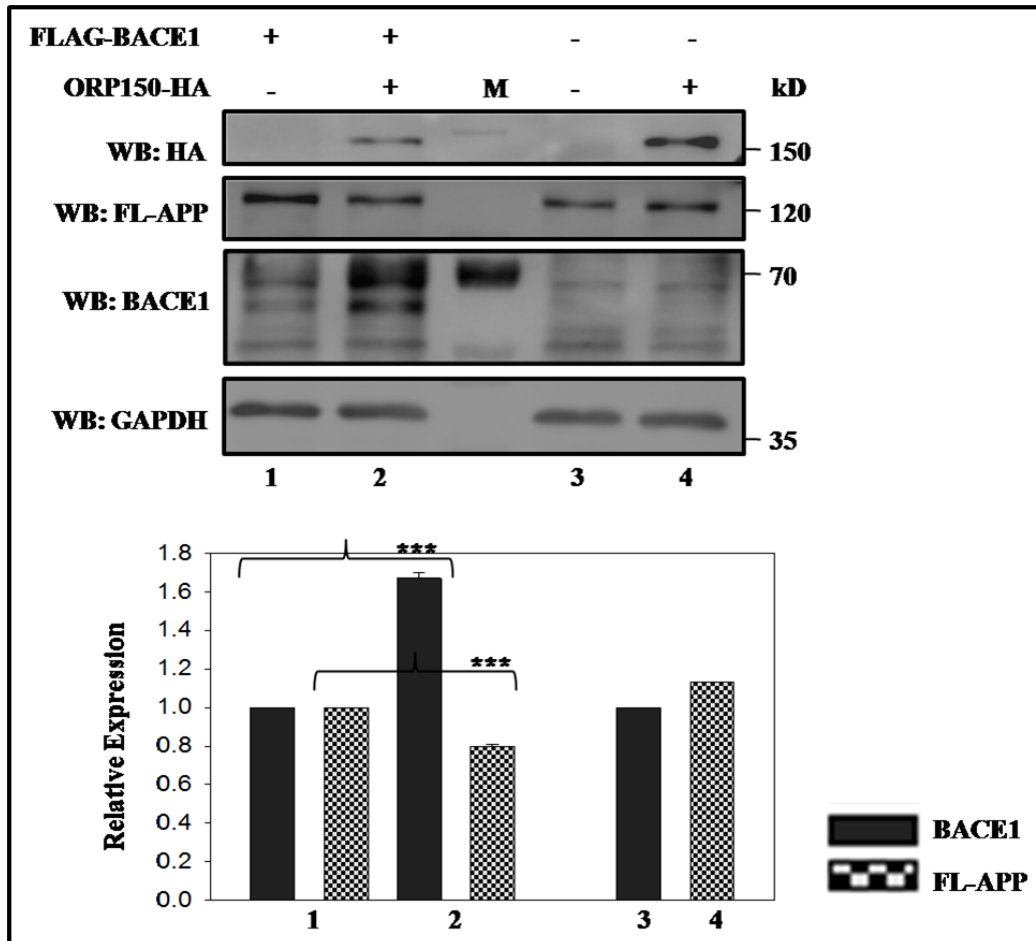
Figure 4: ORP150 decreases FL-APP only by stabilizing BACE1. HEK293-APP stable cells were t ransfected w ith O RP150-HA e xpression pl asmid both i n t he a bsence and pr esence of BACE1. 24 hours post-transfection, expression of ORP150, BACE1 and FL-APP were analyzed by w estern bl otting. GAPDH w as us ed as a loading cont rol. M i s protein molecular w eight marker. Data w as expr essed as m ean ± S E f rom t hree i ndependent expe riments. Statistical analysis was performed by two-tailed t-test for the significance at the * $P \leq 0.05$, ** $P \leq 0.01$ and *** $P \leq 0.001$.

BACE1-mediated A PP processing r esults i n generation of C -terminal fragment of 99 amino-acids (CTF99) which ultimately leads to toxic Amyloid beta42 (Aβ42) peptides. To examine whether ORP150 enhanced generation of CTF99 via BACE1 stabilization, HEK293-BACE1 stable cells were co-transfected with a constant amount of swAPP695 expression vector along with an increasing dose of HA-tagged ORP150. Western blot of whole cell lysate with anti-HA, anti-BACE1, anti-APP, anti-H43 antibodies demonstrated

that ORP150 stabilized BACE1 and subsequently deceased the levels of FL-APP each by 1.4 fold in a dose dependent manner (**Figure 5 – lane 4 and 1**). The levels of CTF99 (C99) fragment were also found to be increased by 1.4 fold with increasing dose of ORP150 (**Figure 5 – lane 7 and 5**). Thus, this data shows ORP150 promotes generation of CTF99 through β-processing of APP via BACE1 stabilization in HEK293 cells.
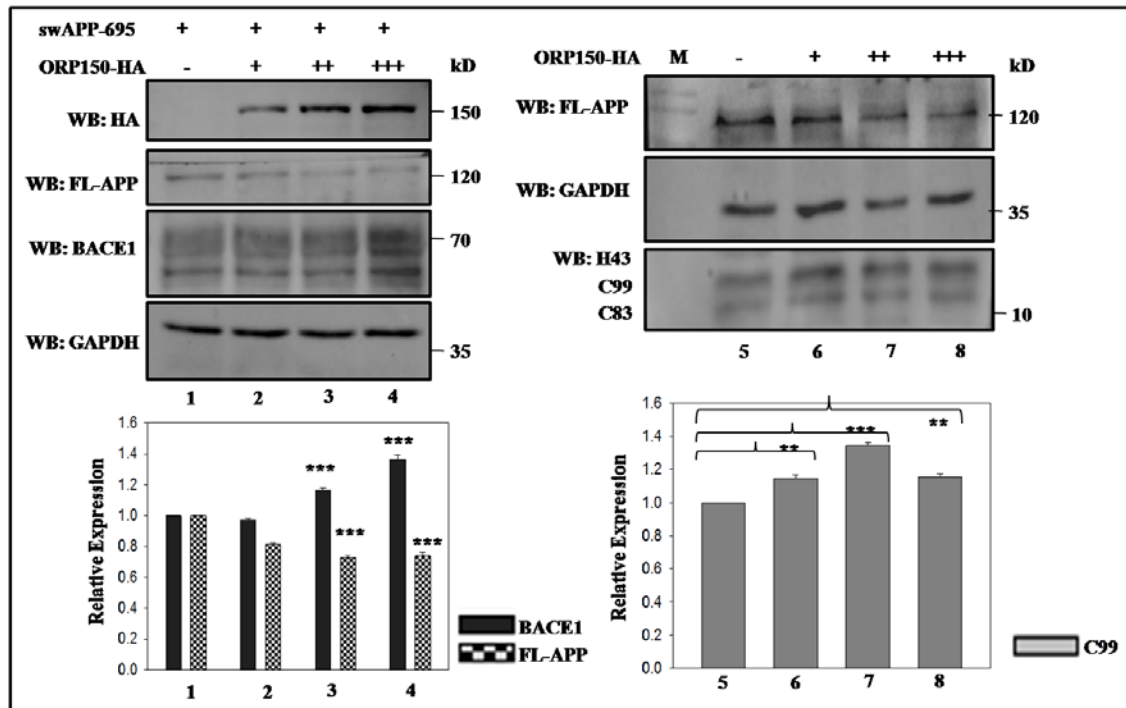
Figure 5: ORP150 promotes β-processing of APP via BACE1 stabilization in a dose dependent mannner. HEK293-BACE1 stable cells were co-transfected with swAPP-695 HA expression plasmid along with increasing amounts of ORP150-HA expression plasmid. After 24 hours of transfection, ORP150, BACE1, FL-APP, C99 levels were determined by western blotting. GAPDH was used as a loading control. M is protein molecular weight marker. Data was expressed as mean ± SE from three independent experiments. Statistical analysis was performed by two-tailed t-test for the significance at the * $P \leq 0.05$, ** $P \leq 0.01$ and *** $P \leq 0.001$.

Further, to study the effect of overexpression of ORP150 on endogenous BACE1 and APP levels, SHSY5Y neuroblastoma cells were transfected with an empty vector or HA–tagged ORP150. Western blotting with specific antibodies confirmed that overexpression of ORP150 stabilized endogenous BACE1 levels by 1.3 fold, reduced FL-APP by 1.9 fold (**Figure 6 – lane 2 and 1**) and subsequently increased C99 fragment by 1.2 fold in SHSY5Y neuroblastoma cells (**Figure 6 – lane 4 and 3**). This result suggests that overexpression of ORP150 increased endogenous level of BACE1 and promoted BACE1-mediated APP processing in neuroblastoma cells.
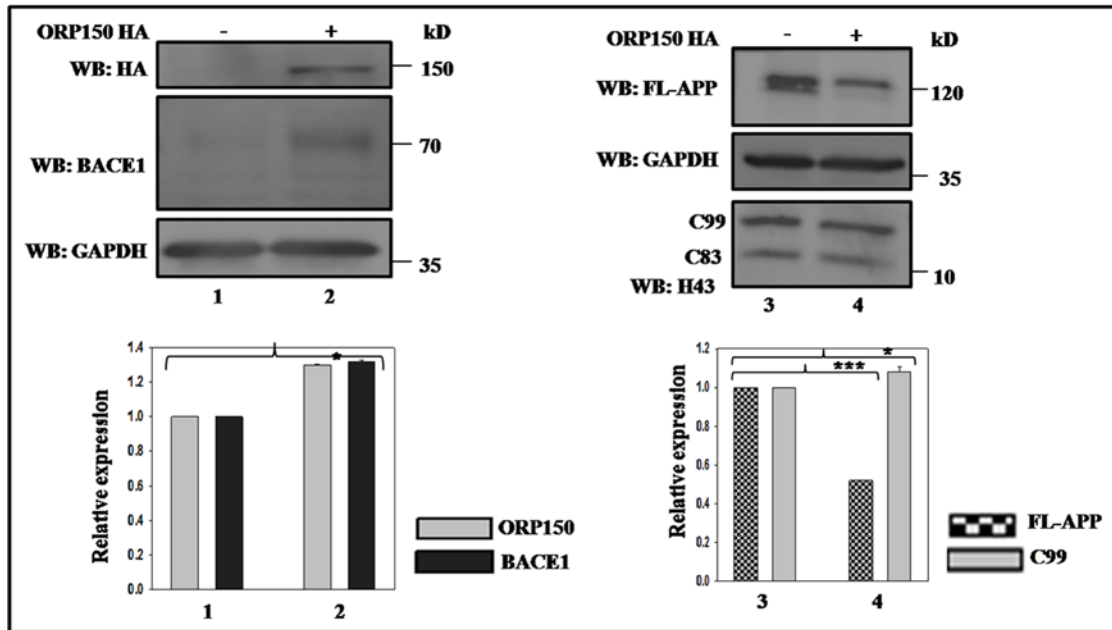
Figure 6: ORP150 promotes β-processing of APP via BACE1 stabilization in SHSY5Y neuroblastoma cells. SHSY5Y cells were transfected either with ORP150-HA or empty plasmid. After 24 hours of transfection, ORP150, BACE1, FL-APP, C99 levels were analyzed by western blotting. GAPDH was used as a loading control. Data was expressed as mean ± SE from three independent experiments. Statistical analysis was performed by two-tailed t-test for the significance at the * P ≤ 0.05, ** P ≤ 0.01 and *** P ≤ 0.001.

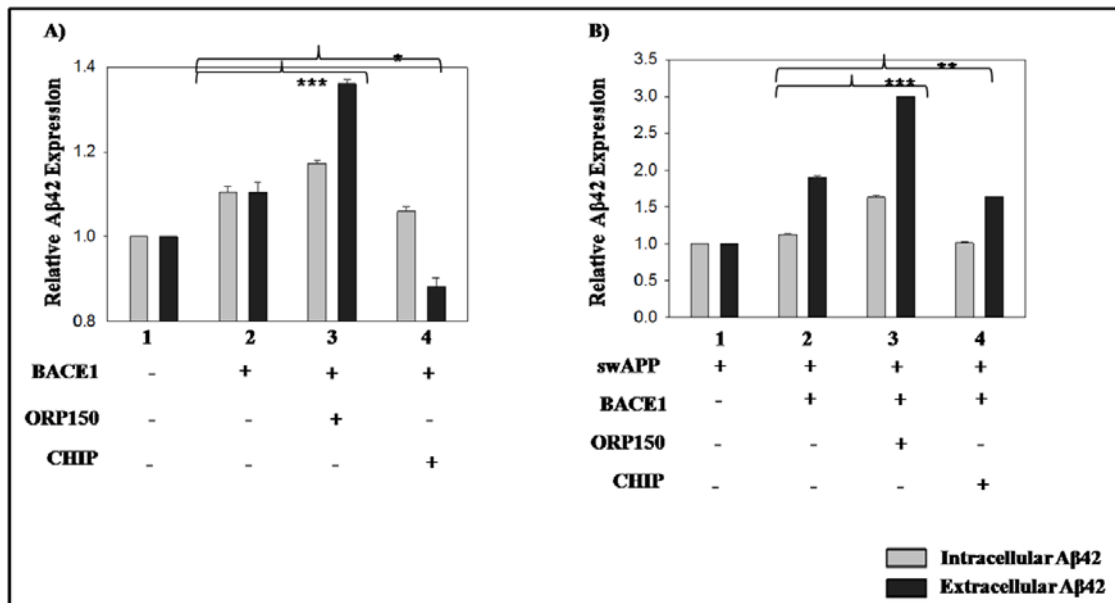Next, HEK-APP stable cells or SHSY5Y neuroblastoma cells transiently transfected with swAPP695 plasmid were used to examine the effect of overexpression of ORP150 on Aβ42 generation. Each cell type was transfected with an empty vector (negative control) and a constant amount of BACE1 expression plasmid. BACE1 transfection was accompanied either with an empty vector (positive control), HA-tagged ORP150 (experimental) or myc-tagged CHIP (experimental). 24 hours post-transfection, media was replaced with conditioned media for 18 hours. Cell lysate and conditioned media were used for estimation of intracellular and secreted extracellular Aβ42. ELISA confirmed an increase in the levels of both intracellular Aβ42 levels by 1.5 fold and extracellular Aβ42 levels by 1.6 fold in the presence of ORP150 (**Figure 7A and 7B-lane 3 and 2**). CHIP showed a decrease in the levels of both intracellular and extracellular Aβ42 each by 1.2 fold (**Figure 7A and 7B-lane 4 and 1**). Thus, this result confirms the role of ORP150 in promoting β-processing of APP and Aβ42 generation via BACE1 stabilization both in HEK293 cells and neuroblastoma cells.

Figure 7: ORP150 increased cellular Aβ42 levels while CHIP decreased Aβ42 levels both in HEK-APP stable and in SHSY5Y neuroblastoma cells. A) BACE1 was co-transfected either with empty plasmid or ORP150-HA or myc-CHIP in HEK293-APP stable cells. ELISA was performed to measure intracellular and extracellular Aβ42 levels. Only cells were used as a control. **B)** ELISA was similarly performed in SHSY5Y neuroblastoma cells transiently expressing swAPP695 plasmid. Data was expressed as mean ± SE from three independent experiments. Statistical analysis was performed by two-tailed t-test for the significance at the * P ≤ 0.05, ** P ≤ 0.01 and *** P ≤ 0.001.

IV. Effect of silencing of ORP150 on endogenous BACE1 level

Since ectopic expression of ORP150 stabilized endogenous BACE1 levels both in HEK293-BACE1 stable cells and in SHSY5Y neuroblastoma cells, it was next investigated whether the depletion of endogenous ORP150 destabilizes BACE1. To study this, siORP150 was transfected in a dose-dependent manner in HEK293-BACE1 stable cells. 72 hours post-transfection, cells were processed for mRNA and protein extraction. Real-time analysis confirmed the efficiency of siORP150 with nearly 80% silencing of ORP150 transcripts achieved with 1μg of siORP150 (**Figure 8**).

At protein level, silencing of ORP150 by 2.4 fold decreased the levels of BACE1 by 1.7 fold in a dose-dependent manner in HEK293-BACE1 stable cells. Scramble silencer was used as a control for the experiment (**Figure 9**).
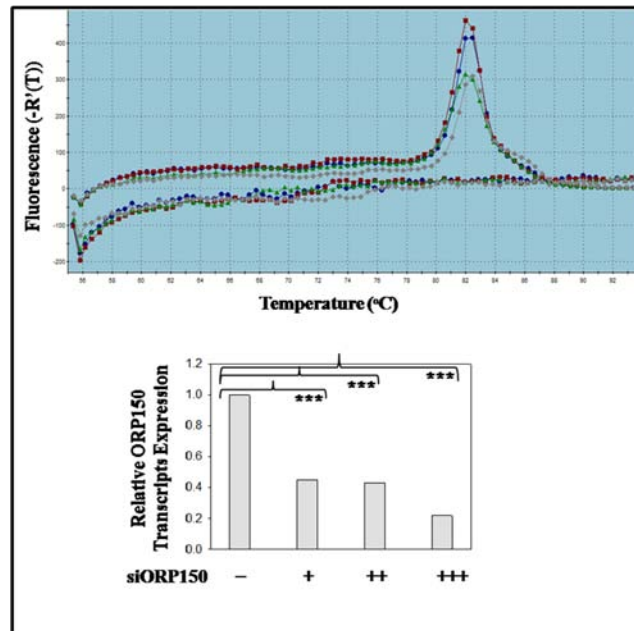
Figure 8: Silencing of ORP150 in HEK293-BACE1 stable cells. Increasing dose of siORP150 was t ransfected in HEK293-BACE1 stable cells. Relative O RP150 t ranscript levels w ere calculated no rmalized to GAPDH. Data w as exp ressed as m ean ± S E from t hree i ndependent experiments. Statistical a nalysis w as p erformed by t wo-tailed t-test for t he s ignificance at t he * P ≤ 0.05, ** P ≤ 0.01 and *** P ≤ 0.001.
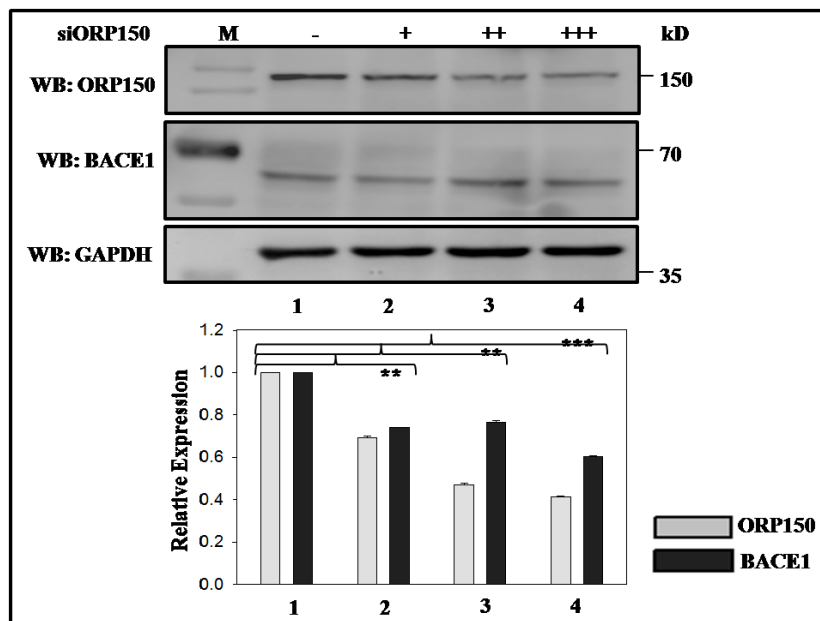
Figure 9: Silencing of ORP150 destabilizes BACE1 in HEK293-BACE1 stable cells. Increasing dos e of s iORP150 w as transfected i n H EK293-BACE1 stable c ells. Expression of ORP150 and BACE1 was analyzed by western blotting. GAPDH was used as a loading control. Data was expressed as mean ± SE from three independent experiments. M is protein molecular weight marker. Statistical analysis was performed by two-tailed t-test for the significance at the * P ≤ 0.05, ** P ≤ 0.01 and *** P ≤ 0.001.

Similarly, silencing of ORP150 by 1.3 fold in SHSY5Y neuroblastoma cells destabilized BACE1 by 1.2 fold when compared to scramble silencer control (**Figure 10 – lane 2 and 1**). Thus, this data validates that ORP150 stabilizes BACE1 in physiological conditions.
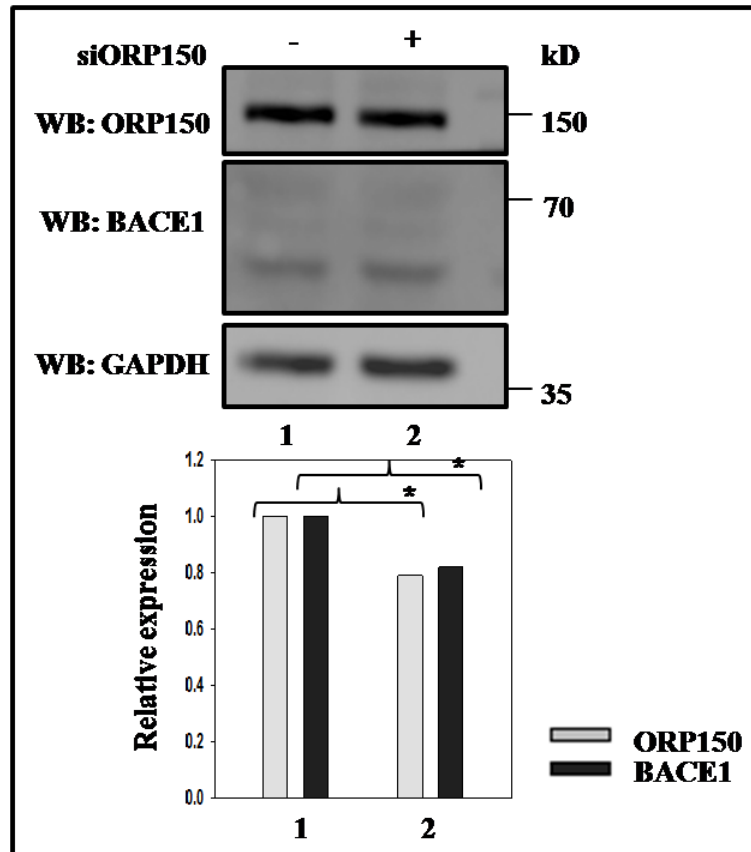
Figure 10: Silencing of ORP150 destabilizes BACE1 in SHSY5Y neuroblastoma cells. SHSY5Y ne uroblastoma cel ls w ere transfected with either Scramble si lencer or siORP150. Expression of ORP150 and BACE1 were analyzed by western blotting. GAPDH was used as a loading c ontrol. D ata w as e xpressed a s m ean ± SE f rom t hree i ndependent e xperiments. Statistical analysis was performed by two-tailed t-test for the significance at the * P ≤ 0.05, ** P ≤ 0.01 and *** P ≤ 0.001.

## V. Effect of ORP150 on BACE1 gene transcription

A l arge num ber of t ranscription factors (S p1, HIF1, Y Y1, NᵔB etc.) are known to regulate BACE1 at transcription level (Sastre et al. 2006; Zhang et al. 2007; Chami et al. 2012; Marwarha et al. 2013) . Having shown the stabilization of BACE1 by ORP150 at protein l evels, it w as next inve stigated whether ORP150 a lso r egulates B ACE1 gene transcription. For this, Real-time PCR was performed to analyze the transcript levels of BACE1 in the presence ORP150. HEK293 cells were transfected with increasing dose of ORP150. RNA isolation was performed using trizol reagent. Quality and purity of RNA

was c onfirmed b y a garose ge l e lectrophoresis a nd s pectrophotometrically respectively. cDNA was s ynthesized from tot al R NA b y reverse tr ansription kit (thermo-scientific). Real time P CR w as pe rformed in triplicate us ing cDNA, d ynamo SYBR green PCR Master M ix, a nd pr imers s pecific f or B ACE1, ORP150 a nd G APDH. Relative B ACE1 gene expression was calculated using the $2^{-\Delta\Delta CT}$ method, in which the relative amount of BACE1 m RNA e xpression l evel w as nor malized t o a n e ndogenous hous ekeeping gene (GAPDH). The result showed that ORP150 does not affect BACE1 transcripts level, not even i n a dos e de pendent m anner **(Figure 11)**. The experiment w as repeated 3 times. Thus, it can be concluded that ORP150, not being a transcription factor, does not regulate BACE1 t ranscription e ither di rectly or i ndirectly t hrough a ny ot her t ranscription f actor. Hence, this result indicates post-translational regulation of BACE1 by ORP150.
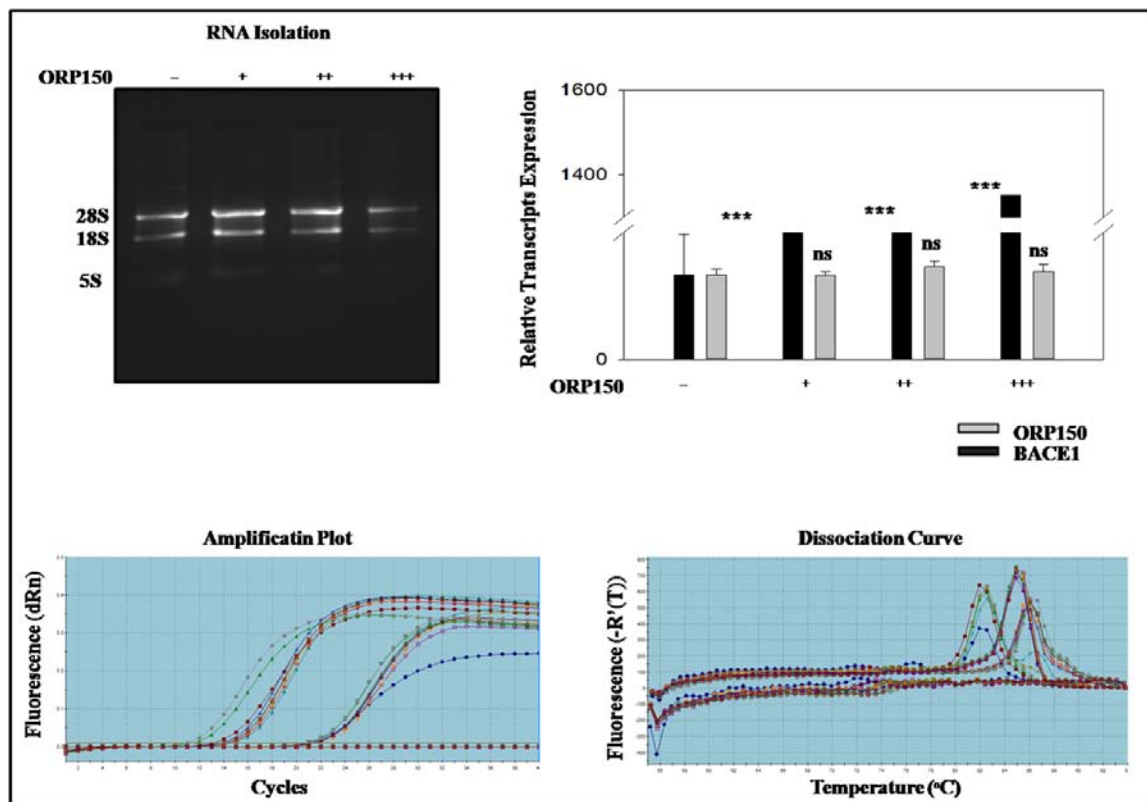
Figure 11: ORP150 does not affect BACE1 gene transcription. HEK293-cells were transfected w ith i ncreasing dos e of O RP150 e xpression pl asmid. The t otal a mount of D NA f or transfection was kept constant in each reaction with empty plasmid**.** Quantitative real time PCR analysis was performed on RNA samples. The endogenous BACE1 mRNA level was analyzed by quantitative real time PCR. GAPDH was used as internal control. Data was expressed as mean ± SE from three independent experiments. Statistical analysis was performed by two-tailed t-test for the significance at the * $P \le 0.05$, ** $P \le 0.01$ and *** $P \le 0.001$.

VI. Effect of ORP150 on BACE1 protein stability

To investigate the post-translational regulation of BACE1 by ORP150, cyclohexamide time-course experiment was performed to determine the half-life of BACE1 in the presence as well as absence of ORP150. HEK293-BACE1 stable cells were transiently transfected with HA-tagged ORP150 expression plasmid. After 16 hours of transfection, cells were treated with 100 μg/ml of cycloheximide (CHX) at an interval of every 3 hours up to 12 hours after which cells were collected at 12th hr and the protein level of BACE1 was estimated. As shown in **Figure 12**, the level of BACE1 and its rate of stabilization gets marginally increased in the presence of ORP150. The marginal increase could be a result of decrease in the level of ORP150 itself with CHX treatment. This result suggests that ORP150 promotes stabilization of BACE1 directly at the protein level.

Taken together, these observations suggest ORP150 enhances APP processing via stabilizing steady-state levels of BACE1, the rate limiting enzyme in the generation of Aβ biogenesis. Moreover, this chaperoning of BACE1 by ORP150 is a post-translational event.
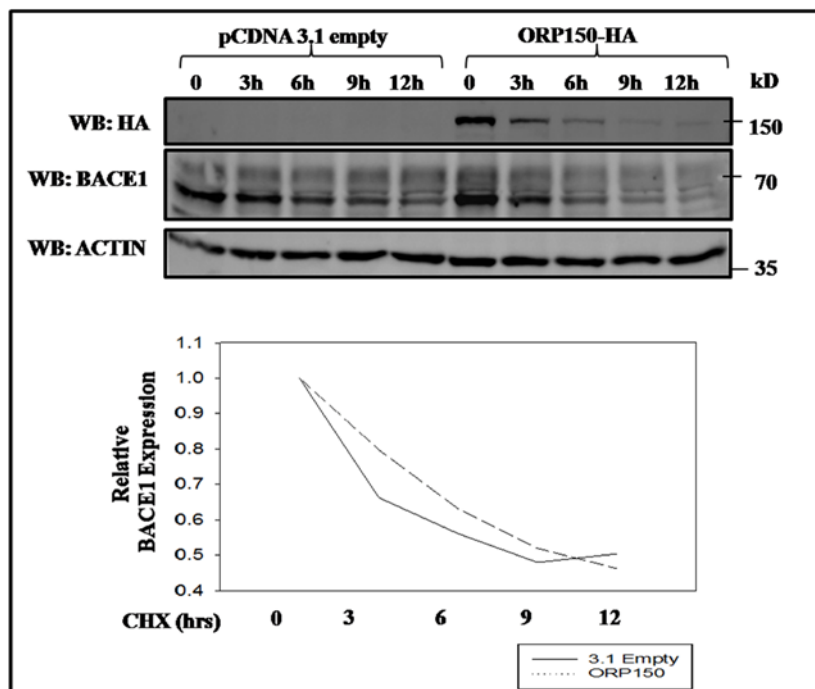
Figure 12: ORP150 stabilizes BACE1 by increasing its half life at the protein level. HEK293-BACE1 stable cells were transfected in the presence of ORP150. pcDNA3.1 empty was used as a transfection negative control. After 16 hours of transfection, cells were treated with 100 μg/ml of cyclohexamide (CHX) to inhibit protein synthesis. At indicated time points, cells were harvested and ORP150, BACE1 levels were analyzed. GAPDH was used as loading control.

47

Role of ORP150 on stress-mediated (oxidative stress, Endoplasmic Reticulum (ER)-stress, hypoxia) BACE1 regulation

A l arge num ber of cellular s tresses i ncluding o xidative s tress, E R s tress, h ypoxia are associated with AD effected brain (Jomova et al. 2010; M adeo et al. 2013; Rosini et al. 2013). B ACE1 i s t he ke y enzyme i nduced t ranscriptionally a nd t ranslationally und er these st ress c onditions (Chami a nd C hecler 201 2; M outon-liger et a l. 2012). Knowing ORP150 as an ER-resident stress-responsive pr otein, it was further investigated whether ORP150 r egulates BACE1 unde r varying physiological s tress c onditions. T o examine this, the cellular le vels of the two stress-responsive pr oteins, O RP150 and B ACE1 were first observed under varying stress conditions.

I. Expression profile of ORP150 and BACE1 under oxidative and ER stress conditions

For ox idative s tress, HEK293-BACE1 s table cells were treated w ith increasing dos e of cumene h ydroperoxide (CHP) - a pha rmacological ox idative s tress i nducer, at 100 a nd 200 μM f or 2 hours e ach. After t reatment, cells w ere ha rvested and ex amined for expression of endogenous ORP150 and BACE1. Immunoblotting with specific antibodies revealed a s ignificant increase in the levels of both ORP150 by 1.3 fold and BACE1 by 1.4 fold with increasing dose of cumene hydroperoxide **(Figure 13 – lane 3 and 1)**. This correlated expression profile of O RP150 a nd BACE1 unde r ox idative s tress c onditions indicates role of ORP150 in regulation of BACE1 expression in oxidative stress.
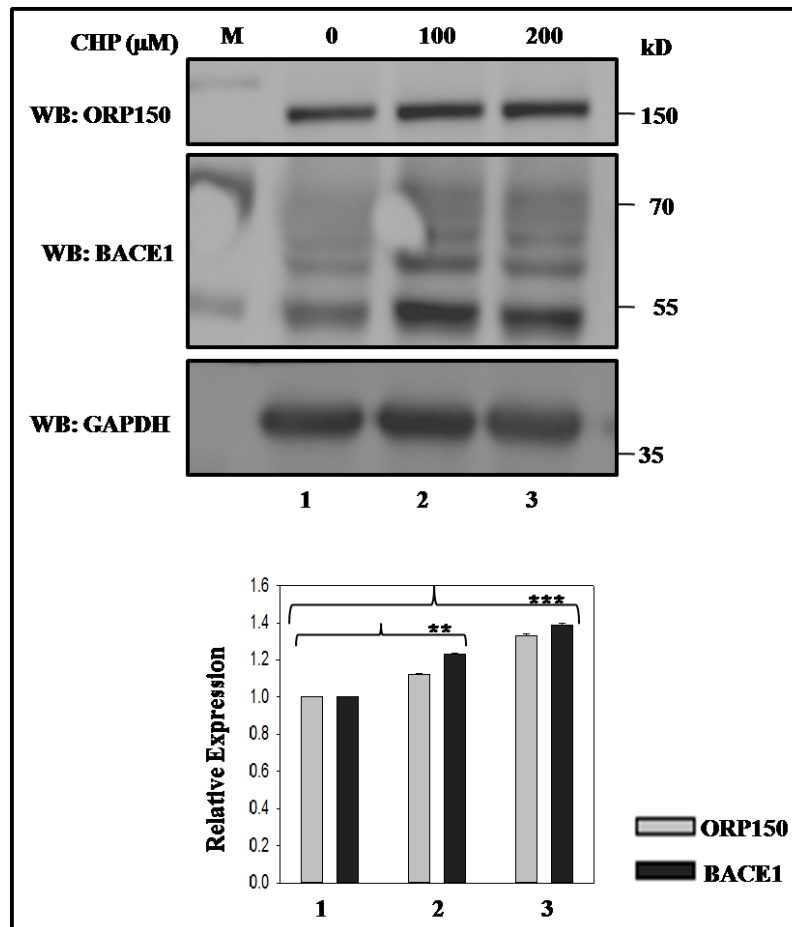
Figure 13: Increasing dose of oxidative stress increased the levels of both ORP150 and BACE1. Oxidative stress was induced in HEK293-BACE1 stable cells using cumene hydrogen peroxide (CHP) at increasing indicated doses for 2 hours each. Endogenous levels of ORP150 and BACE1 were analyzed by western blotting. GAPDH was used as a loading control. M is protein molecular weight marker. Data was expressed as mean ± SE from three independent experiments. Statistical analysis was performed by two-tailed t-test for the significance at the * P ≤ 0.05, ** P ≤ 0.01 and *** P ≤ 0.001.

For ER stress, HEK293-BACE1 stable cells were treated with increasing dose of tunicamycin (Tu) - a N-linked glycosylation inhibitor at a concentration for 4 and 10 μg/ml for 5 and 24 hours each. After treatment, cells were harvested and examined for expression of endogenous ORP150 and BACE1. GAPDH was used as a loading control. Immunoblotting with specific antibodies revealed significant decrease in N-linked glycosylated form of ORP150 by 1.5 fold at 24 hour time point for each of the two doses which coincided with a simultaneous significant decrease in BACE1 levels by 1.9 fold **(Figure 14, lane 2-3 and 1)**. GRP78 was used as a positive control in this experiment whose expression is known to be induced under ER stress. The decrease in BACE1 level

under ER stress is suggestive of either a UPR-mediated translational control response or decrease in BACE1 stabilization because of unglycosylated ORP150.
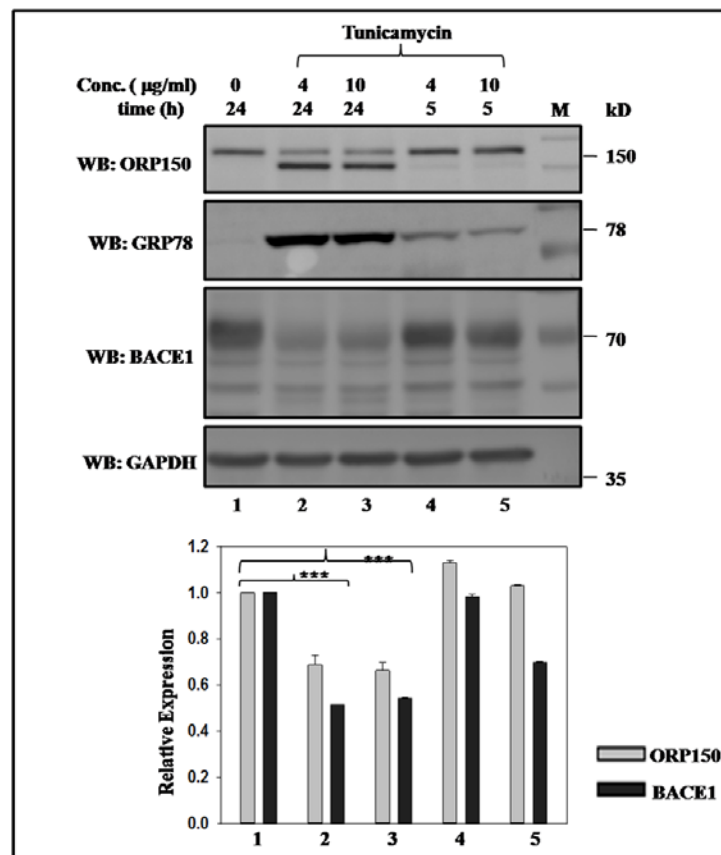
Figure 14: Inhibition of glycosylation of ORP150 correlated with reduced BACE1 levels under ER stress. Endoplasmic r eticulum st ress w as i nduced in HEK293-BACE1 stable ce lls using t unicamycin at 4 and 10 μg /ml e ach for 5 and 24 hours. Western b lotting was pe rformed with anti-ORP150, a nti-BACE1 (M83), a nti-GRP78 a nd anti-GAPDH a ntibodies. GRP78 was used as a positive control for the experiment. GAPDH was used as a l oading control. Data was expressed as m ean ± S E f rom t hree i ndependent ex periments. M i s protein molecular w eight marker. Statistical ana lysis was performed by t wo-tailed t-test for the significance at the * P ≤ 0.05, ** P ≤ 0.01 and *** P ≤ 0.001.

II. Role of ORP150 in BACE1 regulation under ER and oxidative stress conditions

Next s tep w as t o i nvestigate w hether O RP150 r egulates B ACE1 levels under E R and oxidative s tress conditions. To e xamine t his, HEK293-BACE1 stable cells were treated with scramble silencer or siORP150 for 72 hours and were kept under normal conditions, ER s tress [Tunicamycin - 4 μg/ml f or 24 hours] a nd ox idative s tress [cumenehydroperoxide – 200 μM for 2 hours]. After treatment for respective time-points, cells w ere ha rvested and endogenous l evels of ORP150 and B ACE1 were monitored by

western blotting with respective antibodies. Silencing of endogenous ORP150 by 2.1 fold reduced BACE1 levels significantly by 1.7 fold under normal conditions **(Figure 15, lane 2 and 1)**. Cells transfected with scramble silencer and subsequently treated with tunicamycin showed reduction in the levels of BACE1 by 1.6 fold **(Figure 15, lane 3 and 1)**. However, silencing of ORP150 and subsequent treatment with tunicamycin reduced BACE1 levels further to 2.5 fold **(Figure 15, lane 4 and 1)**. Thus, this result indicates ORP150 regulates BACE1 under ER-stress condition where N-linked glycosylation of ORP150 is required for BACE1 stabilization. Also, silencing of ORP150 under oxidative stress conditions reduced BACE1 levels to normal levels compared to 1.3 fold increase under oxidative stress and scramble silencer **(Figure 15, lane 6 and 5)**. Consequently, these results suggest that ORP150 might be regulating BACE1 levels in the stressed environment in Alzheimer's disease.
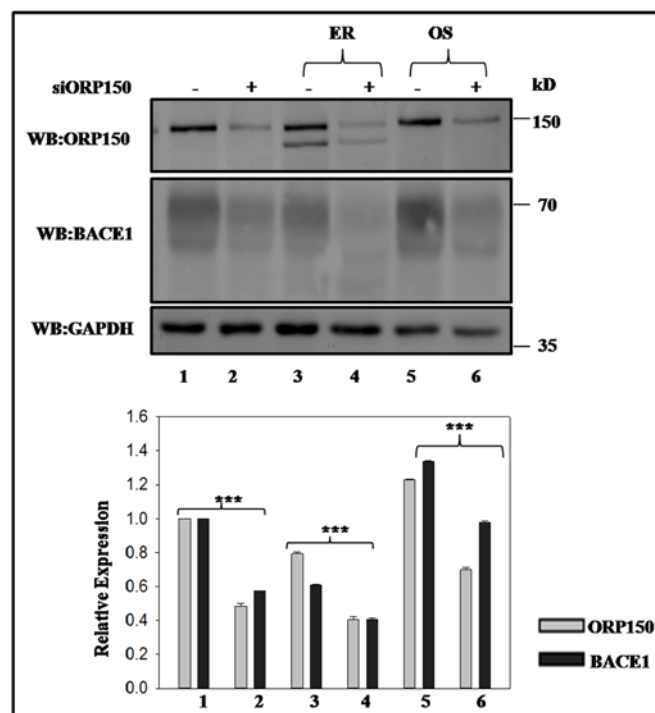
Figure 15: ORP150 regulates BACE1 under Endoplasmic Reticulum (ER) and oxidative stress (OS) conditions. HEK293-BACE1 stable cells were transfected with scramble silencer or siORP150 for 72 hours and the pair was further either kept untreated or treated with tunicamycin (4 μg/ml for 24 hours) for ER stress or with CHP (200 μM for 2 hours) for OS for respective time points. Respective levels of ORP150 and BACE1 were analyzed by western blotting. GAPDH was used as a loading control. Data was expressed as mean ± SE from three independent experiments. Statistical analysis was performed by two-tailed t-test for the significance at the * P ≤ 0.05, ** P ≤ 0.01 and *** P ≤ 0.001.

III. Role of ORP150 in BACE1 regulation under hypoxia

Hypoxia is another major factor predisposing an ageing brain to AD. Previous studies have shown hypoxia increased amyloid biogenesis by alteration in BACE1 and Y-secretase-mediated amyloidogenic processing of APP (Gugleilmotto and Aragno 2009; Guglielmotto et al. 2009; Koike et al. 2010; Zhang et al. 2007). Thus, it was investigated next whether ORP150 also contributes to hypoxia-induced BACE1 stabilization. To study this, HEK293-BACE1 stable cells were exposed to 0.1% oxygen **(Figure 16A)** and 1% oxygen **(Figure 16B)** maintained through a hypoxic chamber in a time-dependent manner up to 72 hours followed by 24 hours of re-oxygenation. After treatment for respective time points, cells were harvested and endogenous levels of ORP150 and BACE1 were monitored. GAPDH was used as loading control. Western blotting with respective antibodies revealed a constant increase in BACE1 levels by 2.8 fold at 0.1% oxygen up to 72 hours followed by an increase at 24 hour re-oxygenation by 3.7 fold. However, levels of ORP150 decreased by 1.3 fold at 0.1% oxygen with increase in time until re-oxygenation **(Figure 16A).** Also, at 1% oxygen, levels of ORP150 showed a constant fall by 2.7 fold while there was no constant pattern for BACE1 expression which showed increase by 1.2 fold at 24 hours of hypoxic exposure **(Figure 16B)**. Thus, ORP150 did not show a direct relation with BACE1 under hypoxia which suggests that unlike ER and OS, ORP150 might not be playing any role in BACE1 stabilization under hypoxic conditions. Recently involvement of CHIP-p53 loop has been shown in BACE1 destabilization (Singh and Pati 2015). Also, previous publications have shown HIF1α as a positive regulator in hypoxic induction of BACE1 (Guglielmotto et al. 2009). Thus, we next examined the levels of p53, CHIP and HIF1α at 0.1 and 1% of oxygen. On probing with respective antibodies, we found levels of p53 to be decreased under both low oxygen concentrations up to 72 hours while CHIP levels remained unchanged. HIF1α showed a constant increase by 2 fold at 0.1% oxygen and 1.5 fold peak at 48 hours of hypoxic exposure to 1% oxygen. Thus, this data suggests that increase in BACE1 under low concentrations of oxygen might be regulated by both increase in HIF1α levels (positive regulator of BACE1) and decrease in p53 levels (negative regulator of BACE1).
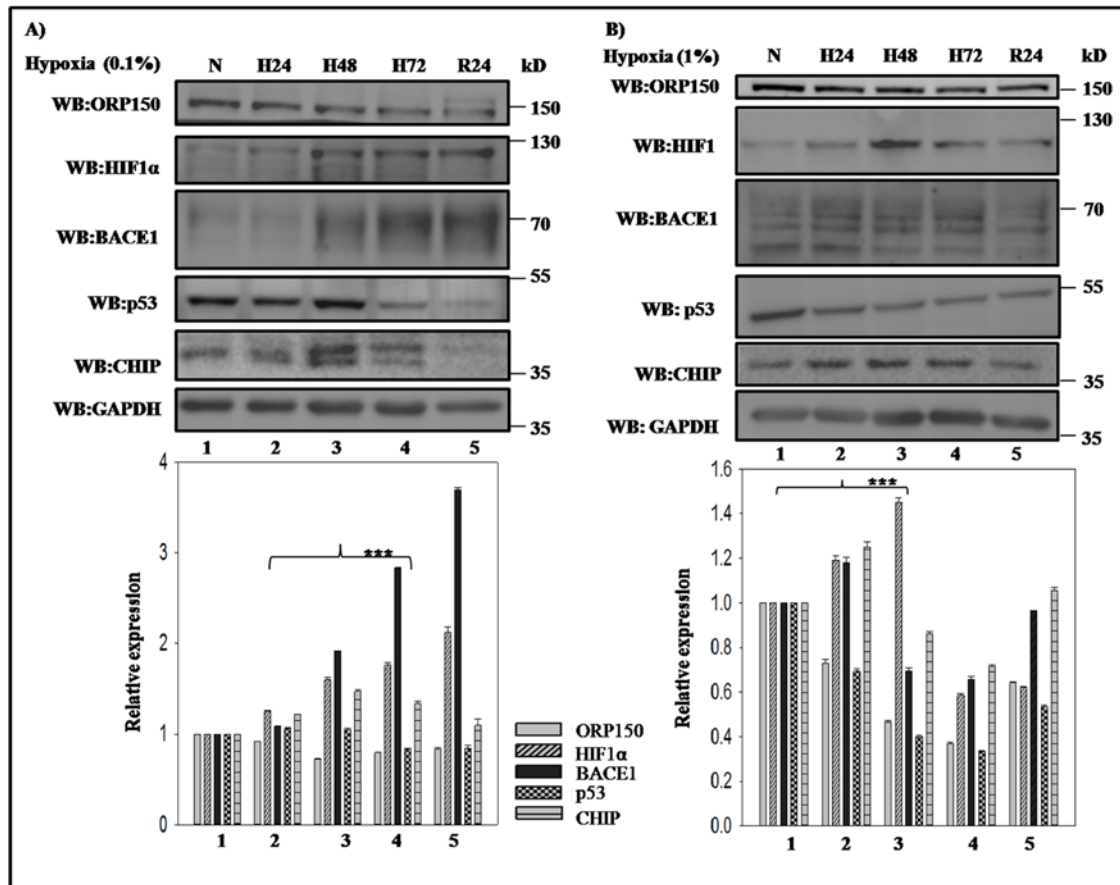
Figure 16: Unlike ER and OS, ORP150 did not show direct relation with BACE1 levels in hypoxic stress. HEK293-BACE1 stable cells were either kept under normal condition (N) or at 0.1% hypoxia (A) or at 1% hypoxia (B) for increasing time up to 72 hours (H24, H48, H72) followed by 24 hours re-oxygenation (R24). Expression of ORP150, HIF1α, BACE1, p53 and CHIP were analyzed by western blotting. GAPDH was used as a loading control. Data was expressed as mean ± SE from three independent experiments. Statistical analysis was performed by two-tailed t-test for the significance at the * $P \leq 0.05$, ** $P \leq 0.01$ and *** $P \leq 0.001$.

Studies on interaction between ORP150 and BACE1

The chaperoning activity of ORP150 has been observed with its role in ER to Golgi transport of newly synthesized proteins (including GP80 and VEGF), thus facilitating their maturation and secretion (Bando et al. 2000; Ozawa et al. 2001). Upon observing a synchronised expression of ORP150 and BACE1 in cellular stressed conditions as well as stabilization of cellular BACE1 by ORP150, it was next investigated whether ORP150 interacts with BACE1 in cell.

I. Subcloning of ORP150 and BACE1 into EGFP and dsRED mammalian fluorescent expression plasmids

To study the subcellular localization of the two proteins, ORP150 and BACE1, their cDNA were sub-cloned into EGFP and DsRED Ex mammalian fluorescent expression vectors respectively. ORP150 cDNA (3kb) and BACE1 cDNA (1.5Kb) were PCR amplified with specific primers by using pCHA-ORP150 and FLAG-BACE1 as template respectively. Amplified PCR products were digested with Nhe1/EcoR1 and EcoR1/Sal1 restriction endonucleases respectively. Digested PCR products were then ligated on the same respective restriction sites in EGFP and dsRED mammalian fluorescent expression vectors which were also respectively digested with Nhe1/Ecor1 and EcoR1/Sal1 restriction enzymes. Ligated products were transformed in *E. coli* DH5α strain. Screening of clones was done by colony PCR and positive clones were confirmed by restriction digestion, PCR amplification and sequencing (**Figure 17**).
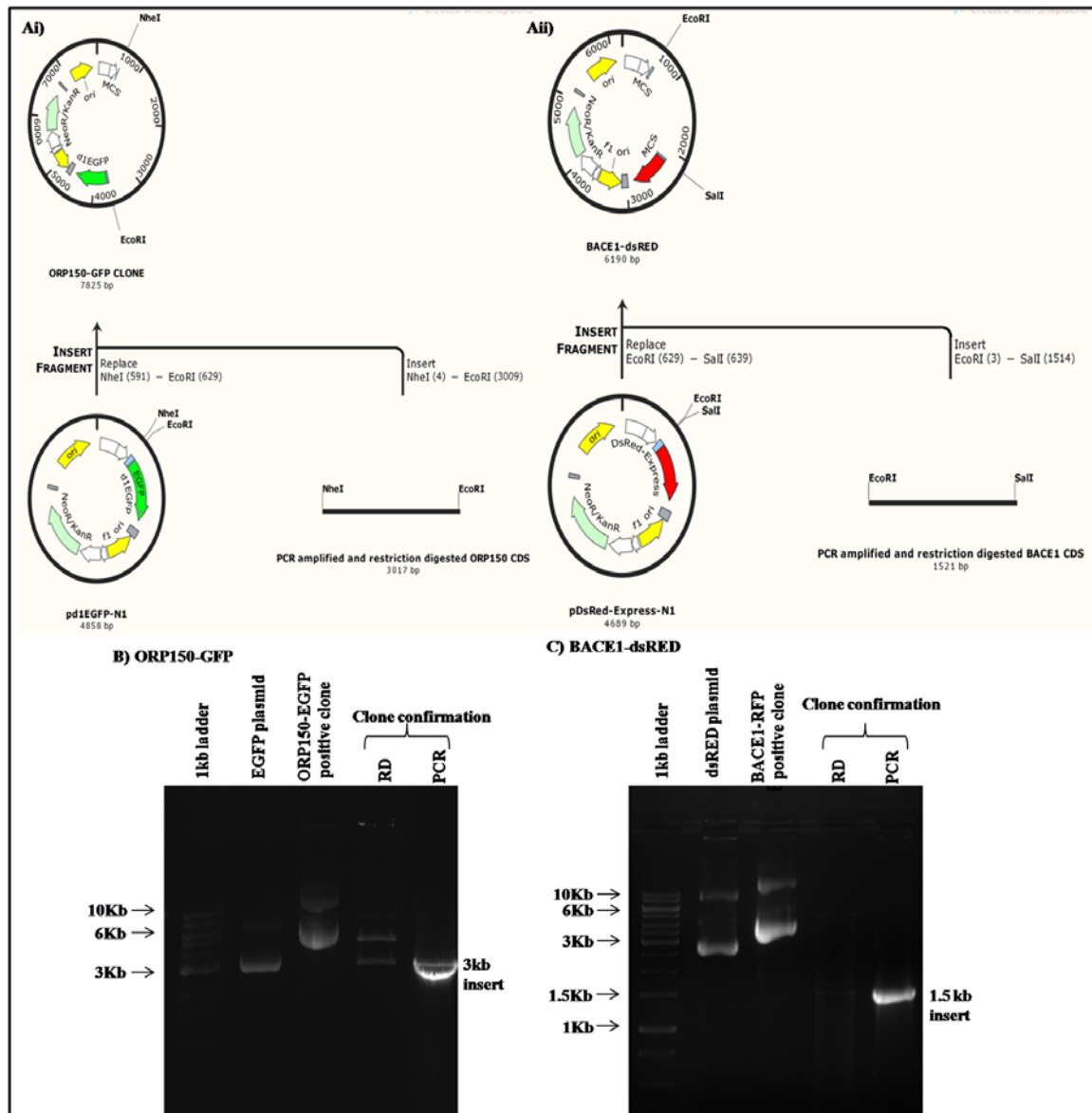
Figure 17: Construction of ORP150-GFP and BACE1-DsRED Ex mammalian fluorescent expression vectors A) Schematic representation of cloning strategy of ORP150 cDNA (Ai) in EGFP and BACE1 cDNA (Aii) in DsRED Ex fluorescent expression vectors. **B)** Clone confirmation of ORP150 in EGFP vector confirmed by PCR and insert fall by restriction digestion (Nhe1/Ecor1) on 1% agarose. **C)** Clone confirmation of BACE1 in DsRED Ex vector confirmed by PCR and by restriction digestion (EcoR1/Sal1) on 1% agarose.

II. Subcellular colocalization and FRET between ectopic ORP150-GFP and BACE1-DsRED Ex in HEK293 cells

To study the subcellular localization and interaction between ORP150 and BACE1 through FRET, ORP150-EGFP and BACE1-DsRED Ex expression vectors were co-transfected transiently in HEK293 cells. 24 hours post-transfection, cells were fixed and images were captured using confocal microscope. Both ORP150 (green) and BACE1

(red) l ocalized j ust out side t he nuc leus, w hich pos sibly i s a n e ndoplasmic r eticulum. Colocalization of the two proteins can be seen from the yellow signal in the merged image **(Figure 18A)**. Only EGFP and DsRED constructs were used as negative control **(Figure 18B)**. FRET efficiency was calculated as described in Materials and Methods.
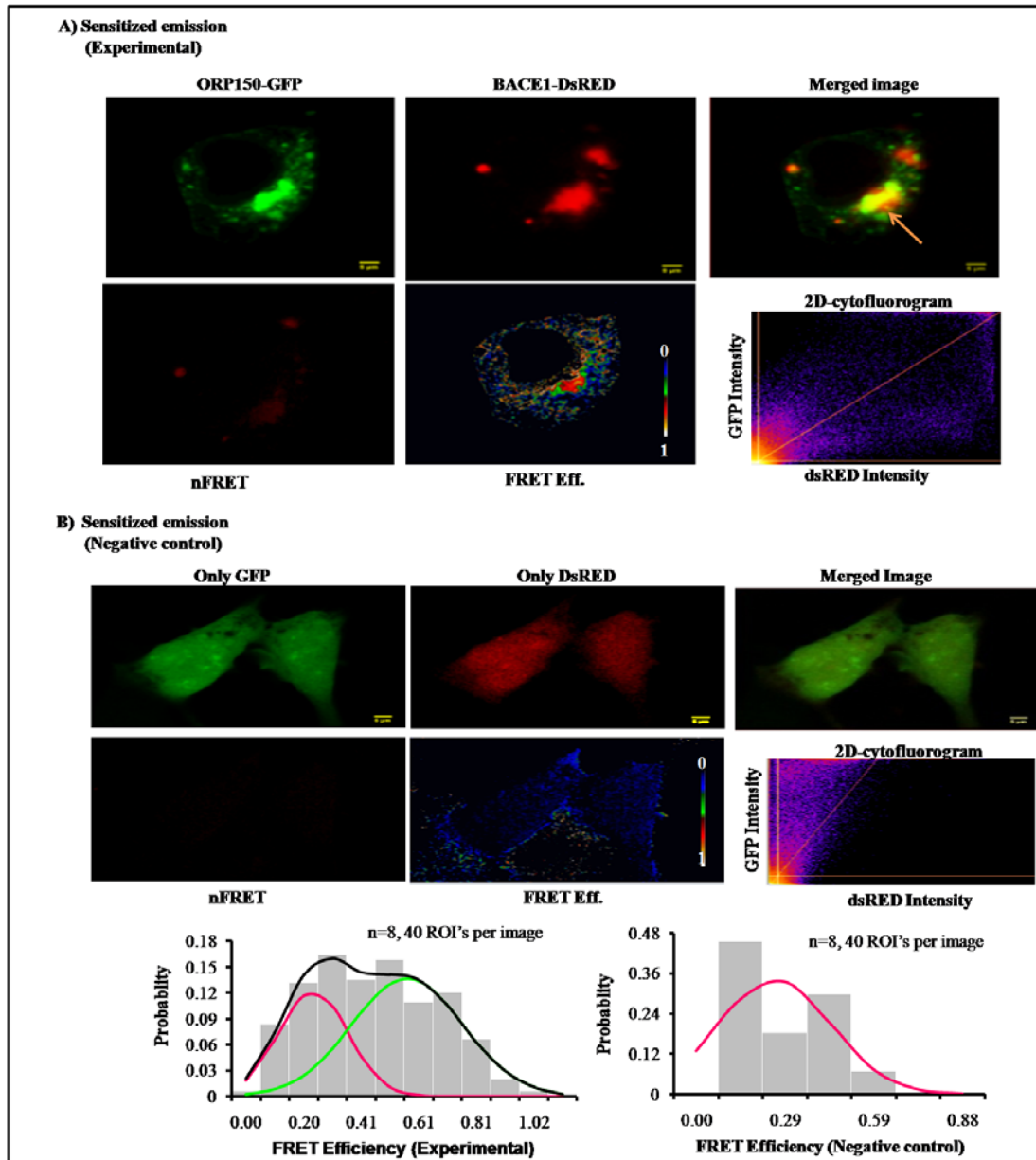
Figure 18: Subcellular Colocalization and FRET (by sensitized emission) between ORP150 and BACE1: A) Colocalization be tween O RP150-GFP and BACE1-dsRED Ex is shown in the merged image of HEK293 cells as indicated by an arrow. 2D cytofluorogram confirms the degree of colocaliztion. F RET analysis b etween O RP150-GFP don or a nd BACE1-DsRED Ex acceptor by sens itized emission is shown. Scale b ar = 5 μm. **B)** No c olocalization w as obs erved w ith negative c ontrol Only GFP and only Ds RED constructs. Scale bar = 5 μm. **C)** FRET e fficiency was calculated for Experimental and Negative control. ROI's stands for region of interest.

FRET efficiency was also calculated by acceptor photobleaching (Material and Methods). BACE1 signal (Acceptor) was bleached approximately 95% using 543 nm laser beam, a corresponding increase in ORP150 signal (Donor) was observed **(Figure 19).**
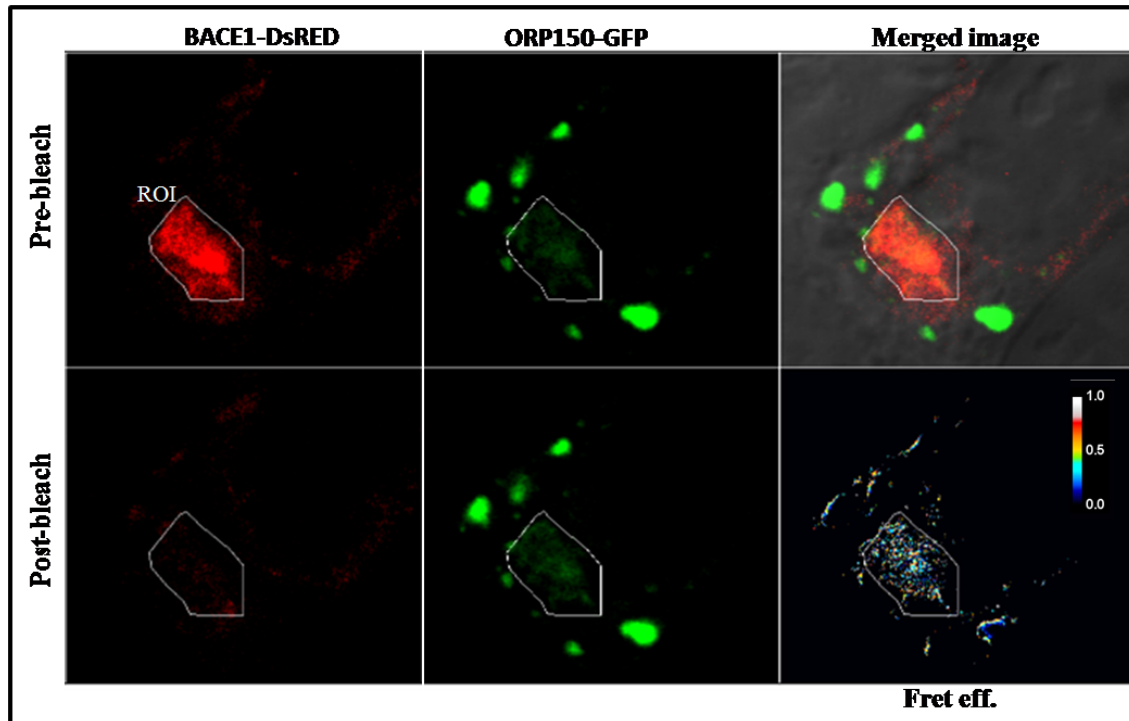
Figure 19: Subcellular Colocalization and FRET (by acceptor photobleaching) between ORP150 and BACE1: A) FRET by Acceptor photobleaching was performed for ORP150-GFP and BACE1-DsRED Ex using confocal laser scanning microscope. Images were taken before and after photobleaching of t he acceptor at selected ROI for 30 seconds with a 543 nm laser beam. Scale bar = 5 μm. ROI stands for region of interest.

Observing colocalization and interaction between ORP150 and BACE1 microscopically, physical i nteraction be tween t he t wo pr oteins was ne xt investigated by co - immunoprecipitation assay.

III. Co-immunoprecipitation between ORP150 and BACE1

For co-immunoprecipitation, O RP150-HA was transfected i n H EK293-BACE1 s table cells. After 24 hours o f t ransfection, cells w ere l ysed and whole cel l l ysates w ere subjected to immunoprecipitation either with anti-BACE1 antibody **(Figure 20A)** or with anti-HA antibody **(Figure 20B)**. IgG antibody was used as non-specific (NSP) antibody control. Immunoprecipitated c omplexes w ere s eparated on S DS-PAGE f ollowed b y immunoblotting with ORP150 a nd B ACE1 a ntibodies. O RP150 w as f ound t o be c o-

immunoprecipitated with BACE1-specific pull **(Figure 20A)** but not with non-specific antibody pull. Similarly, 50kD form of BACE1 was found to be co-immunoprecipitated with ORP150-specific HA-pull **(Figure 20B)** but not with non-specific antibody pull.
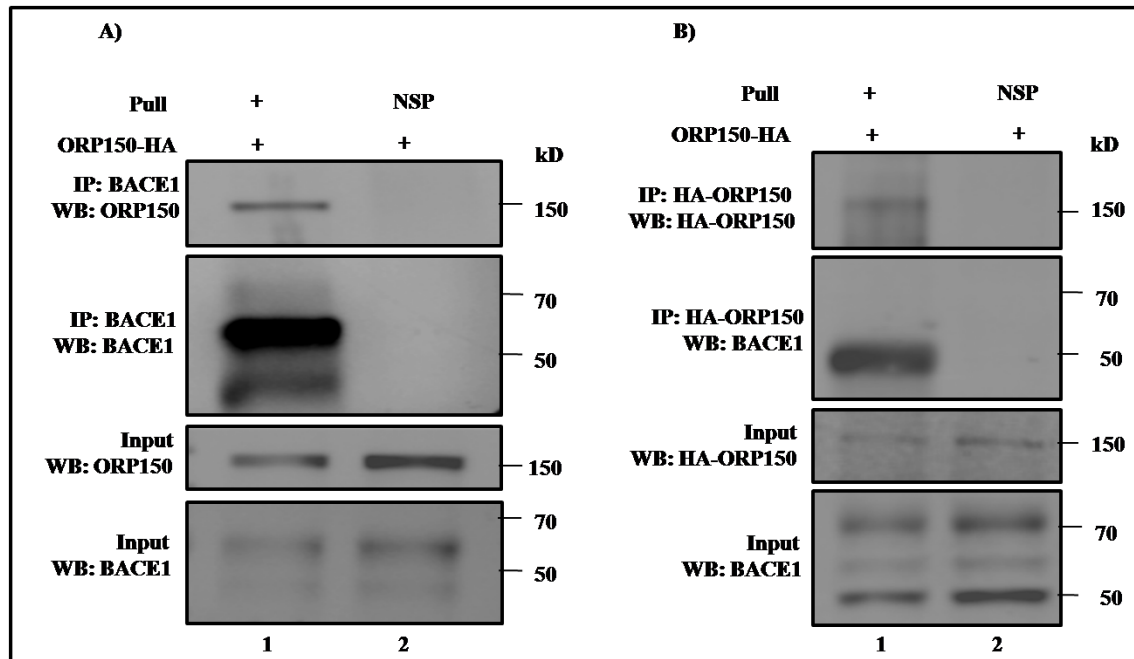
Figure 20: ORP150 associates with BACE1 in cell. HEK293-BACE1 stable cells were transfected with ORP150. Whole cell lysate was subjected to immunoprecipitation either with anti-BACE1 (A) or anti-HA (B) antibody. IgG was used as non-specific (NSP) antibody control in each IP. Immunoblotting to detect ORP150 and BACE1 from the immunoprecipitated complex was done with anti-ORP150 and anti-BACE1. Input constitutes 5% of whole cell lysate.

Observing co-immunoprecipitation between the ORP150 and BACE1 under normal conditions, the interaction between the two was further investigated under varied stress conditions using normal conditions as positive control for the experiment **(Figure 21, lane 1)**. ORP150-HA was transfected in HEK293-BACE1 stable cells. After 24 hours of transfection, cells were either kept under normal conditions or treated for ER stress, oxidative stress or hypoxic stress for indicated doses and time points **(Figure 21)**. Cells were then lysed and whole cell lysates were subjected to immunoprecipitation with anti-BACE1 antibody. Immunoprecipitated complexes were separated on SDS-PAGE followed by immunoblotting with ORP150 and BACE1 antibodies. Surprisingly, both glycosylated and unglycosylated forms of ORP150 interacted with BACE1 under ER stress condition **(Figure 21, lane 2)**. In addition, ORP150 interacted with BACE1 under oxidative stress condition **(Figure 21, lane 3)** but not under hypoxic stress **(Figure 21, lane 4)**.
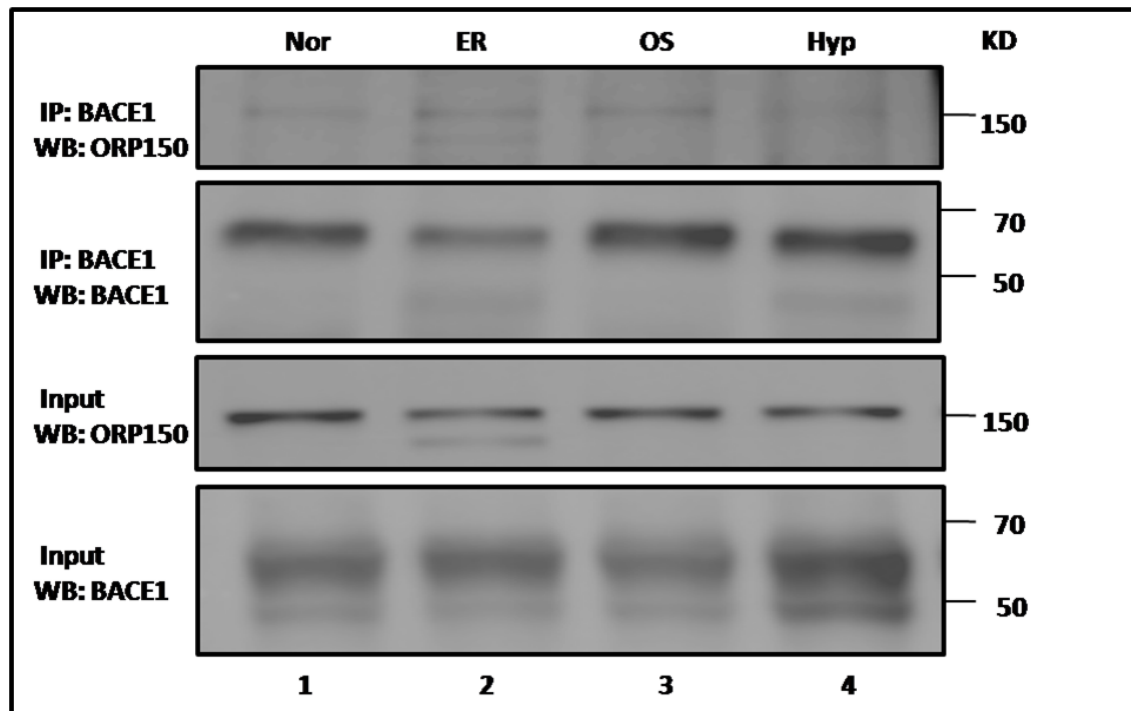
Figure 21: ORP150 associates with BACE1 under ER and oxidative stress but not under hypoxic stress. HEK293-BACE1 stable cells were transfected with ORP150-HA plasmid. 24 hours post-transfection, cells were either left untreated or treated with tunicamycin (4 µg/ml for 24 hours), cumene hydroperoxide (200 µM for 2 hours), or hypoxia (0.1% for 24 hours). Whole cell lysate was subjected to immunoprecipitation with anti-BACE1 antibody. Immunoblotting to detect ORP150 and BACE1 from the immunoprecipitated complex was done with anti-ORP150 and anti-BACE1. Input constitutes 5% of whole cell lysate.

IV. GST-pull down assay between GST-BACE1 and cellular ORP150

BACE 1 undergoes extensive post-translational modifications while passing through the secretory pathway (acetylation, glycosylation etc.), changing from its initially synthesized 50kD form to a 75kD fully matured form. Next, it was examined if there exists an *in vitro* interaction between recombinant GST-BACE1 and ORP150 over-expressing HEK293 whole cell lysate (WCL) using GST-pull down assay. Recombinant GST only and GST-BACE1 (kind gift from Prof. Georges Levesque) proteins were first overexpressed in *E. coli* BL21(DE3) and then purified with glutathione sepharose beads by affinity chromatography. The proteins were dialyzed and their purity was checked by SDS-PAGE **(Figure 22A and 22B)**.
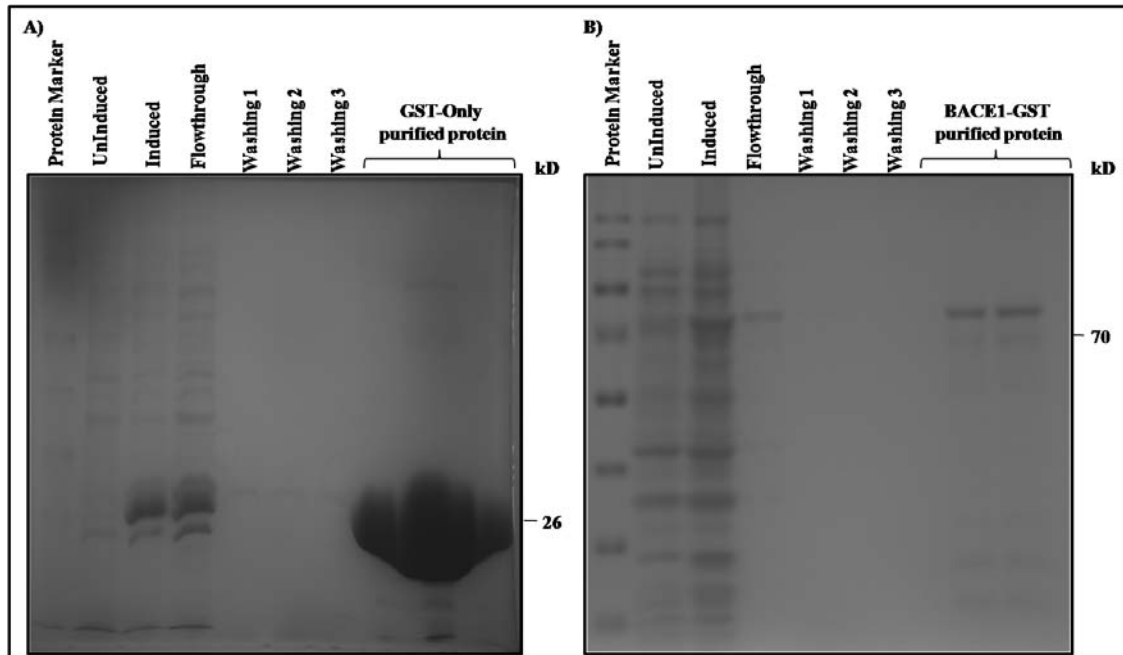
Figure 22: Protein purification of GST only and BACE1-GST proteins. A) Coomassie staining of purified GST-only (26 kD) protein. **B)** Coomassie staining of purified BACE1-GST (71 kD) protein

For GST pull down assay, HA-tagged ORP150 was transiently transfected and expressed in HEK293 cells. 30 hours post-transfection, cell lysis was performed in NP40 lysis buffer. 1 mg of the whole cell lysate was incubated either with recombinant GST only protein or GST-BACE1 protein (5 μg each). Complexes were pulled down by glutathione sepharose beads. After extensive washing to remove unbound proteins, complexes bound to glutathione sepharose beads were eluted and resolved on SDS-PAGE and analyzed with anti-GST antibody. GST only protein was used as a negative control in the assay **(Figure 23 - lane 3)**. GST pull down assay confirmed GST-BACE1 expression but ORP150 was not found to be co-eluted with purified BACE1 **(Figure 23 - lane 2)**. This experiment signifies that ORP150 interacts only with the post-translationally modified form of BACE1.
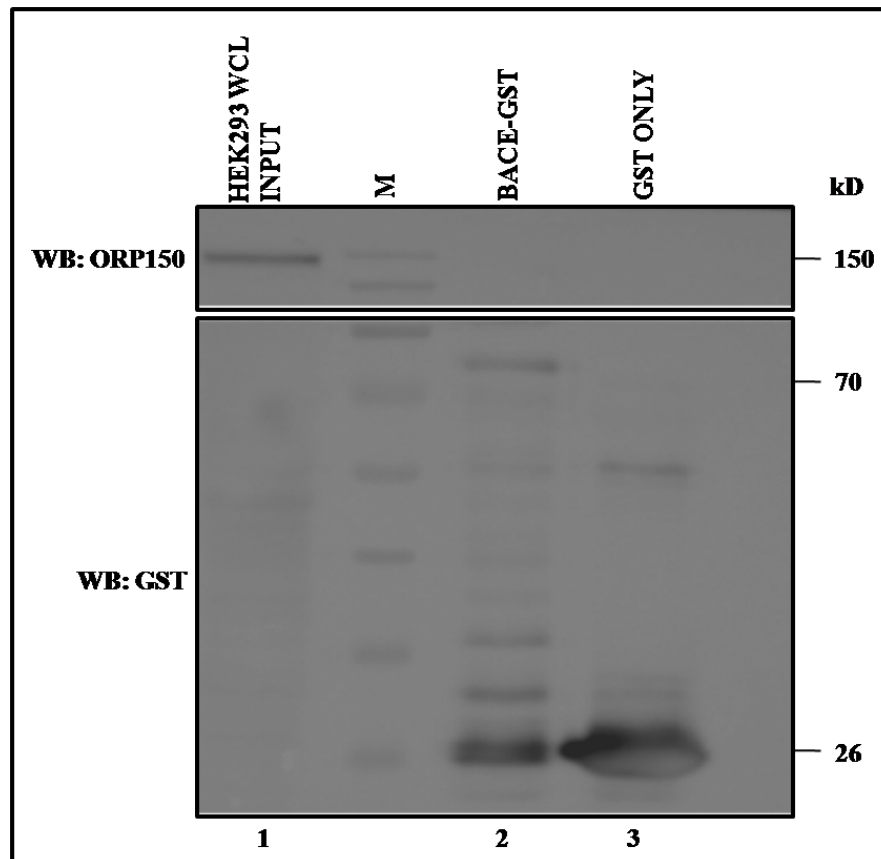
Figure 23: ORP150 does not interact with unmodified immature form of BACE1. HEK293 cells were transiently transfected with ORP150 e xpression plasmid. After 30 hours of transfection, whole cell l ysate (1 mg) w as incubated with purified r ecombinant BACE1-GST or GST-only protein (5 μg each) for 3 hours. GST-pull down assay was performed as described in material and methods. Eluted proteins were subjected to SDS-PAGE for western blot analysis. As a control, whole cell lysate was directly loaded to detect the expression and position of ORP150 (input). M is protein molecular weight marker.

Inverse relation between ORP150 and CHIP

I. Effect of ORP150 on CHIP and of CHIP on ORP150 under normal conditions

Opposing role of E R-resident c haperone (ORP150) a nd o f c ellular c haperone (CHIP) over c ellular B ACE1 l evels a nd ove r B ACE1-mediated APP-processing l ed t o the investigation whether the two chaperones affect each other. To study this, each of the two chaperones, O RP150 a nd C HIP were transfected i n a dos e-dependent m anner i n HEK293-BACE1 stable cells. Increase in ORP150 was found to increase BACE1 levels by 2.2 f old while it significantly r educed CHIP l evels by 3 f old (**Figure 24A – lane 3 and 1**). However, increase in CHIP decreased both BACE1 levels by 1.53 fold as well as ORP150 l evels by 1.32 fold (**Figure 24B – lane 3 and 1**). T hus, t his da ta i ndicates

distinct effect of ORP150 and CHIP over each other where E3 ubiquitin ligase activity of CHIP pl ays ma jor r ole in de creasing bot h B ACE1 a nd O RP150 levels w hile O RP150 predominantly be ing a c haperone s tabilizes BACE1. R educed C HIP l evels i n t he presence of ORP150 might be attributed to the auto-ubiquitylating activity of CHIP in the presence of ORP150.
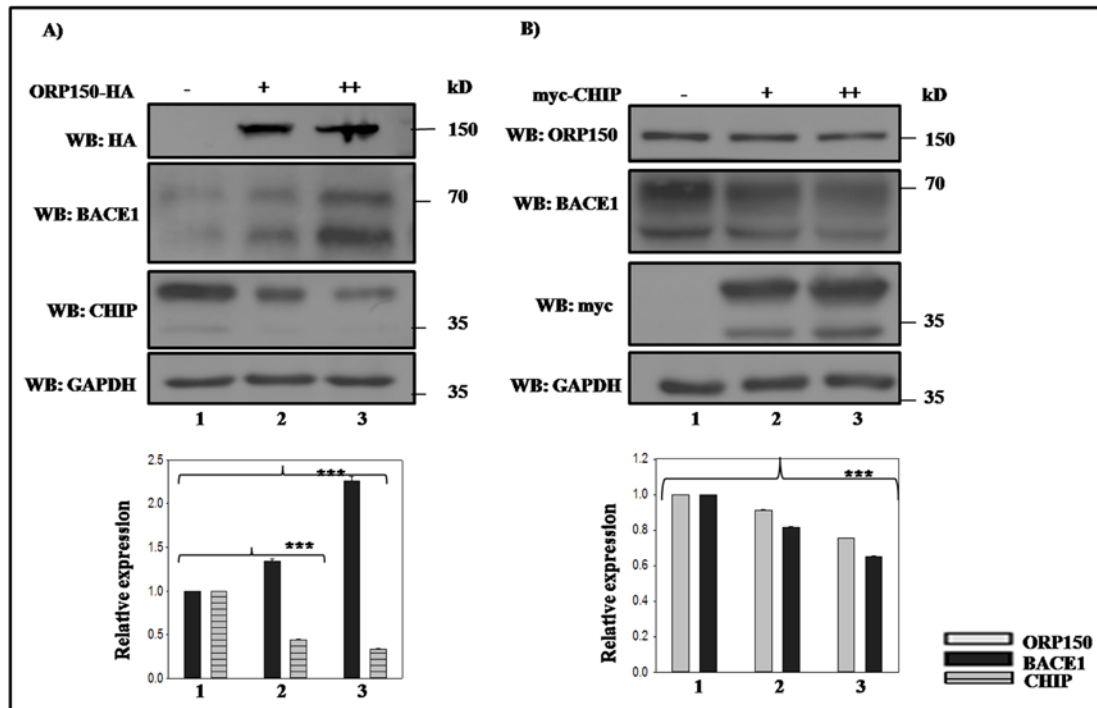
Figure 24: ORP150 stabilizes BACE1 and reduces CHIP whereas CHIP reduces both BACE1 and ORP150. HEK293-BACE1 stable cells were transfected with increasing amounts of either **A)** ORP150-HA or **B)** myc-CHIP expression pl asmids. 30 hours p ost-transfection, ORP150, BACE1, CHIP and GAPDH levels were determined by western blotting with ORP150, M83, CHIP G2, and GAPDH antibodies respectively. Overexpression of ORP150 and CHIP was confirmed using anti-HA and anti-myc antibody respectively. Data was expressed as mean ± SE from three independent experiments. Statistical analysis was performed by two-tailed t-test for the significance at the * P ≤ 0.05, ** P ≤ 0.01 and *** P ≤ 0.001.

II. Mode of degradation of ORP150 by CHIP

CHIP has previously been shown to mediate proteosomal-mediated degradation of many of its c lient proteins. In addition, CHIP acts a molecular switch between lysosomal and proteosomal degradation for α-synuclein (Shin et al. 2005) Regulation of degradation of ORP150 has not been studied so far. On observing a decrease in ORP150 levels on CHIP overexpression, t he m ode of r egulation of O RP150 b y C HIP was elucidated by overexpressing CHIP in H EK293 c ells both in t he presence of pr oteosomal i nhibitor

(MG132/10µM) a nd a n a utosomal i nhibitor (Chloroquine/100 µ M) f or 18 hours. Untreated cells t ransfected with empty pl asmid and myc-CHIP w ere us ed a s c ontrol. **(Figure 25)**. Immunoblotting s howed de gradation of O RP150 b y 1.2 6 f old in t he presence of C HIP **(lane 2).** It was recovered to normal level in the pr esence of M G132 **(lane 3)** and increased by 1.23 fold with respect to normal le vels in the pr esence o f chloroquine **(lane 4)**. Thus, t hese da ta s uggests C HIP m ediates de gradation of O RP150 by both proteosomal and lysosomal pathways.
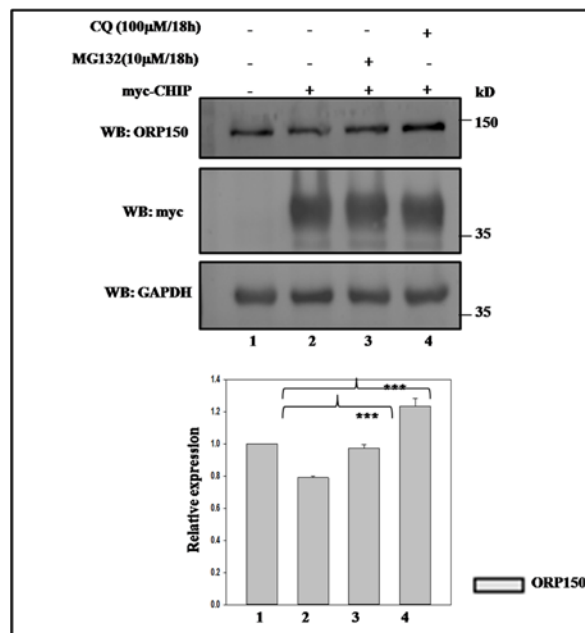
Figure 25: CHIP degrades ORP150 via both proteosomal and lysosomal pathways. HEK293 cells w ere ei ther k ept unt reated or t reated with constant am ounts o f m yc-CHIP e xpression plasmid. 24 hou rs p ost-transfection, m yc-CHIP t rasnfected cells w ere e ither k ept un treated or treated w ith 10 µM M G132 or 100 µM ch loroquine eac h for 18 hou rs. Western blotting w as performed to determine ORP150 levels while overexpression of CHIP was confirmed using anti-myc ant ibody. GAPDH w as us ed as a loading control. Data w as expressed as mean ± SE from three i ndependent expe riments. Statistical ana lysis w as pe rformed by t wo-tailed t-test for t he significance at the * P ≤ 0.05, ** P ≤ 0.01 and *** P ≤ 0.001.

III. Effect of CHIP on BACE1 and ORP150 levels under varied stress conditions

It w as next i nvestigated i f t he t wo cha perones, ORP150 and CHIP al so r egulate each other unde r va ried s tressed c onditions. F or t his, H EK293-BACE1 stable cel ls w ere exposed **(Figure 26)** to Tunicamycin for ER stress**(lane 3 and 4),** cumene hydroperoxide for oxidative stress **(lane 5 and 6),** and hypoxia (0.1%) **(lane 7 and 8)** in the absence and presence of CHIP and level of endogenous ORP150 and BACE1 levels were analyzed by

western bl otting. C HIP w as f ound t o pl ay du al r ole ove r O RP150 a nd B ACE1 b y increasing O RP150 levels b y 1.66 f old and B ACE1 levels b y 1.16 f old under E R stress condition **(lane 4 and 3)** while reducing ORP150 by 1.62 fold and BACE1 levels by 1.18 fold under ox idative stress c ondition **(lane 6 and 5)**. C HIP di d not ha ve a ny si gnificant effect over ORP150 and BACE1 levels under hypoxia **(lane 8 and 7)**.
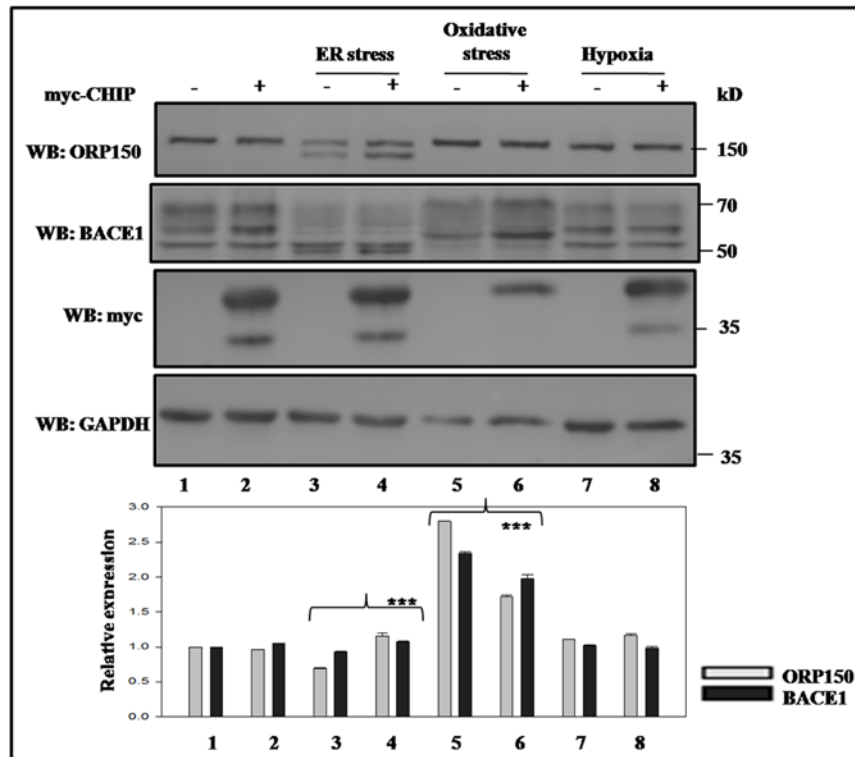
Figure 26: CHIP degrades ORP150 and BACE1 under oxidative stress while stabilizes both under ER stress. HEK293-BACE1 stable c ells w ere t ransfected either w ith empty plasmid or myc-CHIP expression plasmid. 24 hours post-transfection, each pair was either kept untreated or treated with tunicamycin for ER stress (4 μg/ml for 24 hours), or CHP for oxidative stress (200 μM for 2 hours) or hypoxia (0.1% for 24 hours). ORP150 and BACE1 levels were determined by western blotting. Overexpression of CHIP was confirmed using anti-myc antibody. GAPDH was used as a loading control. Data was expressed as mean ± SE from three independent experiments. Statistical analysis was performed by two-tailed t-test for the significance at the * $P \leq 0.05$, ** $P \leq 0.01$ and *** $P \leq 0.001$.

IV. Effect of ORP150 on BACE1 and CHIP levels under varied stress conditions

Similarly, HEK293-BACE1 s table cells w ere e xposed **(Figure 27)** to T unicamycin for ER stress **(lane 3 and 4)**, cumene hydroperoxide for oxidative stress **(lane 5 and 6)**, and hypoxia (0.1%) **(lane 7 and 8)** in the absence and presence of ORP150 and endogenous CHIP and BACE1 l evels w ere a nalyzed. O RP150 s ignificantly reduced C HIP l evels under a ll – ER stress (by 1.3 fold), ox idative stress (by 1.2 fold) and h ypoxic s tress (by

1.3 fold). Also, ORP150 maintained BACE1 levels with significantly increasing its levels especially under oxidative stress **(lane 5 and 6)**. However, overexpression of ORP150 reduced BACE1 levels under hypoxic stress **(lane 7 and 8)**.
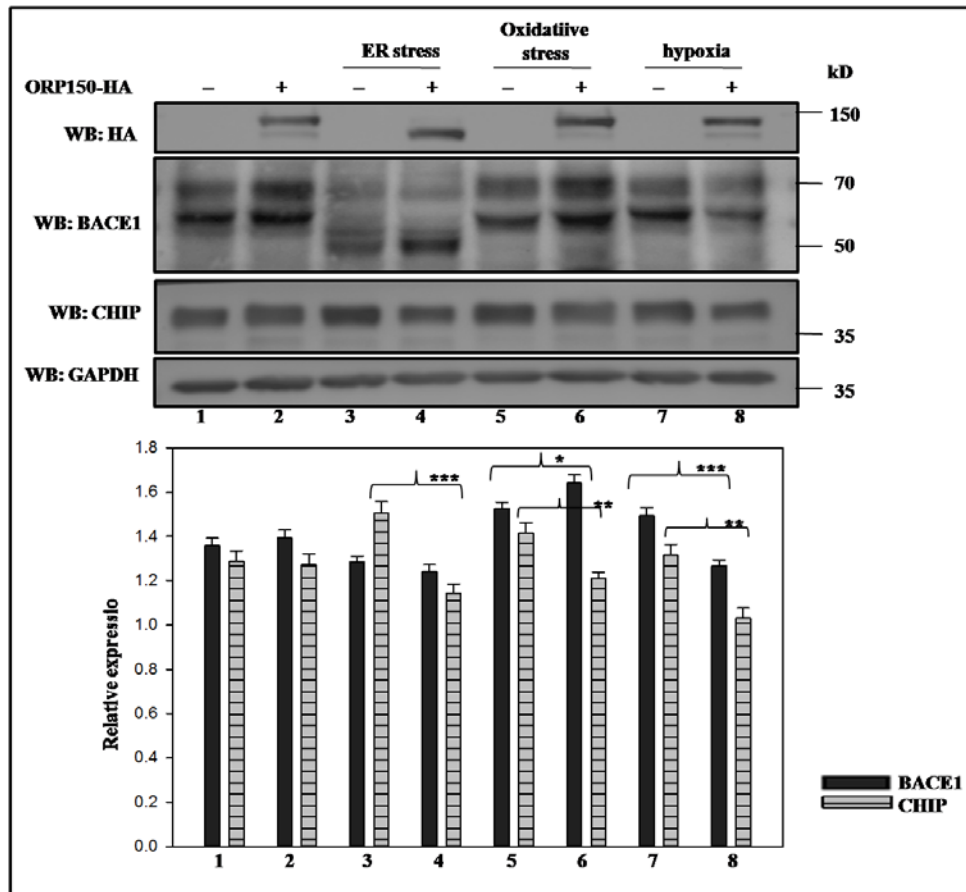
Figure 27: ORP150 degrades CHIP under ER, OS and hypoxic stress while maintaining BACE1 under Oxidative stress. HEK293 cells were transfected either with empty plasmid or ORP150-HA expression plasmid. 24 hours post-transfection, each pair was either kept untreated or treated with tunicamycin for ER stress (4 µg/ml for 24 hours), or CHP for oxidative stress (200 µM for 2 hours) or hypoxia (0.1% for 24hours). CHIP and BACE1 levels were determined by western blotting. Overexpression of ORP150-HA was confirmed using anti-HA antibody. GAPDH was used as a loading control. Data was expressed as mean ± SE from three independent experiments. Statistical analysis was performed by two-tailed t-test for the significance at the * P ≤ 0.05, ** P ≤ 0.01 and *** P ≤ 0.001.

Overexpression studies thus shows inverse effect of chaperones ORP150 and CHIP under stress conditions, where CHIP inhibits Alzheimer's progression by reducing ORP150 and BACE1 specifically under oxidative stress while ORP150 promotes Alzheimer's progression by reducing CHIP and maintaining BACE1 under varied stress conditions.

In vivo expression profile of ORP150, CHIP, BACE1 and Aβ42 in cortex of AD patients

A large number of cellular stresses including oxidative, ER, hypoxia and inflammation are involved in amyloid beta production in human AD brain (Chami et al. 2012). Men and women give different biological response to cellular stress (Verma et al. 2011). To examine the expression of ORP150, CHIP, BACE1 and Aβ42 *in vivo,* cortex from 12 pairs of age and sex-matched AD patients and non-demented controls was analyzed by ELISA and immunoblotting. The samples were further sub-divided into 5 male and 7 female pairs **(Table 1)**. ELISA was performed to detect cellular Aβ42 levels. The Aβ42 levels in AD patients were compared to age and sex-matched non-demented controls **(Figure 28A)**. The plot showed a significant 3 fold increase in Aβ42 levels in all AD patients (n=12) as compared to controls (n=12) confirming the severity of the disease in patient samples. A 3.9 fold increase in Aβ42 levels was observed in AD males (n=5) and a 2.7 fold increase was observed in AD females (n=7) as compared to respective controls.

Next, immunoblotting was performed to detect the levels of ORP150, BACE1 and CHIP in human brain. Frontal cortex from each patient and control was lysed in RIPA lysis buffer in 1:10 (w/v) ratio. The proteins were resolved on SDS-PAGE and probed with anti-ORP150, anti-CHIP, anti-BACE1 and anti-GAPDH antibodies. GAPDH was used as a loading control **(Figure 28B)**. AD females showed a significant increase in CHIP levels by 1.2 fold and a corresponding significant decrease in BACE1 levels by 1.5 fold as compared to AD males **(Figure 28C)**. This data confirms previously published cellular data of inverse relation between CHIP and BACE1 (Singh and Pati 2015). Comparison of male AD patients with non-demented control males revealed a significant increase in the levels of ORP150, CHIP, and BACE1 by 1.3 fold, 1.5 fold and 1.4 fold respectively. While a significant decrease in the levels of ORP150, CHIP and BACE by 1.2 fold, 1.2 fold and 1.3 fold respectively was observed in female AD patients as compared to control females **(Figure 28D, E, F)**. Further, careful analysis of individual patients with their respective controls showed that in 5 male AD patients (patients 1-5) an increase in the levels of ORP150 by 1.3 fold correlated with an increase in BACE1 levels by 1.3 fold along with an increase in Aβ42 levels by 3.9 fold. While in 5 female patients (patient 6-8, 10 and 11), a decrease in the levels of ORP150 by 1.3 fold correlated with a decrease in the levels of BACE1 by 1.5 fold **(Figure 28G)**. Also, in 3 male patients (patient 3-5),

increase i n the levels of CHIP b y 2 fold correlated with an increase i n t he l evels of BACE1 by 1.6 fold while in 6 female patients (patient 6-11), decrease in CHIP levels by 1.2 fold correlated with a decrease in BACE1 levels by 1.4 fold **(Figure 28H)**. Thus, in patient 1 and 2, an increase in ORP150 levels by 1.2 fold, caused a rise in BACE1 levels by 1.2 f old a nd a r ise in A β42 levels b y 4.5 fold. No change i n CHIP l evels w ere observed i n these pa tients. W hile i n pa tient 12 , an increase in CHIP levels b y 1.1 fold caused a de crease i n BACE1 l evels b y 1.2 f old. N o c hange i n O RP150 l evels was observed i n this pa tient pair. T hus, this data s uggests a s trong gender-specific cr osstalk between stress-responsive proteins - ORP150, CHIP and BACE1 in human AD brain.
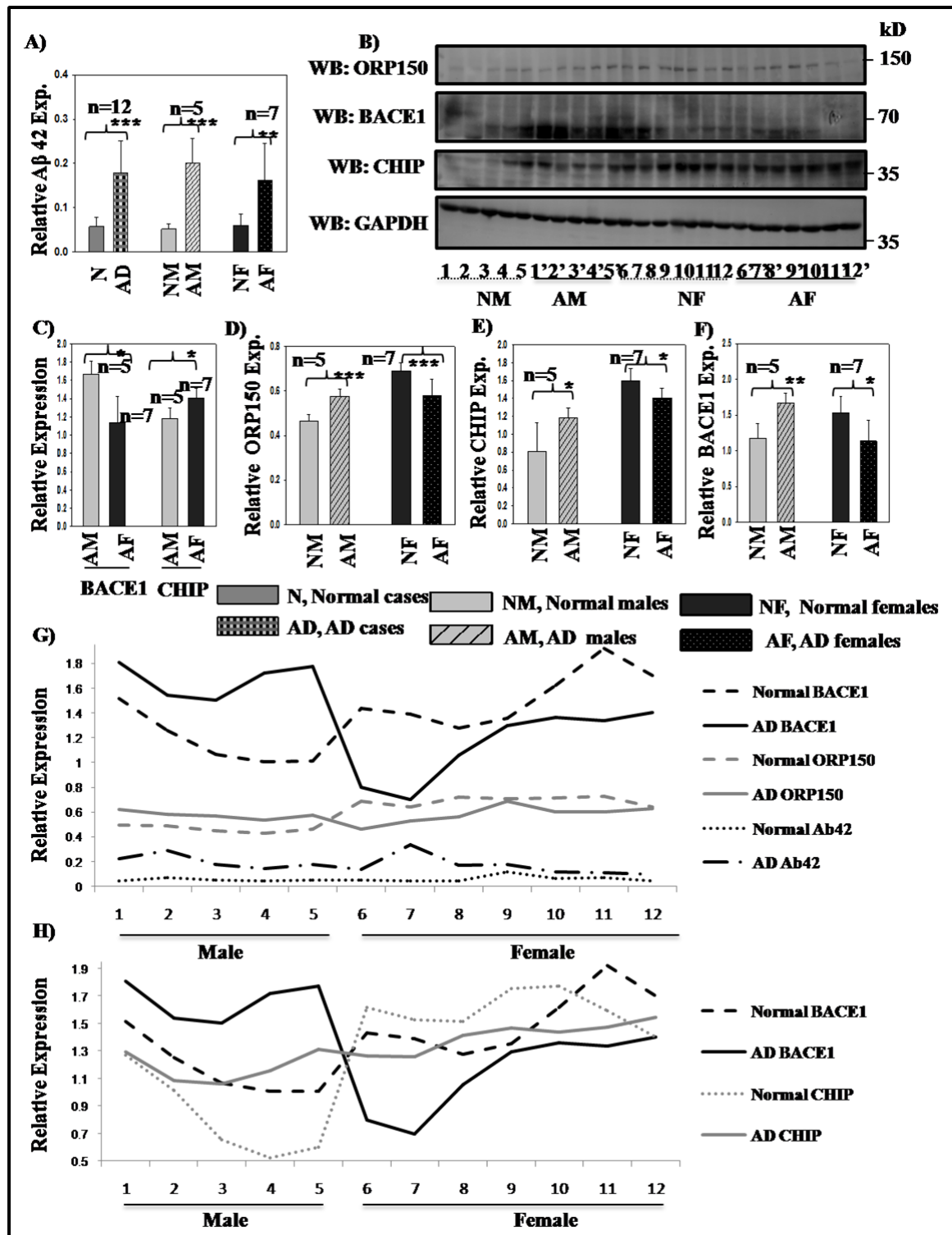
Figure 28: An antagonistic relation exists between CHIP and ORP150 in regard to BACE1 in cortex of AD patient. A) The lysates from human frontal cortices of AD patients and controls were subjected to ELISA and Aβ42 levels were compared in AD patients (AD) compared to non-demented (N) controls. **B)** The lysates from human frontal cortices of AD patients and controls were subjected to immuneblotting and probed with antibody specific for ORP150, BACE1 and CHIP. GAPDH was used as a loading control. The immunosignals were quantified by ImageJ and plotted as follows. **C)** Levels of CHIP and BACE1 were compared in AD males (AM, n=5) and

AD females (AF, n=7). All three proteins **D)** ORP150, **E)** CHIP and **F)** BACE1 were compared between AD males (AM, n=5) and normal males (NM, n=5) and between AD females (AF, n=7) and normal females (NF, n=7). The data was represented as mean ± SEM. **G)** Line pl ot representing direct relation between ORP150, BACE1 and Aβ42 in male and female AD cases. **H)** Line Plot representing inverse relation between BACE1 and CHIP in male and female AD cases. Statistical analysis was performed by two-tailed t-test for the significance at the * P ≤ 0.05, ** P ≤ 0.01 and *** P ≤ 0.001.

DISCUSSION

Discussion

Molecular chaperones display either protective or pathogenic role in the advancement of Alzheimer's disease (Marino Gamazza et al. 2016). BACE1 is at the cross-roads of a toxic vicious cycle involving cellular stress and Aβ production and is a promising therapeutic target in Alzheimer's disease (AD) (Cai et al. 2001; Chami and Checkler, 2012). A cellular chaperone CHIP, mediates stabilization of APP via proteosomal degradation and p53-mediated trans-repression of BACE1 (Singh and Pati 2015). This study shows that silencing of an ER-resident chaperone ORP150 reduces BACE1 levels under oxidative and ER stress. On the other hand, an overexpression of ORP150 stabilizes BACE1 and enhances BACE1-mediated APP processing thus leading to increased Aβ production. The level of ORP150 has direct relationship with BACE1 in post-mortem cerebral cortices of AD patients. Also, ORP150 and CHIP inversely regulate each other and cellular BACE1 levels under stress conditions. These results suggest that a significant balance between ORP150 and CHIP may ultimately influence AD pathophysiology. Thus, this finding might help future implications in designing chaperone-mediated new therapeutics for AD.

ORP150 stabilizes stress-induced BACE1 levels

To uncover the role of stress-induced chaperone ORP150 in BACE1 regulation, their expression profile were analyzed in this study under stress conditions along with silencing of ORP150. Among the varied stress conditions, ER stress, oxidative stress and hypoxic stress were selected as all these stresses are detrimental to Alzheimer's progression (Tan et al. 2013, Guglielmotto et. al. 2009, Lee et al. 2010; Placido et al 2014). Oxidative stress showed a simultaneous increase in both ORP150 and BACE1 levels. Interestingly, silencing of ORP150 reduced BACE1 levels under oxidative stress indicating role of ORP150 in BACE1 elevation under oxidative stress. This data complements with previous studies showing oxidative stress-induced BACE1 expression. The stress-induced upregulation of BACE1, though not completely understood, is shown to be attributed to transcriptional (Marwaha et al. 2012; Kwak et al. 2011), post-transcriptional (O'Connor et al. 2008), translational (Mouton-liger et al. 2012) and post-translational regulation (Kizuka et al. 2016). In addition, ER stress increased the overall level of ER resident chaperones ORP150 as well as GRP78. However, a decrease in the level of N-linked glycosylated ORP150 was associated with a simultaneous decrease in the level of BACE1.

Glycosylation has previously been shown to play an important role in a protein's structure, function a nd s tability (Arey 2012). Silencing of N-linked g lycosylated O RP150 r educed BACE1 levels in tunicamycin-induced E R-stress. T hus, t his finding for the f irst time shows functional r ole of N -linked glycosylation of O RP150 i n s tabilization of BACE1. These r esults i n turn s upport the previously ob served r educed BACE1 a ctivity i n t he presence of ER stress inducers (Sun et al. 2006).

However, unlike O xidative a nd ER st ress, ORP150 a nd B ACE1 w ere inversely r elated under hypoxic s tress (i.e. 0.1 a nd 1% O_2). Increase i n BACE1 expression was associated with a decrease in ORP150 expression. Previous reports show hypoxia inducible factor-1 (HIF1) as a transcriptional a ctivator of BACE1 (Guglielmotto et al. 2009) and p53 as its transcriptional repressor (Singh and Pati 2015). Moreover, an increase in BACE1 level was associated with an increase in HIF1α levels and a decrease in p53 levels under low oxygen concentrations thus indicating their r ole i n i nducing BACE1 expression under h ypoxic stress. This data thus s upports pr eviously publ ished H IF1-mediated i ncrease i n BACE1 transcription under hypoxia (Guglielmotto et al 2009).

ORP150 interacts with BACE1

Subsequently it w as established t hat ORP150 a nd B ACE1 interact and co -localize, and thus it was suggested that ORP150 might affect the regulation of BACE1, possibly through their c ellular i nteraction. B ACE1 s tructure, s ubcellular loc alization and/or a ctivity is modulated by interaction with a large number of proteins including BRI3, GGA's, LRP1, and ni castrin a mong ot hers (Hattori et al. 2002; He et al. 2005; T anokashira et al. 2015). This s tudy c learly s hows c ellular colocalization and interaction between ORP150 a nd BACE1 as confirmed by confocal microscopy and FRET. The colocalization was observed just outside the nuc leus, which possibly is an endoplasmic reticulum-specific localization. BACE1 undergoes extensive post-translational modifications (PTMs) during its maturation including g lycosylation, palmitoylation, a cetylation a nd phos phorylation (Capell et al . 2000). PTM's of BACE1 are necessary for its interactions with many proteins (Venugopal et al. 2008). Moreover, ORP150 interacts only with ~50kD form of BACE1 inside the cell as confirmed by c o-immunoprecipitation but not *in vitro* as obs erved by GST-pull dow n assay. Thus, cellular co-immunoprecipitation experiment further confirmed an ER-specific interaction a s the ~50kD form o f cellular BACE1 corresponds to its ini tially s ynthesized

ER-form which then, while passing through the secretory pathway, undergoes PTMs resulting in increase in its molecular weight to ~75kD (Capell et al. 2000). Consequently, this finding as well as the initial finding of regulation of BACE1 by N-linked glycosylated ORP150 proves that post-translational modification of both the proteins is necessary for regulation of BACE1 by ORP150. However, interestingly both glycosylated and unglycosylated forms of ORP150 interacts with BACE1 under ER stress. In addition, ORP150 interacts with BACE1 under oxidative stress but not under hypoxic stress. This is in synchronization to our finding of regulation of BACE1 by ORP150 under ER and oxidative stress but not under hypoxic stress. Thus it can be concluded that although both glycosylated and unglycosylated ORP150 physically interact with BACE1, it is the glycosylated ORP150 which is involved in regulation of cellular BACE. In addition, glycosylated ORP150 has been observed to be the endogenously expressing form in cells as well as in AD patients.

ORP150 stabilizes BACE1 and mediates β-processing of APP

The chaperoning activity of ORP150 in folding and maturation of secretory and glycoproteins has previously been reported (Lin et al. 1993; Kuznetsov 1998; Ozawa et al. 2001). Hence, it's interaction with BACE1 suggests that the regulation of BACE1 by ORP150 might be consequence of stabilization by ORP150. Overexpression of ORP150 in cellular models of AD increased cellular BACE1 levels which in turn resulted in enhanced β-amyloid processing of APP and a corresponding increase in the levels of C-terminal fragment 99 (CTF99) and Aβ42. Also, a correlated expression of BACE1 has earlier been observed with other proteins like NOGO-B in s-IBM muscle thus affecting its activity over APP (Wojcik et al. 2007). In contrast to this result, a previous study shows reduction in Aβ42 levels by ER chaperones including ORP150 in HEK-APP stable cells (Hoshino et al. 2007). GRP78, another ER-resident chaperone, was shown to mediate stabilization of APP and reduce Aβ42 levels by direct interaction with APP. However, the exact role of ORP150 in reducing Aβ42 levels was not explained. This contradiction might arise by the non-involvement of BACE1 in the study in HEK-APP stable cells (Hoshino et al. 2007). It was however taken into consideration in this study by precisely observing stabilization of BACE1 and enhanced BACE1-mediated APP processing by ORP150 in all cells namely HEK293-BACE1, HEK293-APP and SHSY5Y neurblastoma cells. In addition, recently C-

terminus of HSP70 interacting protein (CHIP) was shown to reduce Aβ42 generation via BACE1 degradation (Singh and Pati 2015). This study further shows inverse regulation of cellular BACE1 levels by CHIP and ORP150 thus, inversely altering cellular Aβ42 production. Similarly, CHIP and USP47 antagonistically regulate Katenin-p60 stability in neuronal cells where USP47 deubiquitinates and stabilizes katenin p60 whereas CHIP ubiquitinates and destabilizes katenin-p60 thus critically influencing katenin-p60-mediated axonal growth (Yang et. al. 2013). Further, silencing of ORP150 reduced endogenous BACE1 levels. This data indicates that the increase in BACE1 levels by ORP150 is a post-translational event as no significant changes are observed in BACE1 mRNA in ORP150 overexpressing cells. Alternatively, BACE1 half-life is increased in the presence of ORP150 after 9 hours of CHX treatment. Post-translational regulation of BACE1 is significantly associated with both physiological and pathological conditions (Araki 2016). Moreover, experimental evidence from this study suggests a significant physiological role of ORP150 in BACE1-mediated APP processing.

AD brain shows gender-specific expression of ORP150, CHIP and BACE1

Levels of cellular chaperones Hsp70, Hsp27 and CHIP are elevated in AD brain and play cytoprotective role in AD (Koren et al 2009; Zhang et al. 2014). Recent study shows silencing of BACE1 *in vivo* promoted translocation of CHIP from nucleus to cytoplasm (Piedrahita et. al 2015). An increase in CHIP was associated with a decrease in BACE1 in female AD patients when compared to male AD patients. This data thus confirms an inverse relation between CHIP and BACE1 (Singh and Pati, 2015). The mRNA level of ORP150 is reported to be high in cellular and mouse models of AD (Hoshino et al. 2007). Correlated but strongly gender-specific expression of ORP150, CHIP and BACE1 were observed in AD affected frontal cortex where female AD patients showed lower levels of ORP150, CHIP and BACE1 while male AD patients showed higher levels of ORP150, CHIP and BACE1 as compared to respective sex-matched controls. Likewise, a different study shows another brain protein, activity-dependent neuroprotective protein (ADNP), showing differential expression in males and females (Malishkevich et al. 2015) thus contributing to gender-specificity in autism and AD. Biological differences between genders determine the gender-specificity of the occurrence of a large number of diseases including Alzheimer's, autism, autoimmune diseases and cardiovascular diseases (Hebert

et al. 2001; Ngo 2014; Regitz-Zagrosek 2006). Alzheimer's disease is more predominant in women than men where increased life span of women, the presence of apoE4 allele and lowered level of estrogen with age are so far considered to be some of the factors responsible for increased incidence of AD in women (Carter et al. 2012; Malishkevich et al. 2015; Viña and Lloret 2010). Also, men and women give different biological response to cellular stress where females are shown to be more vulnerable to oxidative stress resulting in increased anti-oxidative metabolism (Schuessel et al. 2004). As shown at cellular level, ORP150 showed direct relationship with BACE1 and Aβ42 in AD patients as well though in a gender-specific manner. In addition, although CHIP showed inverse relationship with BACE1 in male and female AD cases however direct relationship of CHIP with BACE1 has been observed in AD patients when compared to sex-matched controls. Thus, the observed gender-specific differences in the expression profile of chaperones, ORP150 and CHIP, might be a consequence of the effect of the two chaperones over each other under gender-specific varied stress response. In addition, this study also emphasizes the need to consider gender-specific responses in clinic trials for diseases as they are likely to respond differently.

ORP150 and CHIP inversely regulate each other under varied stress conditions

In vivo data from AD patients reveal direct relation of ORP150 and inverse relation of CHIP in regard to BACE1 levels in a gender-specific manner. Moreover, opposing effect of ORP150 and CHIP, in controlling BACE1 levels as well as Aβ42 production, is confirmed in this study in cellular models of AD. CHIP and USP47 antagonistically regulate katenin-p60-mediated axonal growth during neuronal development (Yang et al. 2013). The expression and activity of molecular chaperones is regulated at both transcriptional and post-transcriptional level under oxidative and proteotoxic stress in various age-related diseases (Niforou et al. 2014). Subsequently, the role of ORP150 in controlling CHIP and that of CHIP in controlling ORP150 was further established in this study. Dose-dependent increase in ORP150 led to a decrease in CHIP levels and an increase in BACE1 levels. The reduced CHIP levels in the presence of ORP150 might be attributed to the auto-ubiquitylating activity of CHIP (Plechanovová et al. 2012). In contrast, overexpression of CHIP resulted in decrease in the levels of both ORP150 and BACE1. CHIP mediates proteosomal and/or lysosmal-mediated degradation for many of

its client proteins (Shin et al. 2005, kumar et al. 2007). However, this data shows both lysosomal and proteosomal-mediated degradation of ORP150 by CHIP. Thus, the antagonistic actions of ORP150 and CHIP in controlling BACE1 levels, either directly or indirectly via controlling each other, should be a critical mechanism for cells to keep BACE1 at appropriate levels in preventing Alzheimer's progression.

Several stresses like ER stress, oxidative stress, hypoxic stress among others regulate prognosis in Alzheimer's disease (Jha et al. 2014). Multiple mechanisms regulate BACE1 under varied stress conditions (Kizuka et al. 2016, Wang et al. 2014). Antagonistic action of ORP150 and CHIP in controlling BACE1 under varied stress conditions was further established. Overexpression of ORP150 decreased CHIP under different stress conditions including ER, oxidative and hypoxic stress thereby maintained BACE1 levels. However, CHIP played a dual role under stress conditions. It reduced both ORP150 and BACE1 under oxidative stress conditions while stabilized both under ER stress condition. The stabilization of ORP150 under ER stress could be attributed to the need for ORP150 as an integral part of an ER stress response. Likewise, previous study shows bi-functional role of CHIP both as a molecular chaperone and an E3 ubiquitin ligase, which controls APP in a proteosome-dependent manner and influence Aβ metabolism (Kumar et al. 2007). Thus, the changes in the level of ORP150 relative to that of CHIP, and vice versa, especially under varied stress conditions would critically influence BACE1 levels and thus influence Aβ42 generation in Alzheimer's disease

Conclusion

The present study confirms the role of ORP150 as positive regulator of BACE1. ORP150 interacts with cellular BACE1 and controls its protein level and functions by promoting stabilization of BACE1 and enhancing BACE1-mediated APP processing and Aβ42 generation. Silencing of ORP150, on the other hand, alleviates BACE1 level in ER and oxidative stress. Multiple chaperones might regulate Alzheimer's progression by regulating the key proteins responsible for Aβ42 generation (Marino Gamazza et al. 2016, Kumar et al. 2007). Interestingly, ORP150 regulates cellular BACE1 levels by inversely regulating CHIP under ER, oxidative and hypoxic stress conditions. By contrast, CHIP reduces ORP150 and BACE1 levels specifically under oxidative stress. Consequently, a direct relationship between ORP150 and BACE1 and an inverse relationship between CHIP and

BACE1 is observed in both male and female AD patients. Thus, *in vivo* data shows simultaneous synergy and antagonism between ORP150 and CHIP in AD patients in a gender-specific manner in regard to BACE1 levels. Based on the present findings, a model is proposed for control of BACE1 levels by antagonistic actions of ER resident chaperone, ORP150 and the cellular chaperone, CHIP **(Figure 29)**. Consequently, modifying the level of these chaperones in human brain can significantly regulate BACE1 levels and thus this study can be exploited therapeutically in designing chaperone-mediated treatment of AD.
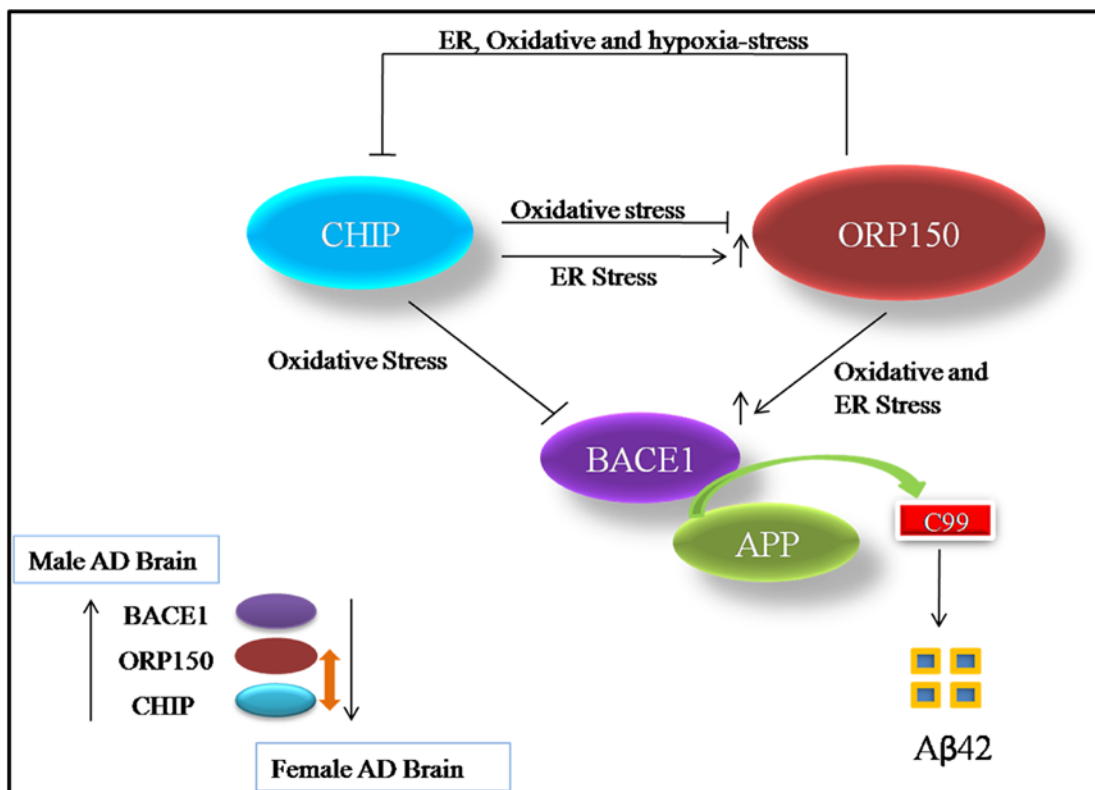

Figure 29: Model depicting inverse regulation of BACE1 by chaperones ORP150 and CHIP in Alzheimer's disease.

BIBLIOGRAPHY

Bibliography

Aleshin AN, Sawa Y, Kitagawa-Sakakida S, Bando Y, Ono M, Memon IA, Tohyama M, Ogawa S, Matsuda H. (2005) 1 50-kDa oxyg en-regulated protein attenuates m yocardial ischemia–reperfusion injury in rat heart. *Journal of molecular and cellular cardiology*. 38: 517-25.

Arnouk H, Zynda ER, Wang XY, Hylander BL, Manjili MH, Repasky EA, Subjeck JR, Latif Kazim A. (2010) T umour secreted grp170 c haperones f ull-length pr otein s ubstrates and induces an adaptive ant i-tumour i mmune r esponse i n v ivo. *International Journal of Hyperthermia*. 26: 366-75.

Angeletti B, Waldron KJ, Freeman KB, Bawagan H, Hussain I, Miller CC, Lau KF, Tennant ME, Dennison C, Robinson NJ, Dingwall C. (2005) B ACE1 c ytoplasmic dom ain interacts w ith t he c opper chaperone for s uperoxide dismutase-1 a nd bi nds c opper. *Journal of Biological Chemistry*. 280: 17930-7.

Araki W. (2016) Post-translational regulation of the β-secretase BACE1. *Brain research bulletin*. 126: 170-7.

Arey BJ. (2012) The Role of Glycosylation in Receptor Signaling, *INTECH* 12: 273-286

Arrington DD, Schnellmann RG. (2008) T argeting of t he molecular c haperone oxy gen-regulated pr otein 150 (ORP150) t o m itochondria a nd i ts i nduction by cellular s tress. *American Journal of Physiology-Cell Physiology*. 294: 641-50.

Asahi H, Koshida K, Hori O, Ogawa S, Namiki M. (2002) Immunohistochemical detection of the 150-kDa oxygen-regulated protein in bladder cancer. *BJU international*. 90: 462-6.

Bando Y, Ogawa S, Yamauchi A, Kuwabara K, Ozawa K, Hori O, Yanagi H, Tamatani M, Tohyama M. (2000) 150 -kDa oxyg en-regulated pr otein (ORP150) f unctions as a nov el molecular ch aperone in MDCK cel ls. *American Journal of Physiology-Cell Physiology*. 278: C1172-82.

Benjannet S, Elagoz A, Wickham L, Mamarbachi M, Munzer JS, Basak A, Lazure C, Cromlish JA, Sisodia S, Checler F, Chrétien M. (2001) P ost-translational Processing of β-Secretase (β-Amyloid-converting E nzyme) a nd I ts E ctodomain S hedding The pr o- and transmembrane/cytosolic domains af fect i ts ce llular ac tivity and amyloid-beta p roduction. *Journal of Biological Chemistry*. 276: 10879-87.

Bertram L, Lill CM, Tanzi RE. (2010) The genetics of A lzheimer di sease: back t o the future. *Neuron*. 68: 270-81.

Bourne KZ, Ferrari DC, Lange-Dohna C, Roßner S, Wood TG, Perez-Polo JR. (2007) Differential regulation of BACE1 promoter activity by nuclear factor-κB in neurons and glia upon exposure to β-amyloid peptides. *Journal of neuroscience research*. 85: 1194-204.

Bruijn RF, Ikram MA. (2014) C ardiovascular r isk f actors an d future r isk of A lzheimer's disease. *BMC medicine*. 12: 130.

Cai H, Wang Y, McCarthy D, Wen H, Borchelt DR, Price DL, Wong PC. (2001) BACE1 is the major β-secretase for generation of Aβ peptides by neurons. *Nature neuroscience.* 4: 233-4.

Cao X, Südhof TC. (2001) A transcriptively active complex of APP with Fe65 and histone acetyltransferase Tip60. *Science.* 293: 115-20.

Capell A, Steiner H, Willem M, Kaiser H, Meyer C, Walter J, Lammich S, Multhaup G, Haass C. (2000) Maturation and pro-peptide cleavage of β-secretase. *Journal of Biological Chemistry.* 275: 30849-54.

Carter CL, Resnick EM, Mallampalli M, Kalbarczyk A. (2012) Sex and gender differences in Alzheimer's disease: recommendations for future research. *Journal of Women's Health.* 21: 1018-23.

Chami L, Buggia-Prévot V, Duplan E, Delprete D, Chami M, Peyron JF, Checler F. (2012) Nuclear factor-κB regulates βAPP and β-and γ-secretases differently at physiological and supraphysiological Aβ concentrations. *Journal of Biological Chemistry.* 287: 24573-84.

Chami L, Checler F. (2012) BACE1 is at the crossroad of a toxic vicious cycle involving cellular stress and β-amyloid production in Alzheimer's disease. *Molecular neurodegeneration.* 7: 52.

Chen S, Ou R, Tang J, Deng X, Wu Y, van Velkinburgh JC, Ni B, Xu Y. (2013) Enhanced anti-tumor effects of HPV16E7 49–57-based vaccine by combined immunization with poly (I: C) and oxygen-regulated protein 150. *Cancer epidemiology.* 37: 172-8.

Chen Y, Huang X, Zhang YW, Rockenstein E, Bu G, Golde TE, Masliah E, Xu H. (2012) Alzheimer's β-secretase (BACE1) regulates the cAMP/PKA/CREB pathway independently of β-amyloid. *Journal of Neuroscience.* 32: 11390-5.

Chouliaras L, Rutten BP, Kenis G, Peerbooms O, Visser PJ, Verhey F, Van Os J, Steinbusch HW, van den Hove DL. (2010) Epigenetic regulation in the pathophysiology of Alzheimer's disease. *Progress in neurobiology.* 90: 498-510.

Christensen MA, Zhou W, Qing H, Lehman A, Philipsen S, Song W. (2004) Transcriptional regulation of BACE1, the β-amyloid precursor protein β-secretase, by Sp1. *Molecular and cellular biology.* 24: 865-74.

Chyung AS, Greenberg BD, Cook DG, Doms RW, Lee VM. (1997) Novel β-secretase cleavage of β-amyloid precursor protein in the endoplasmic reticulum/intermediate compartment of NT2N cells. *The Journal of cell biology.* 138: 671-80.

Coburger I, Dahms SO, Roeser D, Gührs KH, Hortschansky P, Than ME. (2013) Analysis of the overall structure of the multi-domain amyloid precursor protein (APP). 8: 2-12

Cole SL, Vassar R. (2007) The Alzheimer's disease β-secretase enzyme, BACE1. *Molecular neurodegeneration.* 2: 22.

Cook DG, Forman MS, Sung JC, Leight S, Kolson DL, Iwatsubo T, Lee VM, Doms RW. (1997) Alzheimer's Aβ (1–42) is generated in the endoplasmic reticulum/intermediate compartment of NT2N cells. *Nature medicine.* 3: 1021-3.

Dai Q, Zhang C, Wu Y, McDonough H, Whaley RA, Godfrey V, Li HH, Madamanchi N, Xu W, Neckers L, Cyr D. (2003) CHIP activates HSF1 and confers protection against apoptosis and cellular stress. *The EMBO journal.* 22: 5446-58.

De Strooper B, Craessaerts K, Dewachter I, Moechars D, Greenberg B, Van Leuven F, Van Den Berghe H. (1995) Basolateral secretion of amyloid precursor protein in Madin-Darby canine kidney c ells is d isturbed by a lterations o f in tracellular pH a nd by int roducing a m utation associated with familial Alzheimer's disease. *Journal of Biological Chemistry.* 270: 4058-65.

Dingwall C. (2007) A c opper-binding s ite i n the cytoplasmic dom ain of B ACE1 i dentifies a possible l ink t o metal homoeostasis and oxidative stress in A lzheimer's disease. *Biochemical Society Transactions.* 35: 571-573.

Dislich B, Lichtenthaler SF. (2012) The membrane-bound aspartyl protease BACE: molecular and functional properties in Alzheimer's disease and beyond. *Frontiers in physiology.* 17: 3-8.

Du ZN, Rong CT, Hui S, Peng Z, Jin SH, Li SJ, Wang HY, Li JY. (2016) Expression and function of HSP110 family in mouse testis after vasectomy. *Asian journal of andrology.* 19: 355-361

Easton DP, Kaneko Y, Subjeck JR. (2000) The H sp110 a nd G rp170 s tress proteins: ne wly recognized relatives of the Hsp70s. *Cell stress & chaperones.* 5: 276-90.

Esser C, Scheffner M, Höhfeld J. (2005) The chaperone-associated ubiquitin ligase C HIP i s able to target p53 for proteasomal degradation. *Journal of Biological Chemistry.* 280: 27443-8.

Feder ME, Hofmann GE. (1999) H eat-shock pr oteins, m olecular c haperones, a nd t he s tress response: evolutionary and ecological physiology. *Annual review of physiology.* 61: 243-82.

Flores-Diaz M, Higuita JC, Florin I, Okada T, Pollesello P, Bergman T, Thelestam M, Mori K, Alape-Giron A. (2004) A c ellular U DP-glucose de ficiency caus es ov erexpression of glucose/oxygen-regulated proteins independent o f the end oplasmic r eticulum st ress e lements. *Journal of Biological Chemistry.* 279: 21724-31.

Ghosh AK, Osswald HL. (2014) BACE1 (β-secretase) i nhibitors f or t he t reatment o f Alzheimer's disease. *Chemical Society Reviews.* 43: 6765-813.

Guglielmotto M, Aragno M, Autelli R, Giliberto L, Novo E, Colombatto S, Danni O, Parola M, Smith MA, Perry G, Tamagno E. (2009) The up-regulation of BACE1 mediated by hypoxia and ischemic injury: role of oxidative stress and HIF1α. *Journal of neurochemistry.* 108: 1045-56.

Guglielmotto M, Tamagno E, Danni O. (2009) Oxidative stress a nd hypoxia contribute to Alzheimer's di sease pa thogenesis: two s ides of t he s ame c oin. *The Scientific World Journal.* 9: 781-91.

Haass C, Hung AY, Schlossmacher MG, Oltersdorf T, Teplow DB, Selkoe DJ. (1993) Normal Cellular Processing of the β-Amyloid Precursor Protein Results i n the Secretion of the Amyloid β Peptide and Related Moleculesa. *Annals of the New York Academy of Sciences.* 695: 109-16.

Hachet-Haas M, Converset N, Marchal O, Matthes H, Gioria S, Galzi JL, Lecat S. (2006) FRET and colocalization analyzer—A method to validate measurements of sensitized emission FRET acquired by confocal microscopy and available as an ImageJ Plug-in. *Microscopy research and technique.* 69: 941-56.

Hamos JE, Oblas B, Pulaski-Salo D, Welch WJ, Bole DG, Drachman DA. (1991) Expression of heat shock proteins in Alzheimer's disease. *Neurology*. 41: 345-355.

Hardy J, Selkoe DJ. (2002) The a myloid hy pothesis of A lzheimer's di sease: pr ogress and problems on the road to therapeutics. *Science*. 297: 353-6

Hartl D, Klatt S, Roch M, Konthur Z, Klose J, Willnow TE, Rohe M. (2013) Soluble alpha-APP (sAPPalpha) regulates CDK5 expression and activity in neurons. *PloS one*. 8: e65920.

Hattori C, Asai M, Oma Y, Kino Y, Sasagawa N, Saido TC, Maruyama K, Ishiura S. (2002) BACE1 interacts with nicastrin. *Biochemical and biophysical research communications*. 293: 1228-32.

He W, Lu Y, Qahwash I, Hu XY, Chang A, Yan R. (2004) R eticulon f amily members modulate BACE1 activity and amyloid-β peptide generation. *Nature medicine*. 10: 959-65.

He X, Li F, Chang WP, Tang J. (2005) G GA pr oteins m ediate the r ecycling pa thway of memapsin 2 (BACE). *Journal of Biological Chemistry*. 280: 11696-703.

Heacock CS, Sutherland RM. (1990) Enhanced synthesis of stress proteins caused by hypoxia and relation to altered cell growth and metabolism. *British journal of cancer*. 62: 217.

Hebert LE, Scherr PA, McCann JJ, Beckett LA, Evans DA. (2001) Is the risk of developing Alzheimer's di sease greater for women than for men?. *American journal of epidemiology*. 153: 132-6.

Hoozemans JJ, Van Haastert ES, Nijholt DA, Rozemuller AJ, Scheper W. (2012) Activation of t he un folded protein response i s an early ev ent i n Alzheimer's and Parkinson's d isease. *Neurodegenerative Diseases*. 10: 212-5.

Hoozemans JJ, Veerhuis R, Van Haastert ES, Rozemuller JM, Baas F, Eikelenboom P, Scheper W. (2005) T he unfolded protein response is a ctivated in Alzheimer's disease. *Acta neuropathologica*. 110: 165-72.

Hoshino T, Nakaya T, Araki W, Suzuki K, Suzuki T, Mizushima T. (2007) E ndoplasmic reticulum c haperones i nhibit the production o f a myloid-β peptides. *Biochemical Journal*. 402 : 581-9.

Huse JT, Pijak DS, Leslie GJ, Lee VM, Doms RW. (2000) Maturation and endosomal targeting of β-site amyloid precursor protein-cleaving enzyme The Alzheimer's disease β-secretase. Journal of Biological Chemistry. 275: 33729-37.

Hussain I, Powell D, Howlett DR, Tew DG, Meek TD, Chapman C, Gloger IS, Murphy KE, Southan CD, Ryan DM, Smith TS. (1999) Identification of a novel aspartic protease (Asp 2) as β-secretase. *Molecular and Cellular Neuroscience*. 14: 419-27.

Jha NK, Jha SK, Kar R, Ambasta RK, Kumar P. (2014) Role of oxidative stress, ER stress and ubiquitin proteasome system in neurodegeneration. *MOJ Cell Sci Report*. 1:1-8.

Jomova K, Vondrakova D, Lawson M, Valko M. (2010) Met als, oxidative stress and neurodegenerative disorders. *Molecular and cellular biochemistry*. 345: 91-104.

Kaneda S, Yura T, Yanagi H. (2000) Production of Three Distinct mRNAs of 150 kDa Oxygen-Regulated Protein (ORP 150) by Alternative Promoters: Preferential Induction of One Species under Stress Conditions. *The Journal of Biochemistry.* 128: 529-38.

Kitano H, Nishimura H, Tachibana H, Yoshikawa H, Matsuyama T. (2004) ORP150 ameliorates ischemia/reperfusion injury from middle cerebral artery occlusion in mouse brain. *Brain research.* 1015: 122-8.

Kitao Y, Hashimoto K, Matsuyama T, Iso H, Tamatani T, Hori O, Stern DM, Kano M, Ozawa K, Ogawa S. (2004) ORP150/HSP12A regulates Purkinje cell survival: a role for endoplasmic reticulum stress in cerebellar development. *Journal of Neuroscience.* 24: 1486-96.

Kizuka Y, Nakano M, Kitazume S, Saito T, Saido TC, Taniguchi N. (2016) Bisecting GlcNAc modification stabilizes BACE1 protein under oxidative stress conditions. *Biochemical Journal.* 473: 21-30.

Koh YH, von Arnim CA, Hyman BT, Tanzi RE, Tesco G. (2005) BACE is degraded via the lysosomal pathway. *Journal of Biological Chemistry.* 280: 32499-504.

Koike MA, Green KN, Blurton-Jones M, LaFerla FM. (2010) Oligemic hypoperfusion differentially affects tau and amyloid-β. *The American journal of pathology.* 177: 300-10.

Koren J, Jinwal UK, Lee DC, Jones JR, Shults CL, Johnson AG, Anderson LJ, Dickey CA. (2009) Chaperone signalling complexes in Alzheimer's disease. *Journal of cellular and molecular medicine.* 13: 619-30.

Krętowski R, Stypułkowska A, Cechowska-Pasko M. (2013) Low-glucose medium induces ORP150 expression and exerts inhibitory effect on apoptosis and senescence of human breast MCF7 cells. *Acta Biochim Pol.* 60: 167-73.

Kumar P, Ambasta RK, Veereshwarayya V, Rosen KM, Kosik KS, Band H, Mestril R, Patterson C, Querfurth HW. (2007) CHIP and HSPs interact with β-APP in a proteasome-dependent manner and influence Aβ metabolism. *Human molecular genetics.* 16: 848-64.

Kumar P, Pradhan K, Karunya R, Ambasta RK, Querfurth HW. (2012) Cross-functional E3 ligases Parkin and C-terminus Hsp70-interacting protein in neurodegenerative disorders. *Journal of neurochemistry.* 120: 350-70.

Kumar DK, Choi SH, Washicosky KJ, Eimer WA, Tucker S, Ghofrani J, Lefkowitz A, McColl G, Goldstein LE, Tanzi RE, Moir RD. (2016) Amyloid-β peptide protects against microbial infection in mouse and worm models of Alzheimer's disease. *Science translational medicine.* 8: 72-.

Kusaczuk M, Cechowska-Pasko M. (2013) Molecular Chaperone ORP150 in ER Stress–related Diseases. *Current pharmaceutical design.* 19: 2807-18.

Kuwabara K, Matsumoto M, Ikeda J, Hori O, Ogawa S, Maeda Y, Kitagawa K, Imuta N, Kinoshita T, Stern DM, Yanagi H. (1996) Purification and characterization of a novel stress protein, the 150-kDa oxygen-regulated protein (ORP150), from cultured rat astrocytes and its expression in ischemic mouse brain. *Journal of Biological Chemistry.* 271: 5025-32.

Kuznetsov G, Chen LB, Nigam SK. (1997) Multiple molecular chaperones complex with misfolded large oligomeric glycoproteins in the endoplasmic reticulum. *Journal of Biological Chemistry.* 272: 3057-63.

Kwak YD, Wang R, Li JJ, Zhang YW, Xu H, Liao FF. (2011) D ifferential r egulation of BACE1 expression by oxidative and nitrosative signals. *Molecular neurodegeneration*. 6:17-27.

LaFerla FM, Green KN, Oddo S. (2007) Intracellular amyloid-β in Alzheimer's disease. *Nature Reviews Neuroscience*. 8: 499-509.

Laws KR, Irvine K, Gale TM. (2016) S ex differences in c ognitive impairment in Alzheimer's Disease. *World journal of psychiatry*. 6: 54.

Lee JH, Won SM, Suh J, Son SJ, Moon GJ, Park UJ, Gwag BJ. (2010) Induction of t he unfolded protein response and cell death pathway in Alzheimer's disease, but not in aged Tg2576 mice. *Experimental & molecular medicine*. 42: 386-94.

Lin HY, Masso-Welch P, Di YP, Cai JW, Shen JW, Subjeck JR. (1993) T he 170-kDa glucose-regulated stress protein is an endoplasmic reticulum protein that binds immunoglobulin. *Molecular Biology of the Cell*. 4:1109-19.

Luo Y, Bolon B, Kahn S, Bennett BD, Babu-Khan S, Denis P, Fan W, Kha H, Zhang J, Gong Y, Martin L. (2001) Mice deficient in BACE1, the Alzheimer's β-secretase, have normal phenotype and abolished β-amyloid generation. *Nature neuroscience*. 4: 231-2.

Madeo J, Elsayad C. (2013) The role of oxidative stress in Alzheimer's disease. J Alzheimers Dis Parkinsonism. 3: 5.

Malishkevich A, Amram N, Hacohen-Kleiman G, Magen I, Giladi E, Gozes I. (2015) Activity-dependent neuroprotective protein (ADNP) exhibits striking sexual dichotomy impacting on autistic and Alzheimer's pathologies. *Translational psychiatry*. 5: e501.

Marino Gammazza A, Caruso Bavisotto C, Barone R, Macario EC, JL Macario A. (2016) Alzheimer's d isease and m olecular ch aperones: cur rent k nowledge an d t he f uture o f chaperonotherapy. *Current pharmaceutical design*. 22: 4040-9.

Marwarha G, Raza S, Prasanthi JR, Ghribi O. (2013) Gadd153 and NF-κB crosstalk regulates 27-hydroxycholesterol-induced increase in BACE1 and β-amyloid pr oduction i n hum an neuroblastoma SH-SY5Y cells. *PloS one*. 8: e70773.

Matsushita K, Matsuyama T, Nishimura H, Takaoka T, Kuwabara K, Tsukamoto Y, Sugita M, Ogawa S. (1998) Marked, sustained expression of a novel 150-kDa oxygen-regulated stress protein, in severely ischemic mouse neurons. *Molecular brain research*. 60: 98-106.

Maxwell, Brian and Richard Parsons. 2008. *Post Translational Modifications and Cellular Targeting of β - Secretase*. *Recent Advances in the Biology of Secretases*. 1-41

Meacham GC, Patterson C, Zhang W, Younger JM, Cyr DM. (2001) The H sc70 c o-chaperone C HIP t argets i mmature C FTR for pr oteasomal de gradation. *Nature cell biology*. 3: 100-5.

Miyagi T, Hori O, Koshida K, Egawa M, Kato H, Kitagawa Y, Ozawa K, Ogawa S, Namiki M. (2002) A ntitumor e ffect of r eduction of 150 -kDa oxy gen-regulated pr otein e xpression on human prostate cancer cells. *International journal of urology*. 9: 577-85.

Mouton-Liger F, Paquet C, Dumurgier J, Bouras C, Pradier L, Gray F, Hugon J. (2012) Oxidative stress increases BACE1 protein levels through activation of the PKR-eIF2α pathway. *Biochimica et Biophysica Acta (BBA)-Molecular Basis of Disease.* 1822: 885-96.

Mullan M, Crawford F, Axelman K, Houlden H, Lilius L, Winblad B, Lannfelt L. (1992) A pathogenic mutation for probable Alzheimer's disease in the APP gene at the N–terminus of β–amyloid. *Nature genetics.* 1: 345-7.

Müller T, Concannon CG, Ward MW, Walsh CM, Tirniceriu AL, Tribl F, Kögel D, Prehn JH, Egensperger R. (2007) Modulation of gene expression and cytoskeletal dynamics by the amyloid precursor protein intracellular domain (AICD). *Molecular biology of the cell.* 18: 201-10.

Murayama KS, Kametani F, Saito S, Kume H, Akiyama H, Araki W. (2006) Reticulons RTN3 and RTN4-B/C interact with BACE1 and inhibit its ability to produce amyloid β-protein. *European Journal of Neuroscience.* 24: 1237-44.

Newnam GP, Wegrzyn RD, Lindquist SL, Chernoff YO (1999) Antagonistic interactions between yeast chaperones Hsp104 and Hsp70 in prion curing. *Molecular and cellular biology.* 19: 1325-33.

Ngo ST, Steyn FJ, McCombe PA. (2014) Gender differences in autoimmune disease. *Frontiers in neuroendocrinology.* 35: 347-69.

Ni M, Lee AS. (2007) ER chaperones in mammalian development and human diseases. *FEBS letters.* 581: 3641-51.

Niforou K, Cheimonidou C, Trougakos IP. (2014) Molecular chaperones and proteostasis regulation during redox imbalance. *Redox biology* 2: 323-32.

O'Connor T, Sadleir KR, Maus E, Velliquette RA, Zhao J, Cole SL, Eimer WA, Hitt B, Bembinster LA, Lammich S, Lichtenthaler SF. (2008) Phosphorylation of the translation initiation factor eIF2α increases BACE1 levels and promotes amyloidogenesis. *Neuron.* 60: 988-1009.

Oddo S, Caccamo A, Tseng B, Cheng D, Vasilevko V, Cribbs DH, LaFerla FM. (2008) Blocking Aβ42 accumulation delays the onset and progression of tau pathology via the C terminus of heat shock protein70-interacting protein: a mechanistic link between Aβ and tau pathology. *Journal of Neuroscience.* 28: 12163-75.

Okada H, Zhang W, Peterhoff C, Hwang JC, Nixon RA, Ryu SH, Kim TW. (2010) Proteomic identification of sorting nexin 6 as a negative regulator of BACE1-mediated APP processing. *The FASEB Journal.* 24: 2783-94.

Ozawa K, Kuwabara K, Tamatani M, Takatsuji K, Tsukamoto Y, Kaneda S, Yanagi H, Stern DM, Eguchi Y, Tsujimoto Y, Ogawa S. (1999) 150-kDa oxygen-regulated protein (ORP150) suppresses hypoxia-induced apoptotic cell death. *Journal of Biological Chemistry.* 274: 6397-404.

Ozawa K, Kondo T, Hori O, Kitao Y, Stern DM, Eisenmenger W, Ogawa S, Ohshima T. (2001) Expression of the oxygen-regulated protein ORP150 accelerates wound healing by modulating intracellular VEGF transport. *The Journal of clinical investigation.* 108: 41-50.

Ozawa K, Miyazaki M, Matsuhisa M, Takano K, Nakatani Y, Hatazaki M, Tamatani T, Yamagata K, Miyagawa JI, Kitao Y, Hori O. (2005) The endoplasmic reticulum chaperone improves insulin resistance in type 2 diabetes. *Diabetes*. 54: 657-63.

Ozawa K, Tsukamoto Y, Hori O, Kitao Y, Yanagi H, Stern DM, Ogawa S. (2001) Regulation of tumor angiogenesis by oxygen-regulated protein 150, an inducible endoplasmic reticulum chaperone. *Cancer research*. 61: 4206-13.

Parsons CG, Danysz W, Dekundy A, Pulte I. (2013) Memantine and cholinesterase inhibitors: complementary mechanisms in the treatment of Alzheimer's disease. Neurotoxicity research. 24: 358-69.

Plácido AI, Pereira CM, Duarte AI, Candeias E, Correia SC, Santos RX, Carvalho C, Cardoso S, Oliveira CR, Moreira PI. (2014) The role of endoplasmic reticulum in amyloid precursor protein processing and trafficking: implications for Alzheimer's disease. *Biochimica et Biophysica Acta (BBA)-Molecular Basis of Disease*. 1842: 1444-53.

Plechanovová A, Jaffray EG, Tatham MH, Naismith JH, Hay RT. (2012) Structure of a RING E3 ligase and ubiquitin-loaded E2 primed for catalysis. *Nature*. 489:115-20.

Piedrahita D, Castro-Alvarez JF, Boudreau RL, Villegas-Lanau A, Kosik KS, Gallego-Gomez JC, Cardona-Gómez GP. (2015) β-secretase 1's targeting reduces hyperphosphorylated tau, implying autophagy actors in 3xTg-AD mice. *Frontiers in cellular neuroscience*. 9: 1-19.

Puglielli L, Ellis BC, Saunders AJ, Kovacs DM. (2003) Ceramide stabilizes β-site amyloid precursor protein-cleaving enzyme 1 and promotes amyloid β-peptide biogenesis. *Journal of Biological Chemistry*. 278: 19777-83.

Qing H, Zhou W, Christensen MA, Sun X, Tong Y, Song W. (2004) Degradation of BACE by the ubiquitin-proteasome pathway. *The FASEB journal*. 18: 1571-3.

Regitz-Zagrosek V. (2006) Therapeutic implications of the gender-specific aspects of cardiovascular disease. *Nature reviews Drug discovery*. 5: 425-239.

Reitz C, Brayne C, Mayeux R. (2011) Epidemiology of Alzheimer disease. *Nature Reviews Neurology*. 7: 137-52.

Roberds SL, Anderson J, Basi G, Bienkowski MJ, Branstetter DG, Chen KS, Freedman S, Frigon NL, Games D, Hu K, Johnson-Wood K. (2001) BACE knockout mice are healthy despite lacking the primary β-secretase activity in brain: implications for Alzheimer's disease therapeutics. *Human molecular genetics*. 10:1317-24.

Rosini M, Simoni E, Milelli A, Minarini A, Melchiorre C. (2013) Oxidative Stress in Alzheimer's Disease: Are We Connecting the Dots? Miniperspective. *Journal of medicinal chemistry*. 57: 2821-31.

Sahara N, Murayama M, Mizoroki T, Urushitani M, Imai Y, Takahashi R, Murata S, Tanaka K, Takashima A. (2005) In vivo evidence of CHIP up-regulation attenuating tau aggregation. *Journal of neurochemistry*. 94: 1254-63.

Sarajärvi T, Haapasalo A, Viswanathan J, Mäkinen P, Laitinen M, Soininen H, Hiltunen M. (2009) Down-regulation of seladin-1 increases BACE1 levels and activity through enhanced GGA3 depletion during apoptosis. *Journal of Biological Chemistry*. 284: 34433-43.

Sastre M, Dewachter I, Rossner S, Bogdanovic N, Rosen E, Borghgraef P, Evert BO, Dumitrescu-Ozimek L, Thal DR, Landreth G, Walter J. (2006) Nonsteroidal anti-inflammatory drugs repress β-secretase gene promoter activity by the activation of PPARγ. *Proceedings of the National Academy of Sciences.* 103: 443-8.

Schuessel K, Leutner S, Cairns NJ, Müller WE, Eckert A. (2004) Impact of gender on upregulation of antioxidant defence mechanisms in Alzheimer's disease brain. *Journal of neural transmission.* 111: 1167-82.

Selkoe DJ. (2001) Alzheimer's disease: genes, proteins, and therapy. *Physiological reviews.* 81: 741-66.

Semenza GL. (2001) Regulation of hypoxia-induced angiogenesis: a chaperone escorts VEGF to the dance. *The Journal of clinical investigation.* 108: 39-40.

Shimizu H, Tosaki A, Kaneko K, Hisano T, Sakurai T, Nukina N. (2008) Crystal structure of an active form of BACE1, an enzyme responsible for amyloid β protein production. *Molecular and cellular biology.* 28: 3663-71.

Shimura H, Schwartz D, Gygi SP, Kosik KS. (2004) CHIP-Hsc70 complex ubiquitinates phosphorylated tau and enhances cell survival. *Journal of Biological Chemistry.* 279: 4869-76.

Shin Y, Klucken J, Patterson C, Hyman BT, McLean PJ. (2005) The co-chaperone carboxyl terminus of Hsp70-interacting protein (CHIP) mediates α-synuclein degradation decisions between proteasomal and lysosomal pathways. *Journal of Biological Chemistry.* 280: 23727-34.

Singh AK, Pati U. (2015) CHIP stabilizes amyloid precursor protein via proteasomal degradation and p53-mediated trans-repression of β-secretase. *Aging cell.* 14: 595-604.

Sinha S, Anderson JP, Barbour R, Basi GS, Caccavello R, Davis D, Doan M, Dovey HF, Frigon N, Hong J, Jacobson-Croak K. (1999) Purification and cloning of amyloid precursor protein β-secretase from human brain. *Nature.* 402: 537-40.

Stankowski JN, Zeiger SL, Cohen EL, DeFranco DB, Cai J, McLaughlin B. (2011) C-terminus of heat shock cognate 70 interacting protein increases following stroke and impairs survival against acute oxidative stress. Antioxidants & redox signaling. 14: 1787-801.

Stojadinovic A, Hooke JA, Shriver CD, Nissan A, Kovatich AJ, Kao TC, Ponniah S, Peoples GE, Moroni M. (2007) HYOU1/Orp150 expression in breast cancer. *Medical Science Monitor.* 13: BR231-9.

Sun X, He G, Qing H, Zhou W, Dobie F, Cai F, Staufenbiel M, Huang LE, Song W. (2006) Hypoxia facilitates Alzheimer's disease pathogenesis by up-regulating BACE1 gene expression. *Proceedings of the National Academy of Sciences.* 103: 18727-32.

Sun X, Tong Y, Qing H, Chen CH, Song W. (2006) Increased BACE1 maturation contributes to the pathogenesis of Alzheimer's disease in Down syndrome. *The FASEB journal.* 20: 1361-8.

Takeuchi S. (2006) Molecular cloning, sequence, function and structural basis of human heart 150 kDa oxygen-regulated protein, an ER chaperone. *The Protein Journal.* 25: 517-28.

Tamatani M, Matsuyama T, Yamaguchi A, Mitsuda N, Tsukamoto Y, Taniguchi M, Che YH, Ozawa K, Hori O, Nishimura H, Yamashita A. (2001) O RP150 protects a gainst hypoxia/ischemia-induced neuronal death. *Nature medicine*. 7: 317-23.

Tan JL, Li QX, Ciccotosto GD, Crouch PJ, Culvenor JG, White AR, Evin G. (2013) Oxidative stress induces redistribution of BACE1 in non-apoptotic conditions and promotes the amyloidogenic pro cessing of Alzheimer's di sease am yloid precursor protein. *PLoS One*. 8: e61246.

Tanokashira D, Motoki K, Minegishi S, Hosaka A, Mamada N, Tamaoka A, Okada T, Lakshmana MK, Araki W. (2015) LRP1 downregulates the Alzheimer's β-secretase BACE1 by modulating its intraneuronal trafficking. *eneuro*. 2: ENEURO-0006.

Tanzi RE, Bertram L. (2005) Twenty years of the Alzheimer's disease amyloid hypothesis: a genetic perspective. *Cell*. 120: 545-55.

Thinakaran G, Koo EH. (2008) Amyloid precursor protein trafficking, processing, and function. *Journal of Biological Chemistry*. 283: 29615-9.

Thornton E, Vink R, Blumbergs PC, Van Den Heuvel C. (2006) Soluble amyloid precursor protein α reduces neuronal injury and improves functional outcome following diffuse traumatic brain injury in rats. *Brain research*. 1094: 38-46.

Tsukamoto Y, Kuwabara K, Hirota S, Ikeda J, Stern D, Yanagi H, Matsumoto M, Ogawa S, Kitamura Y. (1996) 150 -kD oxygen-regulated protein is e xpressed in hum an atherosclerotic plaques and allows mononuclear phagocytes to withstand cellular stress on exposure to hypoxia and modified low density lipoprotein. *Journal of Clinical Investigation*. 98: 1930.

Tsvetkov P, Adamovich Y, Elliott E, Shaul Y. (2011) E3 ligase STUB1/CHIP regulates NAD (P) H : qu inone oxi doreductase 1 (NQO1) a ccumulation in a ged br ain, a p rocess i mpaired in certain Alzheimer disease patients. *Journal of Biological Chemistry*. 286: 8839-45.

Van Den Heuvel C, Thornton E, Vink R. (2007) T raumatic b rain i njury a nd A lzheimer's disease: a review. *Progress in brain research*. 161: 303-16.

Vassar R, Bennett BD, Babu-Khan S, Kahn S, Mendiaz EA, Denis P, Teplow DB, Ross S, Amarante P, Loeloff R, Luo Y. (1999) β-Secretase cleavage of Alzheimer's amyloid precursor protein by the transmembrane aspartic protease BACE. *science*. 286: 735-41.

Velliquette RA, O'Connor T, Vassar R. (2005) Energy inhibition elevates β-secretase levels and activity and is potentially amyloidogenic in APP transgenic mice: possible early events in Alzheimer's disease pathogenesis. *Journal of Neuroscience*. 25: 10874-83.

Venugopal C, Demos CM, Jagannatha Rao KS, Pappolla MA, Sambamurti K. (2008) Beta-secretase: s tructure, f unction, a nd e volution. *CNS & Neurological Disorders-Drug Targets (Formerly Current Drug Targets-CNS & Neurological Disorders)*. 7: 278-94.

Verghese PB, Castellano JM, Holtzman DM. (2011) Apolipoprotein E in Alzheimer's disease and other neurological disorders. *The Lancet Neurology*. 10: 241-52.

Verma R, Balhara YP, Gupta CS. (2011) G ender di fferences i n stress response: R ole o f developmental and biological determinants. *Industrial psychiatry journal*. 20: 4.

Viña J, Lloret A. (2010) Why women have more Alzheimer's disease than men: gender and mitochondrial toxicity of amyloid-β peptide. *Journal of Alzheimer's disease*. 20: 527-33.

Wahle T, Prager K, Raffler N, Haass C, Famulok M, Walter J. (2005) GGA proteins regulate retrograde transport of BACE1 from endosomes to the trans-Golgi network. *Molecular and Cellular Neuroscience*. 29: 453-61.

Wang Y, Wu Z, Li D, Wang D, Wang X, Feng X, Xia M. (2011) Involvement of oxygen-regulated protein 150 in AMP-activated protein kinase-mediated alleviation of lipid-induced endoplasmic reticulum stress. *Journal of Biological Chemistry*. 286: 11119-31.

Wang Q, Xiao B, Cui S, Song H, Qian Y, Dong L, An H, Cui Y, Zhang W, He Y, Zhang J. (2014) Triptolide treatment reduces Alzheimer's disease (AD)-like pathology through inhibition of BACE1 in a transgenic mouse model of AD. Disease models & mechanisms. 7:1385-95.

Wei H, Wang F, Wang X, Yang J, Li Z, Cong X, Chen X. (2013) Lysophosphatidic acid promotes secretion of VEGF by increasing expression of 150-kD Oxygen-regulated protein (ORP150) in mesenchymal stem cells. *Biochimica et Biophysica Acta (BBA)-Molecular and Cell Biology of Lipids*. 1831: 1426-34.

Wojcik S, Engel WK, Yan R, McFerrin J, Askanas V. (2007) NOGO is increased and binds to BACE1 in sporadic inclusion-body myositis and in AβPP-overexpressing cultured human muscle fibers. *Acta neuropathologica*. 114: 517-26.

Wu YB, Li HQ, Ren MS, Li WT, Lv XY, Wang L. (2013) CHOP/ORP150 ratio in endoplasmic reticulum stress: a new mechanism for diabetic peripheral neuropathy. *Cellular Physiology and Biochemistry*. 32: 367-79.

Yang SW, Oh KH, Park E, Chang HM, Park JM, Seong MW, Ka SH, Song WK, Park DE, Baas PW, Jeon YJ. (2013) USP47 and C terminus of Hsp70-interacting protein (CHIP) antagonistically regulate katanin-p60-mediated axonal growth. *The Journal of Neuroscience*. 33: 12728-38.

Yoo BC, Kim SH, Cairns N, Fountoulakis M, Lubec G. (2001) Deranged expression of molecular chaperones in brains of patients with Alzheimer's disease. *Biochemical and biophysical research communications*. 280: 249-58.

Yu LG, Andrews N, Weldon M, Gerasimenko OV, Campbell BJ, Singh R, Grierson I, Petersen OH, Rhodes JM. (2002) An N-terminal Truncated Form of Orp150 Is a Cytoplasmic Ligand for the Anti-proliferative Mushroom Agaricus bisporusLectin and Is Required for Nuclear Localization Sequence-dependent Nuclear Protein Import. *Journal of Biological Chemistry*. 277: 24538-45.

Yu X, Wang XY. (2013) Engineering Grp170-based immune modulators for cancer immunotherapy. *Oncoimmunology*. 2: e24385.

Zhang X, Shi J, Tian J, Robinson AC, Davidson YS, Mann DM. (2014) Expression of one important chaperone protein, heat shock protein 27, in neurodegenerative diseases. *Alzheimer's research & therapy*. 6: 78-90

Zhang X, Zhou K, Wang R, Cui J, Lipton SA, Liao FF, Xu H, Zhang YW. (2007) Hypoxia-inducible factor 1α (HIF-1α)-mediated hypoxia increases BACE1 expression and β-amyloid generation. *Journal of Biological Chemistry*. 282: 10873-80.

Zhao Y, Wang Y, Yang J, Wang X, Zhao Y, Zhang X, Zhang YW. (2012) Sorting nexin 12 interacts w ith BACE1 and regulates B ACE1-mediated A PP pr ocessing. *Molecular neurodegeneration.* 7: 30.

Zong ZH, Du ZX, Zhang HY, Li C, An MX, Li S, Yao HB, Wang HQ. (2016) Involvement of Nrf2 in proteasome inhibition-mediated induction of ORP150 in thyroid cancer cells. *Oncotarget.* 7: 3416.

APPENDIX

Appendix

Bacterial Culture Media

LB Medium

Dissolve 25 g m of LB (Luria-Bertani) powder (Bekton D ickinson) i n 1 litre doubl e distilled water. Sterilize the media by autoclaving for 15 minutes at 121ºC /15 lb/sq. in.

LB Agar Plate

Dissolve 40 gm of LB Agar powder (DIFCO) in 1 litre double distilled water. Sterilize the media by autoclaving for 15 m inutes at 121ºC /15 lb/sq. in. Allow LB Agar to cool and just before pouring the plates, add appropriate antibiotic to the autoclaved media in the required final concentration to be used as a selection marker.

Antibiotics Preparation

Ampicillin Solution (Bacterial)

Dissolve a mpicillin salt in sterile water to make the stock solution of 100 mg/mL and sterilize by filtration through a 0.22 micron disposable filter. Store the solutions at -20ºC for longer use and can be stored at 4°C for routine work. The working concentration was 100 µg/mL for both broth and plates.

Kanamycin Solution (Bacterial)

Dissolve kanamycin salt i n sterile w ater t o make t he s tock solution of 50 m g/ml a nd sterilize by filtration through a 0.22 micron disposable filter. Store the solutions at -20ºC for longer use and can be stored at 4°C for routine work. The working concentration of the antibiotic was 50 µg/mL for both broth and plates.

G418 Solution (Mammalian)

Dissolve G418 i n s terile w ater t o m ake t he s tock s olution of 50 mg/ml a nd steriliz by filtration through 0.22 micron di sposable filter. S tore t he s olution a t 4° C a nd us e it a t respective calculated concentrations for the generating stable mammalian cell lines.

Stock Solutions of Commonly Used Reagents

30 % Acrylamide

Acrylamide	29 gm
N, N'-methylene-bis-acrylamide	1 gm

Add ddH$_2$O to make up the total volume to 100 mL and filter the solution. Store it at 4ºC.

10 % Ammonium persulphate

Add 10 g m a mmonium pe rsulphate pow der i n 100 mL of s terile ddH$_2$O a nd mix it properly. Keep the solution at 4ºC. The solution is stable for 2-4 weeks.

10 M Ammonium Acetate

Dissolve 385.4 gm of Ammonium acetate in 150 mL of water. Make up the volume to 500 ml. Sterilize the solution by autoclaving for 15 minutes at 121ºC /15 lb/sq. in.

1 M CaCl$_2$

Dissolve 147 gm of Calcium C hloride (CaCl$_2$.2H$_2$O) i n 1 liter w ater and sterilize the solution by filtration with a 0.22 micron filter membrane.

1 M DTT (Dithiothreitol)

Dissolve 3.09 gm of Dithiothreitol in 20 mL of 0.01 M Sodium acetate (pH 5.2) and store at -20ºC after filter sterilization with 0.22 micron filter.

0.5 M EDTA

Dissolve 186.1 g m of N a$_2$EDTA.2H$_2$O pow der i n 800 mL of w ater. K eep on s haking vigorously. A djust pH t o 8.0 w ith N aOH (~20 gm of NaOH pellets). E DTA w ill not dissolve completely until the pH of the solution reaches 8.0. F inally, add water to 1 litre and autoclave the solution.

70 % Ethanol

Mix 70 m L of pu re ethanol a nd 30 mL of s terile w ater to make up t he t otal vo lume to

100 mL. Store it at 4ºC.

Ethidium Bromide

Dissolve 100 m g Ethidium bromide tablet in 10 mL of water. Leave overnight at 37ºC shaker to dissolve the tablet completely and store in dark at room temperature.

50% Glycerol

To 50 m L of 100% glycerol, add sterile water to make up vol ume to 100 m l and mix thoroughly. Sterilize it by autoclaving.

1 M HEPES Buffer (pH 7.9, 8.0)

Dissolve 23.83 gm of solid HEPES salt in 80 mL of sterile water. Adjust the pH to the desired value accordingly with the help of 1N NaOH. Make up the final volume to 100 mL with water. Filter the solution with a 0.22 micron disposable filter. The buffer should be stored at 4ºC.

1 M IPTG (Isopropyl-β-D-thiogalactoside)

Dissolve 2.0 gm of IPTG powder in 8 mL of sterile distilled water. Make up to total 10 mL with water to a final concentration of 200 mg/mL and sterilize the solution by filtration through a 0.22 micron disposable filter. Dispense the solution into small aliquots and store them at -20ºC.

1 M KCl

Dissolve 74.6 gm of Potassium Chloride in 1litre of water and autoclave. Store the solution at room temperature.

1 M MgCl$_2$

Dissolve 203.3 gm of Magnesium Chloride (MgCl$_2$.6H$_2$O) dry powder and make up the total volume to 1 litre with water. Sterilize the solution by autoclaving.

5 M NaCl

Dissolve 292.2 gm of Sodium Chloride in 800 mL water and make up the total volume to 1 litre with water. Sterilize the solution by autoclaving.

10% NP-40 (Nonidet P-40) (v/v)

Make 10% solution of NP-40 detergent in sterile water by diluting from 100% stock solution. This solution can be diluted as per requirement.

dNTP's Mix (dATP, dCTP, dGTP, dTTP)

Prepare 10 mM dNTP mix from a commercially available 100 mM dNTP mix in DNase free MQ water and store in small aliquots at -20ºC.

Phenol: Chloroform: Isoamyl alcohol

Mix 25 parts (v/v) Phenol (previously equilibrated in 150 mM NaCl/50 mM Tris-Cl, pH 7.5 and 1 mM EDTA) with 24 parts (v/v) Chloroform and 1 part (v/v) of Isoamyl alcohol. Store in a dark colored glass bottle at 4ºC.

Protease Inhibitors

All the protease inhibitor solutions were made as 100X concentration stock. They should be added to the pre-cooled solutions just before use. All the protease inhibitor solutions are active for 3-4 weeks at a storage temperature of -20ºC. The required concentration of the solutions is 1X.

Leupeptin	100 µg/mL in MQ
Aprotinin	100 µg/mL in MQ
Trypsin Inhibitor	100 µg/mL in MQ

100 mM Phenyl methyl sulphonyl fluoride (PMSF)

Dissolve 174 mg of PMSF powder in 10 mL of isopropanol. Divide the solution in aliquots and store at -20ºC. Wear gloves while handling the chemical. The half-life of PMSF in aqueous solution is 20 minutes. So, it should be added to the solution just before

use.

10 % Sodium Dodecyl Sulphate (SDS)

Dissolve 100 gm of electrophoresis-grade SDS in 900 mL of sterile ddH$_2$O. Heat to 68°C and adjust the pH to 7.2 by adding a few drops of concentrated HCl. Adjust the volume to 1 litre with H$_2$O. Store the solution at room temperature.

1 M Tris (pH 6.8, 7.0, 7.2, 7.4, 7.5, 8.0, 8.8, 9.1, 9.5)

Dissolve 121.1 g m of T ris ba se i n 800 mL of d dH$_2$O. A djust pH t o de sired va lue b y adding concentrated HCl. Make up the final volume to 1 litre with water and sterilize by autoclaving

10% Triton X-100 (v/v)

Add 10 mL of Triton X-100 detergent solution into 90 mL of water to make up the final volume to 100 mL to get a final concentration of 10%.

10% Tween-20 (v/v)

Add 10 mL of Tween-20 de tergent s olution i nto 90 mL of w ater t o make up the f inal volume to 100 mL to get a final concentration of 10%.

Buffers

6X DNA Loading Buffer

Bromophenol blue	0.25% (w/v)
Xylene cyanol FF	0.25% (w/v)
Glycerol	30% (v/v)

4X Sample buffer (SDS gel loading buffer)

Tris-Cl, pH 6.8	200 mM
β-mercaptoethanol	4%
SDS	8% (w/v)
Bromophenol Blue	0.4% (w/v)
Glycerol	40% (v/v)

50X TAE buffer for 1 litre

Tris Base	242 gm
Glacial acetic acid	57.1 ml
Na$_2$EDTA.2H$_2$O	37.2 gm

5X Tris glycine buffer for 1 litre

Tris base	15.1 gm
Glycine	94.0 gm
SDS	5.0 gm

1X Tris transfer buffer for 1 litre

Tris base	48mM
Glycine	39mM
SDS	.037%
Methanol	20%

Buffers for Proteins Purification

Purification with Glutathione Sepharose

Lysis buffer

PBS (pH 7.4)	1X
Triton X-100	0.1%
PMSF	0.5 mM

Wash buffer

PBS (pH 7.4)	1X
Triton X-100	0.1%
PMSF	0.5 mM

Elution buffer

Tris-HCl pH-8.0	50 mM
Reduced Glutathione	20 mM
PMSF	0.5 mM

APPENDIX

Solution for Coomassie stain

Destain

Methanol	45 mL
Water	45 mL
Acetic Acid	10 mL

Coomassie stain

Dissolve 0.25 gm of Coomassie brilliant blue in 100 mL destain solution.